
USDRIVE
DRIVING RESEARCH AND INNOVATION FOR
VEHICLE EFFICIENCY AND ENERGY SUSTAINABILITY

*This report is a document of the U.S. DRIVE Partnership. U.S. DRIVE (Driving Research and Innovation for Vehicle efficiency and Energy sustainability) is a voluntary, non-binding, and non-legal partnership among the U.S. Department of Energy; the United States Council for Automotive Research (USCAR), representing FCA US LLC, Ford Motor Company, and General Motors; five energy companies—BP America, Chevron Corporation, Phillips 66 Company, ExxonMobil Corporation, and Shell Oil Products US; four utilities—American Electric Power, DTE Energy, Duke Energy Corporation, and Southern California Edison; and the Electric Power Research Institute (EPRI).*

*The Net-Zero Carbon Fuels Technical Team (NZTT) is one of 13 U.S. DRIVE technical teams whose mission is to accelerate the development of pre-competitive and innovative technologies tenable of a full range of efficient and clean advanced light-duty vehicles, as well as related energy infrastructure.*

*This report was authored by Peter Chen,[1] John Dees,[2] Hannah Goldstein,[3] Kylee Harris,[4] Zhe Huang,[4] Uisung Lee,[1] Wenqin Li,[2] Pimphan (Aye) Meyer,[5] Ian Rowe,[6] Dan Sanchez,[1] A.J. Simon,[2] Lesley Snowden-Swan,[5] Ling Tao,[4] Michael Wang,[5] and Eunji Yoo.[5]*

*For more information about U.S. DRIVE, please see the U.S. DRIVE Partnership Plan at www.energy.gov/eere/vehicles/us-drive or www.uscar.org.*

[1] Argonne National Laboratory
[2] University of California, Berkeley
[3] Lawrence Livermore National Laboratory
[4] National Renewable Energy Laboratory
[5] Pacific Northwest National Laboratory
[6] Bioenergy Technologies Office

# List of Acronyms

| | |
|---|---|
| AGR | acid gas removal |
| CaO | calcium oxide (lime) |
| CCS | carbon capture and sequestration |
| CCU | carbon capture and utilization |
| $CH_4$ | methane |
| CI | carbon intensity |
| CO | carbon monoxide |
| $CO_2$ | carbon dioxide |
| $CO_2e$ | carbon dioxide equivalent |
| DAC | direct air capture |
| DDGS | dried distillers grains with solubles |
| FT | Fischer–Tropsch |
| GA | green ammonia |
| GGE | gallon gasoline equivalent |
| GHG | greenhouse gas |
| GREET | Greenhouse gases, Regulated Emissions, and Energy use in Technologies |
| $H_2$ | hydrogen |
| HTL | hydrothermal liquefaction |
| LCA | life cycle analysis |
| LUC | land use change |
| MFSP | minimum fuel selling price |
| MMBtu | million British thermal units |
| $N_2O$ | nitrous oxide |
| NG | natural gas |
| NZTT | Net-Zero Carbon Fuels Technical Team |
| RD | renewable diesel |
| RE | renewable electricity |
| RNG | renewable natural gas |
| SAF | sustainable aviation fuel |
| SMR | steam methane reforming |
| TCI | total capital investment |
| TEA | techno-economic analysis |
| THROX | thermal oxidation unit |
| TRL | technology readiness level |
| U.S. DRIVE | Driving Research and Innovation for Vehicle efficiency and Energy sustainability |

# Executive Summary

The Net-Zero Carbon Fuels Technical Team (NZTT) is tasked with investigating the potential to generate carbon-based fuels with much lower carbon intensities (CIs) compared to those of conventional fuels, approaching or exceeding net-zero greenhouse gas (GHG) emissions. In this study, the life cycle GHG emissions of five fuel production pathways and dozens of variants on those pathways are analyzed. Additionally, the overall cost of each pathway is evaluated and calculated as minimum fuel selling price (MFSP). The five pathways and their primary variations are:

1. Conventional corn ethanol production with upgrading to sustainable aviation fuel (SAF), incorporating renewable process inputs and carbon capture and sequestration (CCS) or carbon capture and utilization (CCU).

2. Advanced cellulosic ethanol production using corn stover biomass feedstock and ethanol upgrading to SAF. Similar to Case 1, renewable inputs, CCS, and CCU are assessed.

3. Production of gasoline, jet, and diesel fuel from woody biomass gasification followed by Fischer–Tropsch (FT) synthesis.

4. Production of gasoline, jet, and diesel fuel from the hydrothermal liquefaction (HTL) of wet wastes (sludge from wastewater treatment plants) and subsequent hydrotreating and fractionation.

5. Direct air capture (DAC) of carbon dioxide ($CO_2$) and water/$CO_2$ electrolysis to syngas followed by FT synthesis to produce gasoline, SAF, and diesel.

These pathways represent a diverse set of options for producing net-zero-carbon fuels, covering a range of feedstocks, process inputs, products, coproducts, environmental impacts, and technical maturities. It is not the intention of this report to rank or compare these pathways on specific criteria or overall promise. Rather, this report is intended to show that there are multiple pathways with multiple feedstocks toward net-zero liquid fuels. Factors such as feedstock constraints, carbon disposal logistics, maturation time, capital and operating costs, and renewable energy availability will affect the technical and economic feasibility of each of these pathways. This report lays the groundwork for continual assessment of net-zero options as this landscape evolves.

Section 2 of this report describes the analysis methodologies. Life cycle analysis (LCA)—based primarily on the Greenhouse gases, Regulated Emissions, and Energy use in Technologies (GREET) LCA model—was used to calculate each pathway's CI. Our LCA considers the GHG emissions associated with the operation of upstream conversions and logistics (e.g., biomass growth and transport, fossil fuel production) and process inputs (e.g., electricity generation, hydrogen production, and reagent manufacturing), as well as the GHG consequences of all

products and coproducts, including displacement credits. Carbon usage, emissions, and disposal from the core pathway are accounted for. Techno-economic analysis (TEA) based on a consistent set of assumptions about finance, capital costs, and feedstock prices is used to calculate each pathway's MFSP. Using published engineering methods and standard accounting assumptions, a discounted cash flow rate of return analysis is conducted using capital and operating cost data to calculate MFSPs. This process is shown schematically in Figure ES-1 for a generalized process. Each case and sub-scenario has different connectivity between resources, intermediates, process configuration, and products.

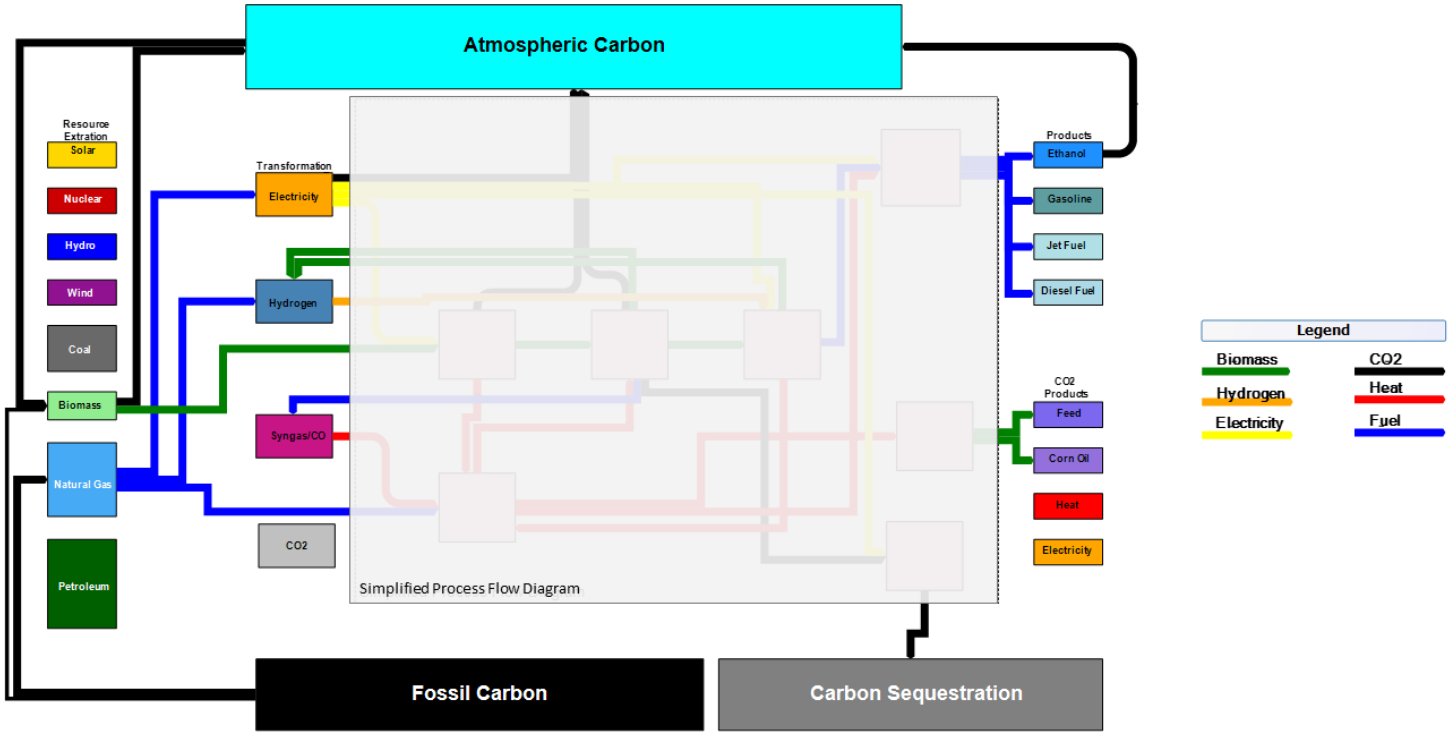


Figure ES-1. Generalized process flow diagram of the life cycle stages considered. The left-hand side of the flow diagram illustrates the upstream conversions, logistics, and process inputs considered. The right-hand side illustrates the downstream process, including products, coproducts, and displacement credits. In the center of the flow diagram (blurred out) are the varying connectivity flows between resources, intermediates, process configuration, and products. This area of the flow diagram varies for each case and sub-scenario.

Section 3 of the report provides details related to each pathway and sub-scenario, including process design, overall mass and energy flows, and LCA and TEA results. The cost impacts of CI reduction interventions are also discussed here.

Section 4 presents the results of the analysis of these five highly diverse pathways in an integrated format. The high-level results, as well as the advantages and disadvantages of each of the pathway cases, are summarized in the following paragraphs. Figure ES-2 shows the overall LCA results of CIs through five cases and their sub-cases. "Conventional" refers to using U.S.

electric mix—fossil natural gas (NG) steam methane reforming (SMR) hydrogen ($H_2$), fossil NG, and conventional ammonia—whereas "renewable" refers to using renewable electricity and $H_2$, landfill-based renewable natural gas (RNG), and green ammonia.

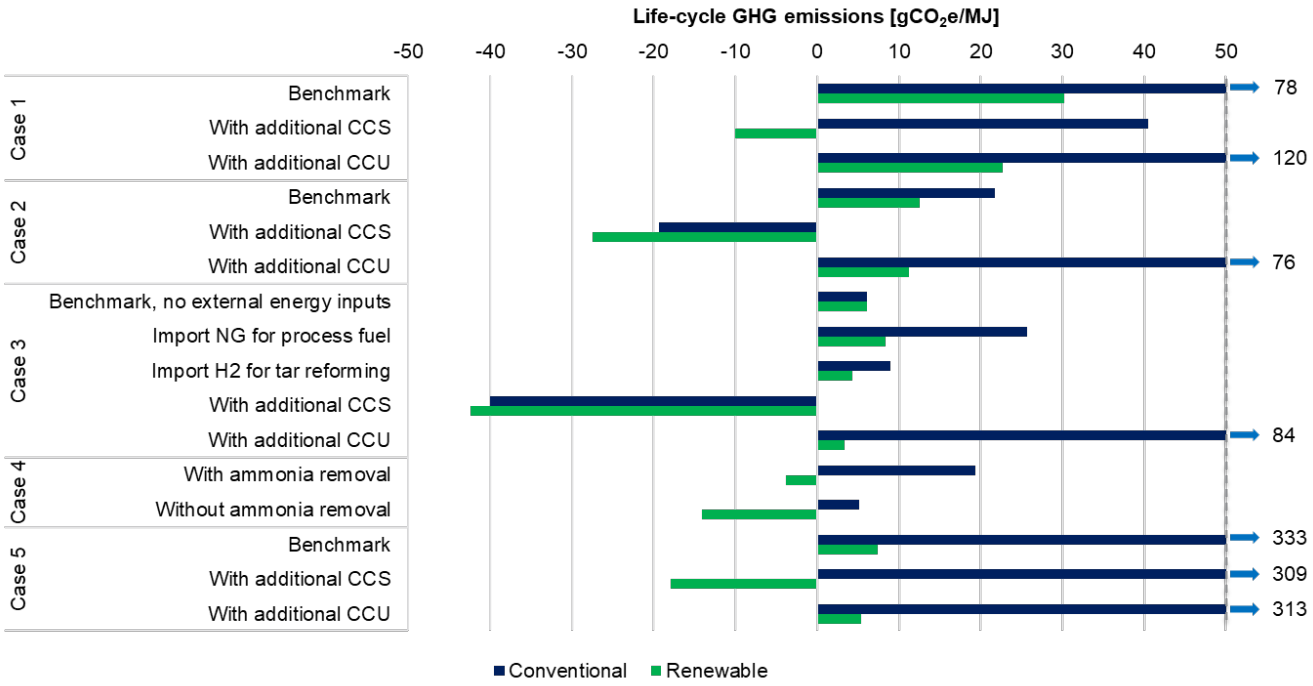


Figure ES-2. Summary of LCA results of carbon intensities of net-zero liquid fuels

**Case 1. Conventional corn ethanol production with upgrading to SAF and with CCS and CCU options.** SAF cost is at $3.24 per gallon gasoline equivalent (GGE) and a CI 7% below conventional fuel without considering either renewable energy inputs or CCS/CCU. Renewable electricity and RNG can substantially reduce the CI by 64%. Much deeper decarbonization is possible by intercepting carbon emissions from the fuel production process, which further reduces the CI by more than 30 g/MJ, making net-zero (and potentially net-negative) jet fuel a near-term possibility. We project that the cost of a net-zero fuel would be approximately $3.90/GGE.

**Case 2. Advanced cellulosic ethanol production using corn stover biomass feedstock and ethanol upgrading to SAF.** Cellulosic ethanol has been demonstrated at commercial scale but is not widely deployed. For a 2,000-dry-ton corn stover conversion facility, the biofuel production (total hydrocarbon) production is about 36 million GGE, with CI of 21.8 g carbon dioxide equivalent ($CO_2e$)/MJ and cost of $4.55/GGE. Incorporating RNG and green hydrogen can reduce CI by 25%. Capturing fermentation $CO_2$ does substantially reduce the CI to net negative of aviation fuel produced from cellulosic biomass converted to ethanol intermediate, but with a small cost penalty, with calculated fuel cost of $4.72/GGE. Adding CCU can improve the carbon efficiency of the process CI by approximately 37 g/MJ, which is more than enough to offset the baseline CI of 22.4 g/MJ. SAF made with cellulosic ethanol in today's electricity,

hydrogen, and ammonia markets would be carbon negative according to our analysis. Substituting green hydrogen and ammonia would further offset emissions such that the net CI would be −21 g/MJ.

**Case 3. Production of gasoline, jet, and diesel fuel from woody biomass gasification followed by FT synthesis.** The pathway technology presents a near-term viable pathway for biomass-derived fuel production and with a low baseline MFSP of $2.58/GGE and a CI starting around 6 g/MJ. Importing green $H_2$ is a near-term option for boosting carbon efficiency; however, current costs for renewable $H_2$ are high and could lead to a cost increase of about $1/GGE. CCS is another near-term carbon mitigation strategy with a high technology readiness level (TRL) that could readily be implemented and remove a large fraction of $CO_2$ emissions with a low cost burden. This enables this pathway to become impressively carbon negative (approximately −40 g/MJ) and with a low cost burden. Since renewable electricity can be purchased at or near grid prices, a fully renewable CCS system is achievable. CCU technologies present a strategy for reincorporating $CO_2$ to fuels, resulting in a significant increase in carbon efficiency—up to 52.9%—but with a large cost burden, especially in the renewable scenario, which would be necessary to approach a net-zero-carbon fuel. Thus, the CCU should be viewed as a long-term strategy for carbon mitigation and utilization in the biomass to fuels via FT pathway.

**Case 4. Production of gasoline, jet, and diesel fuel from HTL of wet wastes.** Wet waste HTL is also a promising pathway using low-cost and abundant feedstocks such as sludge from wastewater treatment plants to generate low-CI transportation fuel. Another benefit of adopting the wet waste feedstock is significant "avoided emissions" accounted due to diversion of the feedstock away from traditional waste disposals. Based on the sizes of existing wastewater treatment plants (highly variable), base case process design assumes ten HTL plants supporting one biocrude upgrading plant. Based on the sizes of existing wastewater treatment plants (highly variable), the base case process design assumes ten HTL plants supporting one biocrude upgrading plant. To process 363,000 dry U.S. tons of sludge per year, 36.8 million GGE of fuel per year could potentially be produced. The economic analysis suggests that production costs of the renewable fuel are between $2.77/GGE (with conventional inputs) and $3.58/GGE (with fully renewable inputs). In addition, CI of the fuel product is 19 g/MJ (5 g/MJ if the HTL aqueous-phase treatment is not required) with conventional inputs and −4 g/MJ (−14 g/MJ if the HTL aqueous-phase treatment is not required) with renewable energy inputs. CCS and CCU options are not considered in Case 4 analysis due to low concentration of $CO_2$ in the flue gas effluent.

**Case 5. DAC of $CO_2$ and water/$CO_2$ electrolysis to syngas, followed by FT synthesis to produce gasoline, SAF, and diesel.** DAC $CO_2$ to FT fuel is an energy-intensive technology that requires 1.2 MJ of $H_2$, 0.4 MJ of NG, and 0.5 MJ of electricity. Thus, without using renewable energy, the DAC $CO_2$ FT process does not provide CI reduction benefits. Using conventional energy sources makes the CI of FT fuel 3.9 times higher (333 $gCO_2e$/MJ) compared to conventional jet fuel (84.5 $gCO_2e$/MJ). CCS or CCU may not help reduce the CIs if the same

conventional energy sources are used. With a fully decarbonized energy system, including zero-carbon electricity and zero-carbon hydrogen, such fuels could achieve near-zero net emissions. They are, however, projected to cost between $10 and $15/GGE.

The LCA results of the five pathways with various conditions present that there is potential to produce low- or zero-carbon fuels. First, the use of renewable energy inputs (electricity, $H_2$, and NG) reduces the CIs of the fuel production pathways by reducing the upstream impacts associated with energy input production. In addition, the CCS option that captures and sequesters $CO_2$ emissions from the conversion processes provides significant emission reductions with a slight increase in electricity consumption for $CO_2$ capture and compression. With this, even negative CIs could be achieved for some pathways. Additional CI reduction is estimated at 24–41 $gCO_2e/MJ$, depending on available $CO_2$ emissions per megajoule of fuel production. When captured $CO_2$ is rather utilized, we need significant additional energy inputs (electricity and $H_2$) to convert $CO_2$ into fuels. Thus, it is essential to use renewable energy inputs for CCU to lower the CIs. CCU coupled with renewable energy can reduce the CIs while providing additional fuel outputs from the same amount of feedstocks. Although CCU cases may not make carbon-negative fuels due to emissions from $CO_2$-derived fuels, they generate additional energy products with low CI values.

# Table of Contents

# List of Figures

# List of Tables

# 1. Introduction

The scope for the Net-Zero Carbon Fuels Technical Team (NZTT) is to investigate and propose solutions for generating liquid carbon-based fuels with a reduced carbon intensity (CI) such that, from a life cycle carbon accounting standpoint, they have a net greenhouse gas (GHG) emissions profile approaching zero. Carbon dioxide ($CO_2$) is the primary GHG emitted into the atmosphere through human activities. In the United States, $CO_2$ accounts for approximately 80% of all 6.5 gigatonnes U.S. greenhouse gas emissions in 2019 [1]. NZTT also performs process analyses to examine the conditions required for economic viability and allow eventual demonstration of the most promising technologies. As stated, the relevance of liquid fuels in the transportation sector points toward the need for carbon-based fuels derived from low-CI sources. The main renewable option for liquid fuel is commonly considered biofuels, which are typically made from organic matter such as corn, oilseeds, algae, and woody or herbaceous biomass, or from waste materials including fats, oils, and greases; agricultural residues; and municipal solid waste. This NZTT effort will investigate both conventional biofuel production and more novel fuel production pathways using renewable electricity and hydrogen, as well as $CO_2$ feedstocks from point sources or captured directly from the air.

Life cycle analysis (LCA) and techno-economic analysis (TEA) approaches are used to determine the challenges and opportunities across five representative biofuel production pathways, in addition to four other biofuel production pathways analyzed in fiscal year 2020 [2]. We developed a biorefinery model to complete mass and energy balances and generate life cycle inventory data for LCA and TEA. In an applied R&D setting, where technology exploration is directly tied to practical applications and possible commercial deployment, the unit operations and process design for the renewable fuel being developed are often optimized to achieve the lowest minimum fuel production cost possible. Thus, the fuel pathway design is optimized in a TEA, followed by the same parameters used to perform an LCA to determine the GHG emissions and other environmental impacts.

An LCA is performed as “cradle-to-grave” analysis to assess the environmental impacts associated with the various stages of fuel production and use, including resource extraction, feedstock growth and processing, conversion (feedstocks to fuel), fuel distribution, and fuel use. Life cycle GHG emissions of fuel production pathways—their CIs—include emissions of $CO_2$, methane ($CH_4$), and nitrous oxide ($N_2O$) combined together with their 100-year horizon global warming potentials, which are presented in term of $CO_2$ equivalents ($CO_2e$) per megajoule of biofuel produced and used. In addition, TEA is used to provide estimates of the economic performance of complete fuel production processes. TEA is typically used to evaluate the technological maturity and feasibility of various renewable fuel pathways. Such an analysis is done by assessing the overall material and energy inputs, outputs, and costs, as well as the product potential of a process based on its current state of technology development. This information is then used to identify the parameters that most significantly impact costs while

also estimating the technical readiness of the technology for deployment at a relevant scale. In this case, such an analysis can usually be presented as the cost of fuel production for a given volume. Together, TEA and LCA will provide insights into potential projected costs of new fuel pathway technologies and environmental performance improvements compared to existing fuels refined from fossil sources and other fuel production pathways.

For biorefineries, $CO_2$ capture and/or utilization can result in deep GHG reductions. Carbon capture and sequestration (CCS) is designed to significantly reduce process GHG emissions, whereas carbon capture and utilization (CCU) aims to improve the process economics by maximizing the biomass carbon usage. Our analysis here applies CCS and CCU to several pathways and demonstrates their effectiveness to achieve net zero.

Five biofuel technologies are investigated in fiscal year 2021:

- **Case 1 – Corn ethanol:** Conventional corn ethanol production and ethanol upgrading to sustainable aviation fuel (SAF) with CCS and CCU.
- **Case 2 – Corn stover ethanol:** Advanced cellulosic ethanol production using corn stover biomass feedstock and ethanol upgrading to SAF. Both on-site CCU and CCS are investigated as alternatives to reduce carbon emissions.
- **Case 3 – Biomass gasification and Fischer–Tropsch (FT) synthesis:** Production of gasoline, jet, and diesel fuel from woody biomass gasification, followed by FT synthesis.
- **Case 4 – Wet waste hydrothermal liquefaction (HTL):** Production of gasoline, jet, and diesel fuel from the HTL of wet wastes (sludge from wastewater treatment plant) and subsequent hydrotreating and fractionation.
- **Case 5 – Direct air capture (DAC) $CO_2$ to SAF:** DAC of $CO_2$ and water/$CO_2$ electrolysis to syngas followed by syngas FT synthesis to produce gasoline, SAF, and diesel.

For each case study, key challenges and potential opportunities for transformational R&D toward net-zero-carbon fuels with economic viabilities are highlighted and reported with comprehensive LCA and TEA results, offering promising near- and longer-term commercialization opportunities.

# 2. Methodology

## 2.1 LCA

To analyze the environmental impact of various energy conversion technologies and resultant fuels and products, LCA is conducted to account for the life cycle environmental impacts, including GHG emissions through the supply chain of fuels and products. In this report, we analyze the life cycle GHG emissions of the five fuel production pathways using the Greenhouse gases, Regulated Emissions, and Energy use in Technologies (GREET) model developed by Argonne National Laboratory [3]and key data on energy and mass balance developed by TEA and other process modeling. The LCA system in this study includes three major stages: feedstock production and transportation, fuel production and transportation, and fuel combustion (Figure 1). All upstream impacts of key inputs (e.g., energy or chemical inputs) are considered, as well as process emissions from each stage. For biomass feedstocks (corn and woody biomass), the feedstock production stage includes farming crops and collecting biomass and/or residues. There are also processes of feedstock treatment and transportation.

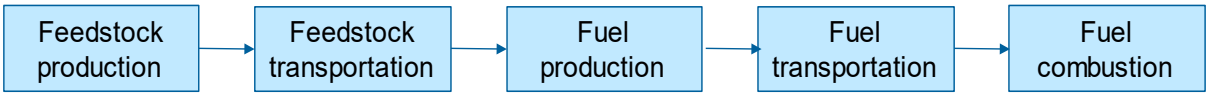


Figure 1. The schematics of the LCA system boundary that consists of feedstock production, feedstock transportation, fuel production, fuel transportation, and fuel combustion stages

The analysis accounts for all emissions from the combustion of process fuel and non-combustion emissions from chemical reaction, leakage, venting, and others. Then, the transportation of fuels from the fuel production plant to the end-use phase is considered. The fuel combustion stage is where fuel is used while emitting combustion emissions. Note that the carbon-neutrality assumption is used because $CO_2$ combustion of biomass- and $CO_2$-derived fuels offsets biological carbon uptake during biomass growth and waste $CO_2$ emissions that are otherwise emitted to the atmosphere, respectively.

For waste feedstocks (corn stover, sludge, manure, and $CO_2$), emissions are accounted starting from collection/recovery, not including upstream emissions for feedstock production. For example, for $CO_2$ feedstocks, the feedstock production stage includes $CO_2$ capture and transmission processes.

The fuel production (i.e., conversion) stage is where feedstock is converted into energy products (e.g., ethanol, SAF, gasoline, and diesel fuels) with process energy and chemical inputs. For LCA Cases 1–5, two major scenarios (conventional and renewable energy supply) are considered (Table 1), mainly driven by the types of input energy sources (electricity, hydrogen [$H_2$], and natural gas [NG]). The conventional scenario represents current U.S. energy systems, whereas the renewable scenario considers alternative energy systems such as renewable

electricity (RE), renewable $H_2$, renewable natural gas (RNG), and green ammonia (GA), which can further reduce the CIs to achieve net-zero-carbon fuels.

All values in Table 1 are from GREET 2021 [3] and are used in this study. For the conventional scenario, electricity use refers to U.S. electricity grid mix in 2020 with the CI of 440 $gCO_2e$/kWh electricity. $H_2$ is produced from fossil NG via steam methane reforming (SMR) with the CI of 79 $gCO_2$/MJ $H_2$. Note that the CI of electrolysis $H_2$ using grid electricity is 170 $gCO_2e$/MJ $H_2$. NG use means conventional fossil NG with the CI of 69 $gCO_2e$/MJ NG, including combustion emissions, and conventional ammonia is produced from fossil NG with the CI of 2,636 $gCO_2e$/kg ammonia.

On the other hand, for the renewable scenario, we assumed on-site renewable electricity (solar or wind) that does not have carbon emissions (0 $gCO_2e$/kWh). While GREET includes GHG emissions of building solar PVs and wind turbines, these infrastructure-related emissions are not included in other pathways (e.g., construction of biofuel plants). For consistency, all infrastructure-related emissions are excluded from the LCA for this study. While GREET includes GHG emissions of building solar PVs and wind turbines, these infrastructure-related emissions are not included in other pathways (e.g., construction of biofuel plants). For consistency, all infrastructure-related emissions are excluded from the LCA for this study. Renewable $H_2$ is produced from on-site electrolysis with renewable electricity (0 $gCO_2e$/MJ $H_2$) except for Case 4, which uses renewable $H_2$ produced from an off-site electrolysis facility and transported 50 miles through pipeline (0.5 $gCO_2e$/MJ $H_2$). This is because renewable hydrogen is assumed to be purchased rather than produced on-site for the Case 4 analysis. Landfill-based RNG with the CI of 11 $gCO_2e$/MJ is assumed for the NG demand. Landfill-derived RNG considers avoided emissions because using landfill gas for fuel production diverts landfill gas from being flared. Green ammonia is produced from nitrogen ($N_2$) and renewable $H_2$. Green ammonia can be used for both the fuel conversion and corn farming processes. Note that the impact of the infrastructure is not considered in this study.

Table 1. The carbon intensities of electricity, $H_2$, and NG of two scenarios used for Cases 2–4: conventional scenario and renewable scenario [3]

| | **Conventional Scenario** | **Renewable Scenario** |
|---|---|---|
| **Electricity** | U.S. grid mix (2020)<br>440 $gCO_2e$/kWh | Renewable electricity<br>0 $gCO_2e$/kWh |
| **$H_2$** | NG SMR (off-site, 50 miles)<br>79 $gCO_2e$/MJ<br>Compare to electrolysis with grid electricity<br>170 $gCO_2e$/MJ (on-site) | Electrolysis with renewable electricity<br>0 $gCO_2e$/MJ (on-site)<br>0.5 $gCO_2e$/MJ (off-site, 50 miles) |
| **NG** | Fossil NG<br>69 $gCO_2e$/MJ | Renewable natural gas from landfill gas<br>11 $gCO_2e$/MJ |
| **Ammonia** | Conventional ammonia<br>2,636 $gCO_2e$/kg | Green ammonia<br>293 $gCO_2e$/kg |

We assumed energy-based allocation for the multiple fuel products (e.g., gasoline, jet, diesel) from the fuel conversion process, while coproduced wax and cogenerated electricity have credits by displacing residual oil and U.S. grid mix electricity, respectively. The life cycle GHG

emissions were calculated in terms of $CO_2e$ using the global warming potentials of 1, 30, and 265 for $CO_2$, $CH_4$, and $N_2O$, respectively, based on the fifth assessment report by the Intergovernmental Panel on Climate Change [4]. The LCA results of each case are compared to the baseline fuel produced from the conventional production pathway. The baseline fuels are conventional petroleum jet (Cases 1, 2, 3, and 5) and conventional low-sulfur diesel (Case 4), the CIs of which are 84.5 $gCO_2e/MJ$ and 90.5 $gCO_2e/MJ$, respectively [3].

## 2.2. TEA

Process economic analysis includes (1) a detailed process flow diagram, informed by a conceptual-level process design based on research data and rigorous material and energy balance calculations via commercial simulation tools such as Aspen Plus; (2) capital and project cost estimations using an in-house model; (3) a discounted cash flow economic model; and (4) the calculation of minimum fuel selling price (MFSP).

The operating expense calculations are based on material and energy balance calculations using process simulations and are consistent with previously developed TEA models [5-10]. Raw materials include feedstocks, chemicals, catalysts, and utilities. In this analysis, we considered displacing fossil energy sources (such as natural gas) using renewable energy sources (such as RNG) to potentially reduce the CIs; Table 2 summarizes the prices of RNG varied by feedstock types. Prices are derived from previous reports [11].

Table 2. Summary of RNG cost sensitivity values

| | **Feedstock** | **Cost Range ($/MMBtu[a])** | | |
|---|---|---|---|---|
| | | **Minimum** | **Baseline** | **Maximum** |
| Anaerobic digestion | Landfill gas | $7.10 | $13.05 | $19.00 |
| | Animal manure | $18.40 | $25.50 | $32.60 |
| | Wastewater sludge | $7.40 | $16.75 | $26.10 |
| | Food waste | $19.40 | $23.85 | $28.30 |
| | RIN[b] | $7.48 | $12.00 | $29.44 |

[a] Million British thermal units; [b] Renewable Identification Number.

The estimated costs of conventional and renewable electricity, hydrogen, and ammonia are listed in Table 3. Conventional process input costs are unlikely to vary substantially and are not subject to a range for sensitivity analysis. Note that baseline $H_2$ price represents the optimistic case from the Hydrogen Analysis (H2A) models [12]. All costs are adjusted to 2016 U.S. dollars using the Plant Cost Index from *Chemical Engineering* magazine [13], the Industrial Inorganic Chemical Index from SRI Consulting [14], and labor indices provided by the U.S. Department of Labor Bureau of Labor Statistics. We did not consider a range of uncertainty for renewable ammonia prices.

Table 3. Summary of renewable electricity and renewable $H_2$ cost sensitivity values

| Resource | Minimum | Baseline | Maximum |
|---|---|---|---|
| Conventional electricity ($/kWh) | | $0.068 | |
| Renewable electricity ($/kWh) | $0.02 | $0.068 | $0.10 |
| Conventional $H_2$ ($/kg) | | $1.38 | |
| Renewable $H_2$ ($/kg) | $1.38 | $4.50 | $6.35 |
| Conventional $NH_3$ ($/kg) | | $0.59 | |
| Renewable $NH_3$ ($/kg) | | $1.37 | |

Material and energy balance and flow rate information is used to determine the number and size of equipment and calculate the capital expenses. Capital costs are primarily based on detailed equipment quotations from previous TEA models. For equipment not listed and for which vendor guidance is not available, the Aspen Icarus Process Evaluator is used to estimate baseline capital costs, assuming a scaling exponent term of 0.6.

Using published engineering methods, a discounted cash flow rate of return analysis was conducted using capital and operating cost data, with the financial assumptions shown in Table 4. We assume 40% equity financing and 3 years of construction plus 6 months for startup. The plant's life is assumed to be 20 years for Case 1 and 30 years for Cases 2–4. The income tax is 21%. Working capital is 5% of the fixed cost investment. The MFSP is the minimum price that the fuel product must sell to generate a net present value of zero for a 10% internal rate of return.

Table 4. Economic assumptions for TEA

| Economic Parameters | Assumed Basis |
|---|---|
| **Basis year for analysis** | 2016 |
| **Debt/equity for plant financing** | 60%/40% |
| **Interest rate and term for debt financing** | 8%/10 years |
| **Internal rate of return for equity financing** | 10% |
| **Total income tax rate** | 21% |
| **Plant life** | 20 years (Case 1, dry-mill facilities)<br>30 years (Cases 2, 3, and 4) |
| **Construction period** | 3 years |
| **Fixed capital expenditure schedule (years 1–3)** | 32% in year 1, 60% in year 2, 8% in year 3 |
| **Startup time** | 0.5 years |
| **Revenues during startup** | 50% |
| **Variable costs during startup** | 75% |
| **Fixed costs during startup** | 100% |
| **Site development cost** | 9% of inside battery limit, total installed cost |
| **Warehouse** | 1.5% of inside battery limit |
| **Indirect Costs** | % of total direct costs |
| **Prorated expenses** | 10% |
| **Home office and construction fees** | 25% |
| **Field expenses** | 10% |
| **Project contingency** | 10% |
| **Other costs (startup and permitting)** | 10% |
| **Fixed operating cost** | Assumed basis |

### 2.2.1 Carbon Capture and Sequestration Assumptions

CCS was introduced to several cases as a high-technology-readiness-level (TRL) carbon abatement strategy. In cases where a high-purity $CO_2$ stream was readily available, CCS was treated as a bolt-on system comprising compression, drying, and final sequestration. If the purity of the $CO_2$-containing stream was not enough for sequestration, an amine purification system was added on. The design and economic assumptions for the amine scrubber were determined based on the system described in the acid-gas removal system of the National Renewable Energy Laboratory's indirect liquefaction design report [15]. The base case design for Case 1 and Case 2 both contained nearly pure $CO_2$ streams (>99%) from fermentation offgases; thus, CCS was used to sequester carbon from those streams. Similarly, Case 3 also contained a high-purity $CO_2$ stream from the acid-gas removal step required to condition syngas prior to fuel synthesis. This $CO_2$ stream was chosen as the sequestration stream. Cases 2, 3, and 4 also had low-concentration flue gas streams; however, since additional cost and complexity would be required to concentrate the $CO_2$ and introduce CCS, these streams were not considered. Therefore, CCS was only used for preexisting high-purity $CO_2$ streams for Cases 1–3. Case 5, however, did not have any pure $CO_2$ streams (excluding the $CO_2$ feedstock), so an amine scrubber and CCS were utilized to capture and sequester $CO_2$ from flue gas in this case.

Costs and performance of the various components of CCS systems were adopted from published engineering studies. Specifically, the energy use for $CO_2$ compression was estimated based on experience at an existing biorefinery [16], and the costs for the required equipment were adapted from the same study. The costs for $CO_2$ sequestration include the costs of drilling and maintaining disposal wells, and the costs of transporting pure compressed $CO_2$ from the biorefinery gate to those wells were adapted from the National Energy Technology Laboratory's analysis [17] (Table 5).

Table 5. Key parameters for CCS

| Parameter | Value |
|---|---|
| Electricity use for $CO_2$ compression | 112 kWh/tonne $CO_2$ |
| $CO_2$ sequestration cost | \$10/tonne $CO_2$ (2016 dollars) |

### 2.2.2 $CO_2$ Electrolysis Assumptions

Electrochemical conversion of $CO_2$ to carbon monoxide (CO) was used as a $CO_2$ mitigation and carbon utilization strategy for four out of the five cases (excluding Case 4) investigated in this assessment. Additionally, Case 5 (DAC $CO_2$ to SAF) utilized $CO_2$ electrolysis to convert a $CO_2$ feedstock to syngas for fuel synthesis. The underlying assumptions for $CO_2$-to-CO electrolysis are presented in this section. The modeled process leveraged key operating parameters including cell voltage, faradaic efficiency, and current density from Ma et al. [18]. In this process, $CO_2$ was reduced to CO over a carbon-nanotube-doped Ag electrocatalyst at a single-pass conversion of $CO_2$ at 43%. A summary of the operating assumptions is given in Table 6.

The required electricity consumption, $E$, in a given period, $t$, is calculated by Equation 1:

$$E = I \cdot V \cdot t = Q \cdot V = \frac{Z \cdot n \cdot F}{\varepsilon_{faradiac}} \cdot V \quad (1)$$

where $I$ is the current, $V$ is the cell voltage, $z$ is the number of required electrons to produce one mole of product ($z$ = 2 to produce CO), $n$ is the number of moles of the given product, $F$ is Faraday's constant, and $Q$ is the total charge passed.

$CO_2$ electrolyzer designs vary significantly in the literature, and thus electrolyzer cost is also highly variable depending on the process design. Since the electrosynthesis of CO from $CO_2$ shares many similarities with $H_2$ synthesis from $H_2O$, the U.S. Department of Energy Hydrogen Analysis (H2A) models were used to establish the cost basis of the modeled $CO_2$ electrolyzer. The electrolyzer installed capital cost was thus set at $600/kW [19].

Table 6. Summary of key metrics for $CO_2$-to-CO electrolysis

| **Metric** | **Assumed Value** | **Reference** |
|---|---|---|
| Cell voltage (V) | 3.0 | [18] |
| Faradaic efficiency (%) | 98.0 | [18] |
| Current density (mA/cm$^2$) | 350.0 | [18] |
| Electrolyzer capital cost ($/kW) | 600.0 | [19] |

# 3. Case Studies

## 3.1 Case 1 – Corn Ethanol

### 3.1.1 Process Design

The total ethanol production capacity in 2019 in the United States was 15,778 million gallons per year, with an operation production capacity of 16,005 million gallons/year [20]. A total of 190 ethanol facilities were in operation and four new facilities were under construction or expansion as of January 2020. With both new facilities and the expansion of existing facilities, the total ethanol production capacity will increase. The average capacity per corn ethanol biorefinery has increased from 31.9 million gallons/year in 1998 to 82.6 million gallons/year as of January 2020 [21]. There are two general types of processing: wet-milling and dry grind. Dry-grind ethanol plants are much more prevalent; more than 91% of U.S. fuel ethanol is produced using the dry-mill process (with the remaining 9% coming from wet mills) [21]. The main difference between the two processes is in the initial treatment of the grain. Dry-grind processes are less capital- and energy-intensive than their wet-mill counterparts. However, they also produce fewer products. Dry-grind plants produce ethanol and animal feed, known as distillers dried grains (DDG) or distillers dried grains with solubles (DDGS). Wet mills, on the other hand, are structured to produce several products, including starch, high-fructose corn syrup, ethanol, corn gluten feed, and corn gluten meal. Wet mills separate starch, protein, and fiber in corn grain prior to processing these components into ethanol and other products. As a result, ethanol yields from wet mills are slightly lower (2.5 gallons per bushel) than from dry-grind processes (2.8 gallons per bushel). Since dry mill is more prevalent, we are modeling the corn ethanol case using the dry-mill technology.

The general process diagram is shown in Figure 2. Corn grain is milled and slurried with water and amylase enzymes. The mixture is cooked and mixed with additional enzyme to complete starch hydrolysis to glucose. The subsequent glucose sugars are fermented to ethanol, $CO_2$, and other minor byproducts using various yeast strains. The ethanol is concentrated and purified through a series of distillation and molecular sieve dehydration steps. The byproduct solids are dewatered and dried through a series of centrifugation, evaporation, and drying steps.

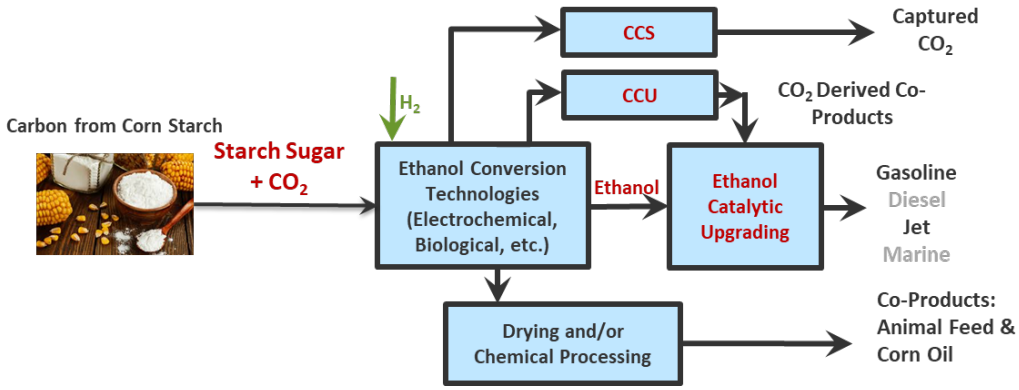


Figure 2. Block flow diagram for the dry-mill ethanol and ethanol-to-hydrocarbon fuel process

After ethanol is dehydrated catalytically to ethylene, the water is removed by a flash drum and a molecular sieve unit as described in literature [22, 23]. The ethylene is then pressurized before entering the oligomerization reactor. In the two-step Ziegler process there are two separate reactions steps [24]. In the first reactor, ethylene oligomerizes by attaching to the recycled and fresh catalyst triethylaluminum at 90°–120°C and 100 bar. In the second reactor, the oligomers are released from the catalyst surfaces with fresh ethylene at 200°–300°C and 10 bar [25]. The oligomers are then separated by the tandem flash tanks and centrifugal separators (details in [24]). The final product are distribution of olefins, which are then hydrotreated to hydrocarbon fuels.

The above conditions were used as the baseline assumptions for each of the Case 1 scenarios. Several scenarios (sub-cases) were introduced to understand the life cycle and economic opportunities and trade-offs for different renewable interventions and process designs. An overview of the sub-cases is given in Table 7. A short description of each intervention and its overall scope and impact follows. Further detail can be found in Sections 2.1 and 2.2.

Table 7. Summary of Case 1 scenarios and key interventions. Fossil $H_2$ refers to $H_2$ derived from fossil NG SMR.

| *Case Number* | *Fermentation $CO_2$* | *Hydrogen* | *Ammonia* | *Notes* |
|---|---|---|---|---|
| *1.1.0* | Vented | Fossil $H_2$ | $NH_3$ | Base case |
| *1.1.1* | Vented | Fossil $H_2$ | $NH_3$ | RE only—feasible today |
| *1.1.2* | Vented | Fossil $H_2$ | $NH_3$ | RE and RNG |
| *1.1.3* | Vented | Renewable $H_2$ | $NH_3$ | RE, RNG, and renewable $H_2$— three proven low-emission technologies. |
| *1.1.4* | Vented | Renewable $H_2$ | GA | All interventions |
| *1.2.0* | CCS | Fossil $H_2$ | $NH_3$ | Base case |
| *1.2.1* | CCS | Fossil $H_2$ | $NH_3$ | RE only—feasible today |
| *1.2.2* | CCS | Fossil $H_2$ | $NH_3$ | RE and RNG |
| *1.2.3* | CCS | Renewable $H_2$ | $NH_3$ | RE, RNG, and renewable $H_2$—three proven low-emission technologies. |
| *1.2.4* | CCS | Renewable $H_2$ | GA | All interventions |
| *1.3.0* | CCU | Fossil $H_2$ | $NH_3$ | Base case—will demonstrate infeasibility of CCU with current grid. |
| *1.3.1* | CCU | Fossil $H_2$ | $NH_3$ | RE only |
| *1.3.2* | CCU | Fossil $H_2$ | $NH_3$ | RE and RNG |
| *1.3.3* | CCU | Renewable $H_2$ | $NH_3$ | RE, RNG, and renewable $H_2$—three proven low-emission technologies. |
| *1.3.4* | CCU | Renewable $H_2$ | GA | All interventions |

Fermentation $CO_2$ capture refers to the practice of diverting the offgas from the fermenter away from its conventional practice of vent to atmosphere, and instead routing that gas to compression and geologic sequestration (CCS) or to an input into an additional chemical conversion process (CCU). Other $CO_2$ emissions from the biorefinery (e.g., from combustion at the steam boilers) are not included in this analysis. Other $CO_2$ emissions from process inputs or product utilization are also not included.

Electricity refers to the life cycle emissions from electricity used at the biorefinery. Electricity use in other parts of the life cycle, such as upstream electricity use in feedstock production, is not included in this analysis, and therefore the RE scenarios do not adjust the carbon intensity of any other process inputs.

Fuel refers only to the fuel used at the biorefinery for process heat. Switching to RNG does not affect the CI of other process or life cycle inputs such as electricity, chemicals, or transportation.

Hydrogen refers only to the hydrogen used as a process input to the ethanol to jet conversion process at the biorefinery. Hydrogen used in the production of ammonia is covered in a separate intervention——green ammonia.

Ammonia refers to both the ammonia used as a process input at the biorefinery and the ammonia used to create fertilizer for feedstock production.

Case 1.1.0 is the base case scenario where the process design is as described above, and no renewable interventions are introduced. Cases 1.1.1, 1.1.2, 1.1.3, and 1.1.4 use either RE, renewable hydrogen, RNG, or a combination of all three renewable inventories. CCS and CCU of fermentation $CO_2$ are considered in case scenarios 1.2.x and 1.3.x, respectively. Note that x refers to scenarios defined in Table 7.

In the CCS case (Case 1.2) we take advantage of the fact that the fermentation $CO_2$ streams are highly concentrated at greater than 90% by mass, and that the impurities in the $CO_2$ are mainly water. Therefore, energy-intensive separation technologies such as amine scrubbers are unnecessary. For simplicity, we model a 100% capture rate by calculating the energetic cost and associated emissions of a multistage $CO_2$ compressor with a suction pressure of 17.4 psia at 81°F and a discharge pressure of 2,214 psia [26]. Assuming a pressure drop of 35 kPa/km (5.07 psia/km) and a minimum outlet pressure of 10.3 MPa (1,494 psia) and excluding elevation, this pressure is sufficient to pump compressed $CO_2$ roughly 140 km. The energetic cost of this process is estimated at 112 kWh/ton $CO_2$ captured.

For CCU scenarios (Case 1.3), $CO_2$ compression for transportation and sequestration is not required assuming conversion to CO through an electrolysis unit. CO is purified from the $CO_2$–CO mixture out of the electrolyzer via pressure-swing adsorption and mixed with imported $H_2$ to create additional syngas with a molar ratio of 2.0 ($H_2$:CO). The syngas is fermented to ethanol, and then $CO_2$-derived ethanol is catalytically upgraded with biomass-derived ethanol.

### 3.1.2 LCA Results and Discussions

*LCA Cases and Inventories*

Figure 3 is the schematic flow diagram showing the supply chain of Case 1, which includes corn farming, corn transportation, ethanol production, jet fuel production, jet fuel transportation and distribution, and jet fuel combustion. Case 1.1 represents base jet fuel production from corn

ethanol, which vents out fermentation $CO_2$ into the atmosphere. In other cases, the fermentation $CO_2$ is captured and sequestrated (Case 1.2) or utilized to produce additional jet fuels (Case 1.3).

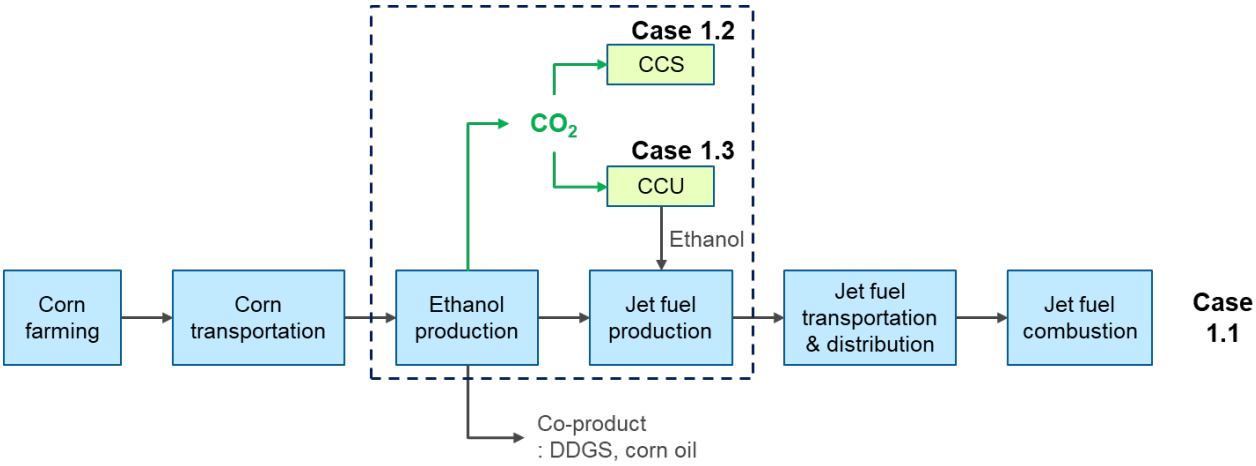


Figure 3. The schematic flow diagram of the supply chain of Case 1, which includes corn farming and transportation, ethanol production, jet fuel production, jet fuel transportation and distribution, and jet fuel combustion. Case 1.2 and Case 1.3 apply CCS and CCU, respectively, for the fermentation $CO_2$ from ethanol production.

Table 8 shows the life cycle inventory of Case 1, which includes energy inputs, materials, and output products per 1 MJ of jet fuel production. The input data are categorized into four processes: ethanol production (corn starch to ethanol), jet production (ethanol upgrading), CCS, and CCU. Each process requires energy and catalyst/chemical inputs. DDGS and corn oil are coproducts from corn ethanol production, which have emission credits by displacing the counterparts (e.g., soybean meal and soy oil). The upstream processes of corn feedstock include energy, fertilizer, pesticide uses for corn farming, and corn transportation [3].

Case 1.1 represents a sustainable jet fuel production pathway from corn starch ethanol without capturing $CO_2$, which requires 0.0046 bushels of corn starch feedstock to produce 1 MJ of jet fuel. Case 1.2 represents the same production pathway as Case 1.1, with the addition of capture of fermentation $CO_2$ and subsequent compression and sequestration of that gas.

In Case 1.3, additional jet fuel is produced by converting captured $CO_2$ into jet fuels; 68% of carbon in jet fuels is from corn ethanol and the remaining 32% is from $CO_2$-derived ethanol. Therefore, Case 1.3 needs less corn starch input (0.0031 bushels) and less energy/material inputs per megajoule for ethanol production compared to Case 1.1, whereas the CCU process needs additional energy and material inputs to capture fermentation $CO_2$ and convert it to ethanol. Similarly, coproducts per megajoule of jet fuel production for Case 1.3 are reduced due to higher jet fuel production. Note that $CO_2$-derived ethanol enters to the jet production process at a lower temperature and lower purity condition compared to corn ethanol, which requires more NG inputs to heat up, separate from water, and purify ethanol compared to Case 1.1.

Table 8. Life cycle inventory of Case 1: jet fuels from corn starch ethanol (Case 1.1) with CCS (Case 1.2) or CCS (Case 1.3). Note that all corn farming parameters rely on GREET.

| [per MJ of jet fuel] | | Unit | Case 1.1 | Case 1.2 | Case 1.3 |
|---|---|---|---|---|---|
| **Ethanol production** | Corn starch (15% moisture) | bushel | 0.0046 | 0.0046 | 0.0031 |
| | Electricity | kWh | 0.012 | 0.012 | 0.008 |
| | NG | MJ | 0.42 | 0.42 | 0.29 |
| | Catalysts/chemicals | g | 0.88 | 0.87 | 0.60 |
| **Jet production** | Electricity | kWh | 0.01 | 0.01 | 0.01 |
| | NG | MJ | 0.07 | 0.06 | 0.08 |
| | $H_2$ | MJ | 0.06 | 0.065 | 0.06 |
| | Catalysts/chemicals | g | 0.01 | 0.01 | 0.01 |
| **CCS** | Electricity | kWh | N/A | 0.004 | N/A |
| | NG | MJ | N/A | N/A | N/A |
| | Catalysts/chemicals | g | N/A | N/A | N/A |
| **CCU ($CO_2$ to ethanol)** | Electricity | kWh | N/A | N/A | 0.06 |
| | NG | MJ | N/A | N/A | 0.12 |
| | $H_2$ | MJ | N/A | N/A | 0.34 |
| | Ammonia | g | N/A | N/A | 0.08 |
| | Other catalysts/chemicals | g | N/A | N/A | 0.57 |
| **Coproduct (output)** | DDGS | g | 29.5 | 28.6 | 20.0 |
| | Corn oil | g | 1.6 | 1.6 | 1.1 |

*LCA Results*

Figure 4 shows life cycle GHG emissions (i.e., CI) of Case 1. Each bar represents the GHG emissions of each contributor defined in the legend. The groups of green, purple, blue, red, and yellow bars represent the GHG emissions of the corn farming, corn ethanol production, jet fuel production, CCU, and CCS, respectively. The net GHG emissions are indicated as black dots, which are the sum of GHG emissions of each process. For jet fuel combustion GHG emissions, only $CH_4$ and $N_2O$ emissions of 0.3 $gCO_2e/MJ$ are accounted for, while $CO_2$ emissions are considered carbon neutral.

For Cases 1.1.0–1.1.3, GHG emissions regarding the corn feedstock production remain the same as 26.8 $gCO_2e/MJ$ with the contribution of 31.9, 7.9, and −12.9 $gCO_2e/MJ$ for corn farming, LUC, and coproduct credits, respectively, which are not changed by the CI reduction strategies in the biorefinery. For Case 1.1.4, GHG emissions regarding the corn feedstock production are 20.8 $gCO_2e/MJ$ because green ammonia is used as a fertilizer for corn farming. Case 1.1.0 produces jet fuel from corn starch using conventional energy sources (i.e., grid electricity, fossil NG, $H_2$ from fossil NG SMR). With this condition, the corn-to-ethanol process and jet fuel production process have GHG emissions of 35.6 and 15.9 $gCO_2e/MJ$, respectively.

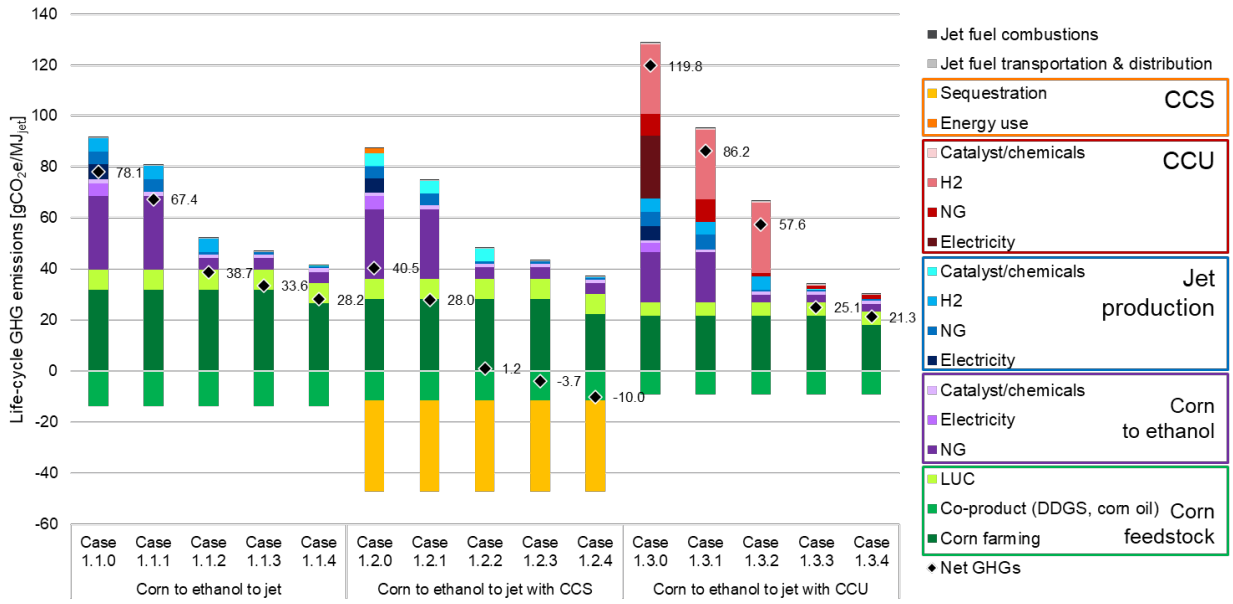


Figure 4. Life cycle GHG emissions ($gCO_2e/MJ$) of jet from corn starch ethanol (baseline). With the fermentation $CO_2$, Cases 1.2.0–1.2.4 and Cases 1.3.0–1.3.4 implement additional CCS and CCU, respectively.

For Cases 1.1.1–1.1.4, the incremental use of renewable electricity, landfill gas RNG, renewable $H_2$, and green ammonia—respectively replacing grid electricity, fossil NG, $H_2$ from NG SMR, and conventional ammonia—reduce the jet fuel CIs by 10.7, 28.7, 5.1, and 3.4 $gCO_2e/MJ$, respectively. The net GHG emission ranges of Cases 1.1.0–1.1.4 become 28.2–78.1 $gCO_2e/MJ$, which are 7%–67% lower compared to the CI of conventional jet fuel (84.5 $gCO_2e/MJ$).

In Cases 1.2.0–1.2.4, we added carbon capture and sequestration. While $CO_2$ emissions of 35.9 $gCO_2e/MJ$ are captured in each of these cases, additional electricity use of 0.004 kWh/MJ for CCS leads to an increase of 1.9 $gCO_2e/MJ$ for Case 1.2.0, resulting in a net reduction of 34 $gCO_2e/MJ$ compared to Case 1.1.0. Small differences in the total carbon intensity stem from independent analysis by different parts of the team for the cases with and without carbon capture and sequestration. Subsequent cases, which use RE to power compression as well as ethanol and conversion steps, reflect the full 35.9-g/MJ reduction.

In Cases 1.3.0–1.3.4, corn starch ethanol to jet with CCU, 68% of jet fuel is produced from corn starch feedstock, while the remaining 32% is from fermentation $CO_2$. As the corn feedstock input is reduced by 32% per megajoule of fuel compared to Case 1.1, corn feedstock and starch ethanol production-related GHG emissions also decrease by 32%. However, due to significant energy and material demand for CCU converting $CO_2$ into jet fuels, the CI of Case 1.3.0 becomes 1.4 times higher (119.8 $gCO_2e/MJ$) even compared to conventional petroleum jet fuels (84.5 $gCO_2e/MJ$). For the CCU process, GHG emissions from conventional energy systems can be reduced by 27.3, 24.4, and 7.3 $gCO_2e/MJ$ by using renewable $H_2$, renewable electricity, and landfill gas, respectively. The impact of catalyst/chemical inputs for CCU is as small as 0.4

$gCO_2$/MJ in Cases 1.3.0–1.3.3, among which 3.8 $gCO_2e$/MJ is further reduced by using green ammonia as in Case 1.3.4. As a result, the CI of the best case of CCU (Case 1.3.4) would be 75% lower than that of the petroleum jet fuel baseline.

### 3.1.3 TEA Results

*MFSP*

A summary of the MFSP results and cost contribution breakdown is given in Figure 5. The TEA results for Case 1 include MFSP and carbon efficiency. The TEA results also include sensitivity assessments around the costs of electricity, hydrogen, and natural gas, where applicable.

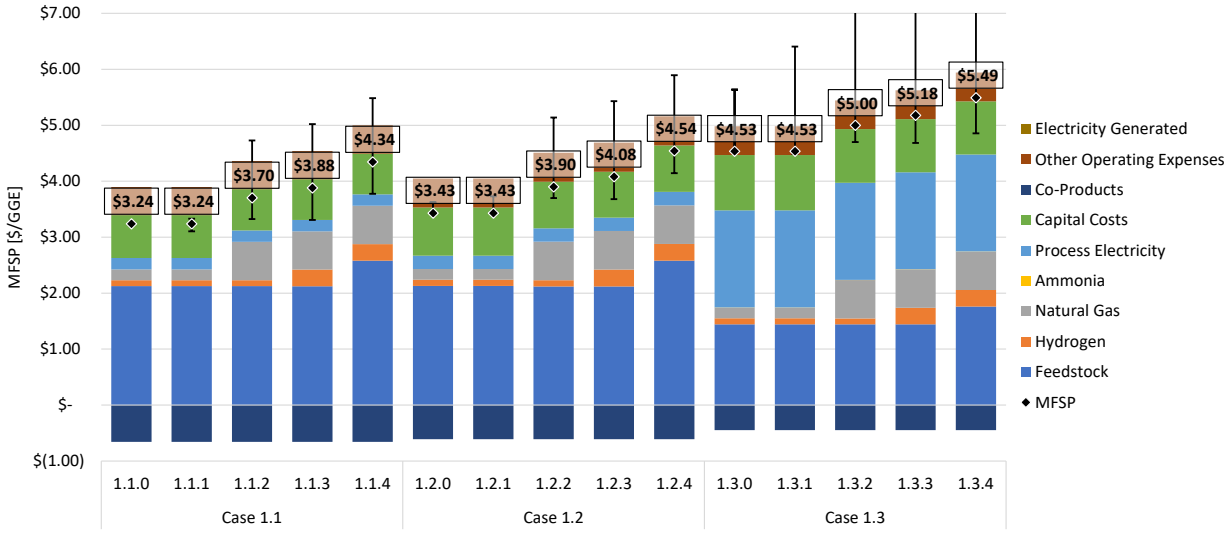


Figure 5. MFSP cost contribution breakdown of Case 1 scenarios in dollars per gallon gasoline equivalent (GGE)

The base case scenario (Case 1.1.0) for the conversion of corn sugar to SAF resulted in an MFSP of $3.24/GGE with a total fuel yield of 25.1 million GGE per year. A coproduct credit of $0.60/GGE was obtained through the sale of the DDGS coproduct. Of the total MFSP, about $1.34/GGE was attributed to capital costs and $2.13/GGE was attributed to corn grain. The total capital investment (TCI) of the base case was nearly $142 million.

Cases 1.1.2 and 1.1.3 use renewable electricity and RNG. The base case scenario with all green interventions (i.e., renewable electricity and RNG) results in an increased MFSP of $3.70/GGE due to higher operating cost for RNG. Another portion of the increase is due to the high baseline cost of green $H_2$, which contributes a total of $3.88/GGE versus only $3.24/GGE in Case 1.1.0.

In Case 1.1.4, we calculated the MFSP for fuel produced with renewable electricity, renewable natural gas, and renewable hydrogen as process inputs. We additionally analyzed the effects of using renewable ammonia, both as a process input at the biorefinery and as an input into the manufacturing of fertilizer for feedstock production. The net GHG and cost impacts of

ammonia as a process input in Cases 1.x.x is negligible, as the quantity of ammonia consumed is very small. However, because corn grain is extensively fertilized in the United States, and because fertilizer is estimated to be about 17% of the cost of producing corn [27], switching to renewable ammonia will have large CI and cost impacts. With an increase in ammonia costs from $0.59/kg to $1.37/kg, we estimate that the feedstock cost for corn grain will escalate from $3.61/bushel to $4.41/bushel. This translates to an MFSP increase of approximately $0.46/GGE.

Case 1.2 assessed the cost of implementing CCS technology to sequester carbon from fermentation offgas. The CCS scenario did not impact the overall fuel yield relative to the base case. The additional costs primarily stem from compression and dehydration capital expenses (estimated to be $9 million), compression power requirements, and the cost of final $CO_2$ storage, estimated to be $10/tonne $CO_2$, which was treated as an operating expense. Since the baseline cost for renewable electricity is assumed to be equal to current grid costs, CCS expenses increased the MFSP to $3.43/GGE in both the gray electricity and renewable electricity scenarios. This $0.19/GGE increase in MFSP, combined with the 35.9-g/MJ CI reduction, corresponds to a cost of carbon abatement of $40.18/tonne $CO_2$. This represents an increase over our fiscal year 2020 estimate of the cost of CCS due to fiscal year 2021's inclusion of sequestration costs, as well as other small adjustments to our analysis and assumptions. This analysis does not consider incentives or credits for $CO_2$ storage. The existing 45Q tax credit at $50/tonne would change the $10/tonne $CO_2$ disposal cost to a $40/tonne $CO_2$ byproduct credit. The cost curve for carbon abatement in Case 1.2.x is shown in Figure 6. Note that x refers to scenarios defined in Table 7.

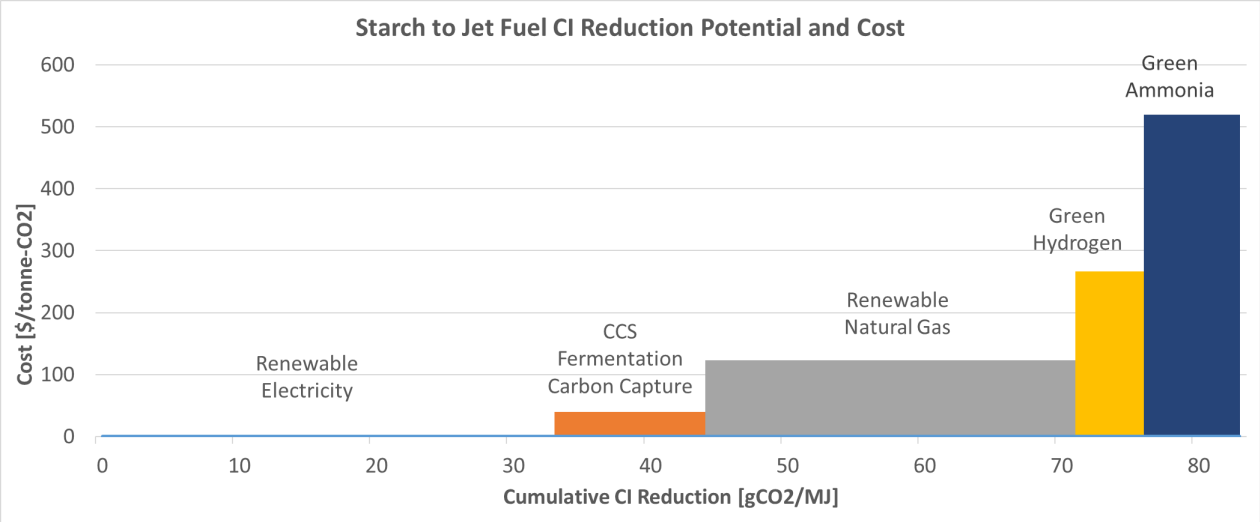


Figure 6. Cost and CI reduction potential of RE, CCS, RNG, green $H_2$, and GA for the starch-to-SAF pathway

Case 1.3 reincorporated acid gas removal (AGR) $CO_2$ into the final fuel product through electrosynthesis of $CO_2$ to CO. Reincorporating carbon lost from fermentation offgas via electrolysis and syngas formation increased the fuel yield significantly from 25.1 million GGE per year (Case 1.1.0) to 37.0 million GGE per year. However, the addition of the electrolyzer

incurred significant capital expenses, nearly doubling the TCI from $142 million in the base case to $271 million. $H_2$ and electricity costs also contributed significantly to the MFSP in Case 1.3, as shown in Figure 5.

### 3.1.4 Key Learnings

Cases 1.1–1.3 represent SAF production pathways whose "front end" (conversion of corn to ethanol) is based on mature technology that has been commercialized for decades. The "back end" of the process, conversion of ethanol to jet fuels via a catalytic upgrading process, has been demonstrated at pilot scale but is not yet commercial. In fact, there are numerous ethanol-to-jet processes in development, including multistep and single-step variants that have differing capital and operating requirements and different needs for electricity, hydrogen, and process heat (supplied by natural gas or otherwise). The numerical results of the TEA and LCA presented here are specific to a single-step process, but the trends can be generalized to many processes that could be "bolted onto" or integrated with existing corn ethanol biorefineries.

*Key Learnings – LCA*

- Conventional aviation fuel has a carbon intensity of 84.5 $gCO_2e/MJ$ [3]. Our analysis shows that the baseline configuration of corn ethanol to SAF with conventional inputs (Case 1.1.0) decreases the CI of aviation fuel by 7% to 78.1 g/MJ. Our subsequent cases explore changes to the process that can bring this pathway closer to net-zero GHG emissions.

- Low carbon "interventions" in the inputs to farming (fertilizer, or "green ammonia"), process heat in the ethanol production and upgrading stages ("green hydrogen" for the latter and RNG for both), and use of renewable electricity across the entire production chain have the potential to significantly decrease the CI of jet fuel production. Cases 1.1.1–1.1.4 explore these interventions and conclude that the CI can be further reduced to 28.2 g/MJ, which is a 64% decrease over conventional aviation fuel. These further interventions, representing decarbonized electricity, heat, and hydrogen, demonstrate that a substantial fraction of the CI of corn-derived jet fuels comes from process inputs.

- Much deeper decarbonization is possible by intercepting carbon emissions from the fuel production process. Over 35 g/MJ is emitted from the fermenter in the ethanol production step. When this carbon is captured, compressed, and injected into the subsurface for permanent storage, the corn-to-SAF pathway can achieve net-zero emissions.

- Another strategy for reducing the overall CI of the process is to divert carbon (in the form of $CO_2$) from the fermenter and energetically upgrade it to fuel. This strategy results in a much higher carbon efficiency for the integrated process, and therefore far more fuel per unit feedstock. In this approach, represented by Cases 1.3.0–1.3.4,

upstream emissions from feedstock production are reduced. However, emissions associated with process inputs such as electricity and hydrogen are very high because the $CO_2$ upgrading process is far more energy-intensive than ethanol production and upgrading. Finally, because feedstock and other upstream emissions cannot be completely eliminated, and there is no carbon removal in this case, the process is not capable of reaching net zero. It is, however, a demonstration of how biomass and non-carbon renewable energy (wind and solar) can be combined to deliver a low-CI carbon-based fuel from limited feedstock.

*Key Learnings – TEA*

- While this analysis does not compare the baseline cost of corn SAF to conventional fuel, it does demonstrate that going from a 20% CI reduction to a 64% CI reduction through the use of more sustainable process inputs is likely achievable at modest cost escalation of $0.64 over the $3.24/GGE baseline price in Case 1.1.0.

- The cost for incorporating CCS is estimated to increase the MFSP by $0.19/GGE. This approach is explored in Cases 1.2.0–1.2.4, which demonstrate an approach to, and eventual achievement of, net zero.

- Incorporating CCU into this process is very cost-intensive. The benefits of improving the carbon efficiency of feedstock utilization are offset by the carbon intensity of most other process inputs unless significant effort is made to decarbonize electricity, hydrogen, natural gas, and fertilizer.

# 3.2 Case 2 – Corn Stover Ethanol

### 3.2.1 Process Design

Second-generation biofuel refers to the biofuel produced from non-food biomass, mostly from lignocellulosic plant materials and waste residues. Lignocellulosic feedstocks include agricultural residues (rice/wheat straw, corn stover, sugarcane baggage), herbaceous crops (switchgrass, alfalfa), wood chips, forest residues, municipal solid waste, paper waste, etc. In lignocellulosic biomass, lignin, hemicellulose, and cellulose create a tightly bonded lignin–carbohydrate structure that is recalcitrant to enzymatic degradation. Cellulosic ethanol production thus requires complex pretreatment of biomass to make the cellulose accessible for the enzymes.

The corn stover ethanol design (Figure 7) uses dilute acid pretreatment followed by enzymatic hydrolysis and co-fermentation with recombinant *Zymomonas mobilis*. The corn stover is first treated with dilute sulfuric acid catalyst at a high temperature (190°C) for a short time (average at 2 minutes), liberating the hemicellulose sugars and other compounds. Before going into enzymatic hydrolysis, proper conditioning is required for acid neutralization and detoxification prior to the biological portions of the process. Detoxification is only applied to the liquor fraction of the pretreated biomass and not the solids. Solids from pretreatment will be internally washed before being remixed with the detoxified liquor for saccharification and fermentation. A purchased cellulase enzyme is added to the hydrolyzate at an optimized temperature for enzyme activity. If saccharification and fermentation steps are conducted at different temperatures, a cooling step is required to ensure growth of fermenting organism *Zymomonas mobilis* at anaerobic conditions. Several days (total 3 to 7 days) are required to convert most of the cellulose and xylose to ethanol. The “beer” liquor with approximately 4–8 wt % ethanol is then sent to recovery and purification, which uses standard adsorption technology. The solids after fermentation are separated and combusted in a fluidized bed combustor to produce high-pressure steam for electricity credits and process heat. After ethanol is recovered and purified, ethanol is catalytically upgraded to hydrocarbon fuels using a similar design described in Section 3.1.1. Ethanol is dehydrated catalytically to ethylene, then oligomerized and hydrotreated to hydrocarbon fuels.

The above conditions were used as the baseline assumptions for each of the Case 2 scenarios. Several scenarios (sub-cases) were introduced to understand the life cycle and economic opportunities and trade-offs for different renewable interventions and process designs. An overview of the sub-cases is given in Table 9.

Case 2.1.0 is the base case scenario where the process design is as described above, and no renewable interventions are introduced. Cases 2.1.1, 2.1.2, and 2.1.3 use either RE, renewable $H_2$, RNG, or a combination of all three renewable inventories. CCS and CCU of fermentation $CO_2$ are considered in Cases 2.2.x and 2.3.x, respectively. Note that x refers to scenarios defined in Table 9.

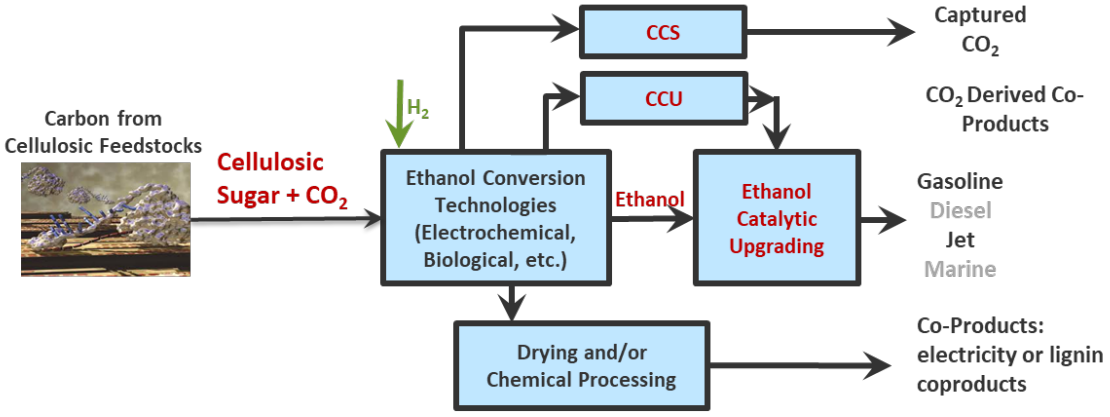


Figure 7. Block flow diagram for the corn stover ethanol and ethanol-to-hydrocarbon fuel process

Table 9. Summary of Case 1 scenarios and key interventions

| Case Number | Fermentation $CO_2$ | Electricity | Hydrogen | Ammonia | Notes |
|---|---|---|---|---|---|
| 2.1.0 | Vented | U.S. mix | Fossil $H_2$ | $NH_3$ | Base case |
| 2.1.1 | Vented | RE | Fossil $H_2$ | $NH_3$ | RE only |
| 2.1.2 | Vented | RE | Renewable $H_2$ | $NH_3$ | RE and renewable $H_2$ |
| 2.1.3 | Vented | RE | Renewable $H_2$ | GA | All interventions |
| 2.2.0 | CCS | U.S. mix | Fossil $H_2$ | $NH_3$ | Base case |
| 2.2.1 | CCS | RE | Fossil $H_2$ | $NH_3$ | RE only |
| 2.2.2 | CCS | RE | Renewable $H_2$ | $NH_3$ | RE and renewable $H_2$ |
| 2.2.3 | CCS | RE | Renewable $H_2$ | GA | All interventions |
| 2.3.0 | CCU | U.S. mix | Fossil $H_2$ | $NH_3$ | Base case |
| 2.3.1 | CCU | RE | Fossil $H_2$ | $NH_3$ | RE only |
| 2.3.2 | CCU | RE | Renewable $H_2$ | $NH_3$ | RE and renewable $H_2$ |
| 2.3.3 | CCU | RE | Renewable $H_2$ | GA | All interventions |

In Case 2.2.x, we take advantage of the relatively pure $CO_2$ stream from the fermentation process with a CCS process that immobilizes $CO_2$ from the biorefinery that would otherwise be emitted to the atmosphere. Note that we do not consider capturing combustion emissions of corn stover in this study. The $CO_2$ from fermentation is produced at a purity greater than 90%, with most of the balance being easily removable water vapor [26]. Therefore, energy-intensive separation technologies such as amine scrubbers are unnecessary. For simplicity, we model a 100% capture rate by calculating the energetic cost and associated emissions of a multistage $CO_2$ compressor with a suction pressure of 17.4 psia at 81°F and a discharge pressure of 2,214 psia [26]. Assuming a pressure drop of 35 kPa/km (5.07 psia/km) and a minimum outlet pressure of 10.3 MPa (1,494 psia) and excluding elevation, this pressure is sufficient to pump compressed $CO_2$ roughly 140 km. The energetic cost of this process is estimated at 112 kWh/ton $CO_2$ captured [16, 26]. Case 2.2.0 applies CCS to the system assessed in Case 2.1.0 (cellulosic ethanol to jet fuel operated on today's grid, with fossil natural gas for process heat, conventional

hydrogen as an ethanol-upgrading feedstock, and conventional ammonia as a chemical reagent). CCS results in a 37.6-g$CO_2$/MJ CI reduction. Case 2.2.1 operates this same system on an electric grid that is GHG-free (renewable electricity case).

Similar to the corn starch cases explored in Case 1, Case 2.2.x represents the same production pathway as Case 2.1, with the addition of capture of fermentation $CO_2$ and subsequent compression and sequestration of that gas. Note that x refers to scenarios defined in Table 9. Removal and storage of this biogenic GHG before it reaches the atmosphere reduces the CI of the cellulosic pathway by nearly 40 g/MJ. For CCU scenarios (Case 2.3), the captured $CO_2$ is routed through an electrolysis unit and electrochemically converted to CO, similar to Case 1. CO is purified from the $CO_2$–CO mixture out of the electrolyzer via pressure-swing adsorption and mixed with imported $H_2$ to create additional syngas with a molar ratio of 2.0 ($H_2$:CO). The syngas is then fermented to ethanol. After ethanol is recovered and purified, ethanol is catalytically upgraded using similar catalytic upgrading to hydrocarbon fuels.

### 3.2.2 LCA Results and Discussions

*LCA Cases and Inventories*

Figure 8 is the schematic flow diagram of Case 2, jet fuel production from corn stover ethanol, which has a very similar system boundary compared to Case 1 except that Case 2 uses corn stover whereas Case 1 uses corn starch. We assumed that corn stover is a waste product of corn production. GHG emissions from the corn farming stage belong to corn starch as in Case 1, whereas corn stover is a residue after corn starch harvest. Thus, the life cycle pathways of Case 2.1 start from corn stover collection followed by stover transportation, cellulosic ethanol production, jet fuel production, jet fuel transportation and distribution, and fuel combustion. In addition, fermentation $CO_2$ is captured and sequestrated in Case 2.2 or utilized for additional jet fuel production as in Case 2.3. Note that corn starch takes all the $CO_2$ emissions from LUC of corn farming, while additional land management practices for corn stover harvesting bring LUC credits of −50 g$CO_2$e per gallon of ethanol.

Table 10 shows the energy and material inputs and outputs of Case 2. The input life cycle inventory data are categorized into four groups: corn stover to ethanol, jet production (ethanol upgrading), CCS, and CCU. Note that we rely on GREET for corn stover collection and transportation. Case 2.1 represents the base case of jet fuel production from corn stover ethanol. For each megajoule of jet fuel production, 150 g (dry) corn stover is needed. During ethanol production, corn stover is used not only as the feedstock of the jet fuel, but also as the process fuel. A portion of corn stover inputs is burned to supply heat and electricity demand for the ethanol and jet production processes. Ethanol production from corn stover in Case 2.1 consumes catalysts and chemicals: 4.0 g sulfuric acid, 3.3 g glucose, 1.8 g corn steep liquor, 1.4 g caustic, 0.9 g lime, 0.62 g ammonia, and 0.4 g other catalysts/chemicals per megajoule of jet fuel production. Because corn stover provides sufficient heat and electricity, there are no external electricity or NG inputs in the ethanol and jet fuel production. In addition, the remaining 0.08 kWh of electricity from corn stover is assumed as a coproduct that displaces grid electricity (U.S. grid mix). Note that based on

discussion with the National Renewable Energy Laboratory, Argonne National Laboratory has updated the parameters regarding corn stover ethanol production pathways in GREET 2021: ethanol yield, coproduced electricity, and catalysts/chemicals inputs.

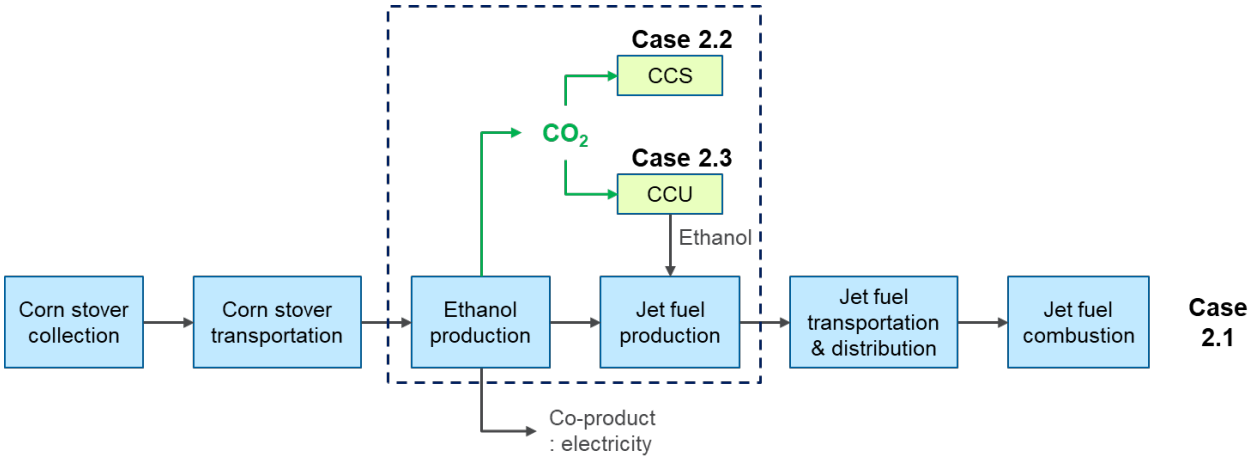


Figure 8. The schematic flow diagram of the supply chain of Case 2, which includes corn stover collection and transportation, ethanol production, jet fuel production, jet fuel transportation and distribution, and jet fuel combustion. Cases 2.2 and 2.3 apply CCS and CCU, respectively, for the fermentation $CO_2$ from ethanol production.

Table 10. Life cycle inventory of Case 2: jet fuels from corn stover ethanol (Case 2.1) with CCS (Case 2.2) or CCS (Case 2.3). Note that all corn stover collection parameters rely on GREET.

| [per MJ of jet fuel] | | Unit | Case 2.1 | Case 2.2 | Case 2.3 |
|---|---|---|---|---|---|
| **Ethanol production** | Corn stover (dry) | g | 150 | 150 | 102 |
| | Ammonia | g | 0.62 | 0.62 | 0.42 |
| | Other catalysts/chemicals | g | 11.7 | 11.7 | 7.9 |
| **Jet production** | $H_2$ | MJ | 0.06 | 0.6 | 0.06 |
| | Catalysts/chemicals | g | 0.01 | 0.01 | 0.01 |
| **CCS** | Electricity | kWh | N/A | 0.004 | N/A |
| | Catalysts/chemicals | g | N/A | N/A | N/A |
| **CCU ($CO_2$ to ethanol)** | Electricity | kWh | N/A | N/A | 0.06 |
| | $H_2$ | MJ | N/A | N/A | 0.34 |
| | Ammonia | g | N/A | N/A | 0.08 |
| | Other catalysts/chemicals | g | N/A | N/A | 0.57 |
| **Coproduct** | Electricity | kWh | 0.008 | 0.004 | N/A |

In Cases 2.2.0–2.2.3, carbon dioxide from the fermentation step is captured, compressed, and sequestered. While $CO_2$ emissions of 35.9 $gCO_2e$/MJ are captured in each of these cases, 0.004 kWh/MJ is required in each of these cases for $CO_2$ compression. In Case 2.2.0, this represents a reduction in renewable electricity that can be sold to the grid as a byproduct and that would displace conventional electricity. Therefore, in Case 2.2.0, there is a reduction of 1.9 $gCO_2e$/MJ in byproduct CI credit, resulting in a net reduction of 34 $gCO_2e$/MJ. Subsequent cases, in which the biorefinery is connected to a fully renewable grid, reflect the full 35.9-g/MJ reduction.

Case 2.3 generates additional jet fuel from captured fermentation $CO_2$-derived ethanol along with corn stover ethanol. The corn stover inputs of 102 g (dry) is used to produce 0.68 MJ of jet fuel, while an additional 0.32 MJ of jet fuel is produced from captured fermentation $CO_2$ through CCU. Thus, Case 2.3 needs less corn stover input per megajoule of jet production, which requires additional energy and material inputs for CCU (i.e., 0.06 MJ of electricity and 0.34 MJ of $H_2$). In this study, only fermentation $CO_2$ is considered, not corn stover combustion emissions. Coproduced electricity from corn stover ethanol production is consumed for CCU, so there is no excess electricity in Case 2.3.

*LCA Results*

Figure 9 shows the life cycle GHG emissions of jet fuel produced from corn stover ethanol. The GHG contributions are categorized and colored based on their specific processes: corn stover feedstock (green), corn stover to ethanol (blue), jet fuel production (purple), CCU (red), and CCS (yellow). For all the cases, $CO_2$ emissions from jet fuel combustion are offset by biogenic carbon uptake; there are only 0.2 $gCO_2e/MJ$ of GHG emissions from $CH_4$ and $N_2O$ emissions. Transportation and distribution of jet fuel generates an additional 0.3 $gCO_2e/MJ$.

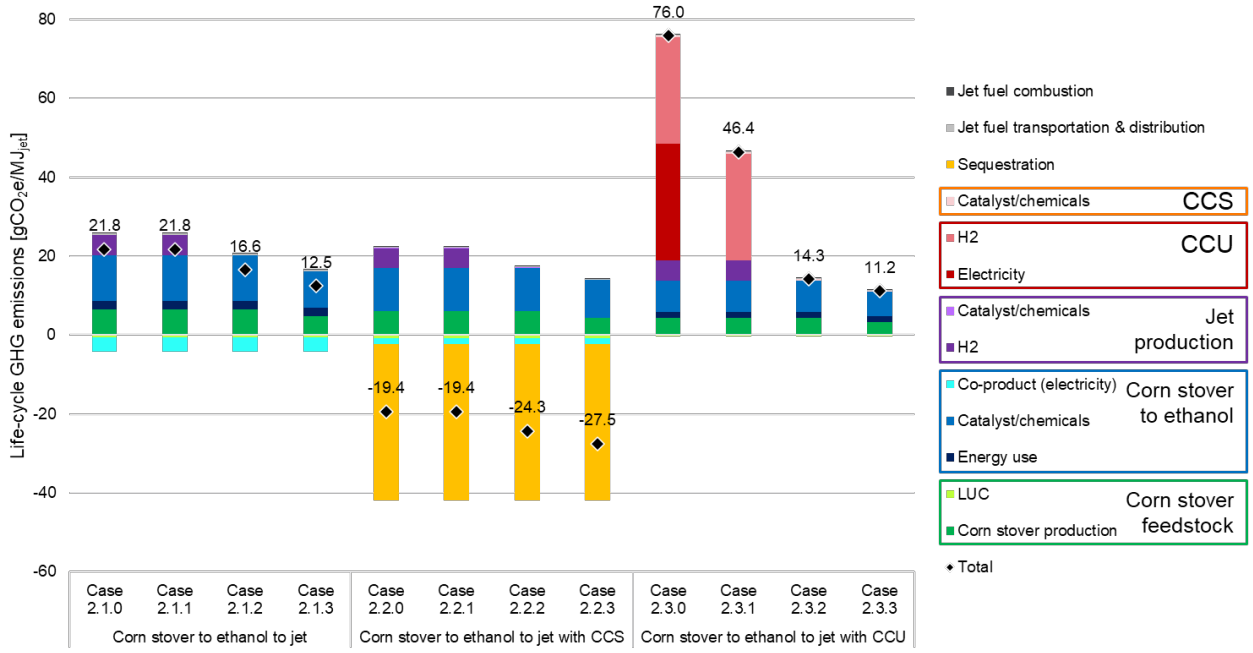


Figure 9. Life cycle GHG emissions ($gCO_2e/MJ$) of jet fuel production from corn stover ethanol. Cases 2.3.0–2.3.3 implement additional CCU with the fermentation $CO_2$.

The CI of Case 2.1.0 is 21.8 $gCO_2e/MJ$, which is 74% lower than conventional jet fuel (CI of 84.5 $gCO_2e/MJ$). This is also 72% lower than Case 1.1.0, with the CI of 78.1 $gCO_2e/MJ$ mainly because corn stover does not take energy use and emissions burdens of corn farming. In addition, there are additional GHG emissions from LUC of corn starch in Case 1.1.0, whereas the impact of LUC of corn stover is −0.7 $gCO_2e/MJ$ due to the GHG sequestration of land management practices for corn stover harvesting. The number is led by a small increase in forest lands resulting

in carbon sequestration, which is slightly higher than the emission impact of conversion of cropland pasture to corn agriculture [28]. For Case 2.1.0, the largest GHG emissions come from catalyst/chemical inputs for the corn-stover-to-ethanol process (11.7 $gCO_2e/MJ$), followed by corn stover production (6.5 $gCO_2e/MJ$), $H_2$ for jet fuel production (5.1 $gCO_2e/MJ$), and others during corn stover to ethanol (2.1 $gCO_2e/MJ$). Note that the corn stover production results in emissions by energy inputs for corn stover field treating, drying, collection and handling, and additional fertilizer use. Meanwhile, the jet fuel gets −3.5 $gCO_2e/MJ$ of credits from coproduced electricity displacing grid electricity. Furthermore, as there is no electricity input, the results of Case 2.1.1 are the same as Case 2.1.0. In Cases 2.1.2 and 2.1.3, renewable $H_2$ and green ammonia reduce the CIs by 5.1 and 4.1 $gCO_2e/MJ$, respectively.

The cost and CI of Case 2.2.1 are the same as Case 2.2.0 because our baseline assumption for renewable electricity is that it costs the same as conventional electricity, and because the cellulosic biorefinery is a net exporter of renewable electricity. Case 2.2.2 assesses the net carbon benefit of supplying the ethanol upgrading process with renewable hydrogen, which results in a CI reduction of 4.8 $gCO_2/MJ$. Case 2.2.3 assesses the impact of supplying the ethanol production process with green ammonia (ammonia produced with minimal GHG emissions), which results in a further CI reduction of 1.4 $gCO_2/MJ$. This is a much lower reduction in CI than the 1.x.x green ammonia cases because ammonia use in the cellulosic cases is confined to small quantities of chemical reagents in the biorefinery, whereas ammonia use in the starch cases is attributed to large quantities used as fertilizer.

The CI of Case 2.2.0 is −19.4 $gCO_2e/MJ$, which is 41.1 g lower than Case 2.1.0 due to the reduction provided by CCS and is already carbon negative. Further CI-reducing interventions such as green hydrogen and green ammonia can push the CI even further into negative territory.

In Case 2.3.0, compared to Case 2.1.0, 32% of jet fuel is produced from captured $CO_2$, which leads to 32% GHG emissions reduction associated with feedstock production/transportation and ethanol production. However, the total GHG emissions increase to 76.0 $gCO_2e/MJ$ due to the use of grid electricity and NG SMR $H_2$ for converting $CO_2$ into jet fuels through CCU. Using renewable electricity reduces 29.6 $gCO_2e/MJ$ in Case 2.3.1. Using renewable $H_2$ further reduces 27.0 $gCO_2e/MJ$ from the CCU process and 5.1 $gCO_2e/MJ$ from the jet production process. Along with the impact of green ammonia in Case 2.3.3, the CI becomes 11.4 $gCO_2e/MJ$, which is 87% lower than the CI of petroleum jet fuels (84.5 $gCO_2e/MJ$).

### 3.2.3 TEA Results and Discussions on Key Metrics (Carbon Efficiency, Energy Efficiency, and Cost)

A summary of the MFSP results and cost contribution breakdown is given in Figure 10. The TEA results for Case 2 include MFSP and carbon efficiency. The TEA results also include sensitivity assessments around the costs of electricity, hydrogen, and natural gas, where applicable.

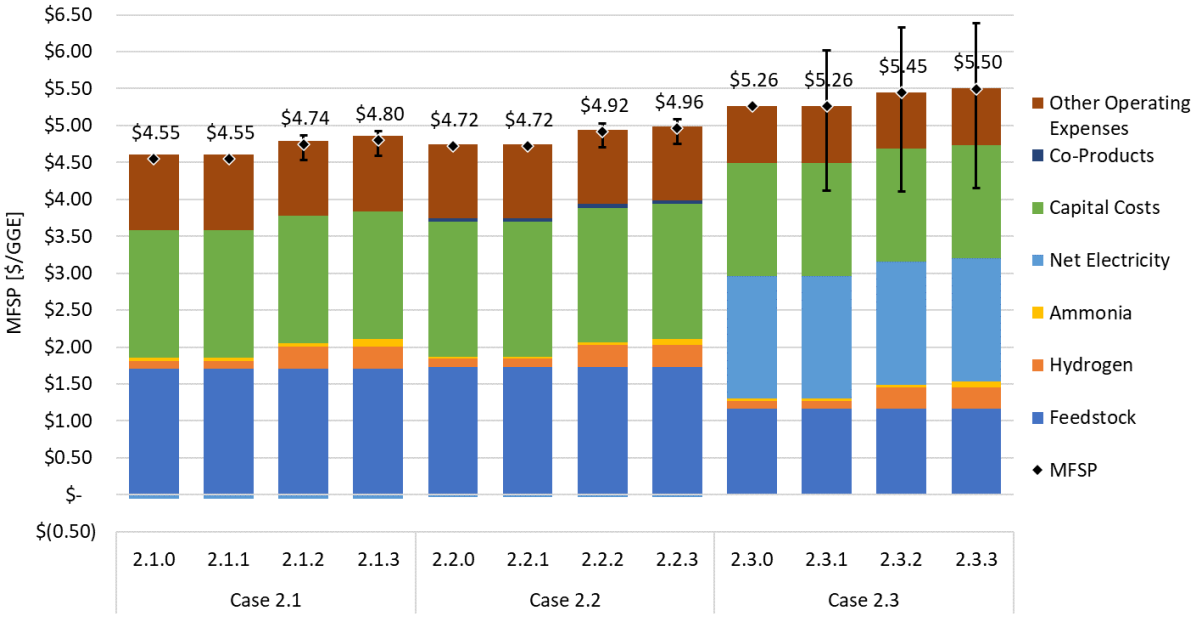


Figure 10. MFSP cost contribution breakdown of Case 2 scenarios ($/GGE)

The base case scenario (Case 2.1.0) for the conversion of corn sugar to SAF resulted in an MFSP of $4.55/GGE with a total fuel yield of 35.8 million GGE per year. A coproduct credit of $0.06/GGE was obtained through on-site combustion of residue lignin via a combined heat and power system and selling excess electricity to the grid. Of the total MFSP, about $1.71/GGE was attributed to cellulosic biomass feedstocks. The TCI of the base case was nearly $486 million.

Case 2.2.0 for the conversion of cellulosic feedstocks to SAF results in an MFSP of $4.72/GGE, which is $0.19 higher than the non-CCS case. The increase in selling price is due to the capital costs for compression and drying equipment, loss of revenue from the electricity that is required for compression (and would otherwise have been sold as byproduct), and costs for $CO_2$ disposal, estimated to be $10/tonne. This analysis does not consider incentives or credits for $CO_2$ storage. The existing 45Q tax credit at $50/tonne would change the $10/tonne $CO_2$ disposal cost to a $40/tonne $CO_2$ byproduct credit.

Case 2.3 reincorporated AGR $CO_2$ into the final fuel product through electrosynthesis of $CO_2$ to CO. Reincorporating carbon lost from fermentation offgas via electrolysis and syngas formation increased the fuel yield significantly, from 35.8 million GGE per year (Case 2.1.0) to 52.7 million GGE per year. However, the addition of the electrolyzer incurred significant capital expenses, increasing the TCI from $486 million in the base case to $654 million. $H_2$ and electricity costs also contributed significantly to the MFSP in Case 1.3, as shown in Figure 5.

### 3.2.4 Key Learnings

Second-generation biofuels such as cellulosic ethanol produced from corn stover have inherently lower CIs than their first-generation counterparts such as ethanol produced from corn

starch. Cellulosic fuels have lower feedstock-related emissions from land use change and fertilizer application. It is assumed that the process heat and electricity for ethanol and jet fuel production is supplied from a carbon-neutral corn stover combustion. It stands to reason, therefore, that SAF produced from second-generation ethanol will have a lower CI; the baseline Case 2.1.0 has a net CI of 21.8 g/MJ, which is 78% lower than conventional aviation fuel.

*Key Learnings – LCA*

- The opportunities for further reducing the CI of aviation fuel produced from a second-generation biofuel platform are limited. Emissions due to electricity production, which play a growing role from Cases 1.1.x to 1.3.x (because electricity demand increases due to $CO_2$ compression in Case 1.2, and then increases much further in Case 1.3 with $CO_2$ upgrading), are not a factor in Cases 2.1 and 2.2 because these cases already use carbon-neutral heat and power (i.e., corn stover combustion). Because the biomass feedstock has inherently low emissions, increasing the carbon efficiency of biomass utilization in Case 2.3 does not substantially reduce CI.

- Modest reductions in the CI of cellulosic ethanol to SAF are feasible with the substitution of green hydrogen for conventional hydrogen as a process input in Cases 2.1 and 2.2. This change reduces CI by about 5 g/MJ, which is a substantial fraction of the net CI but a small percentage of the CI of conventional aviation fuel. Similarly, swapping green ammonia for conventional ammonia used in the pretreatment and conversion of cellulosic biomass reduces the CI by about 1 g/MJ.

- Capturing fermentation $CO_2$ does substantially reduce the CI of aviation fuel produced from cellulosic biomass converted to ethanol and subsequently upgraded to SAF (Cases 2.2.0–2.2.3). This intervention reduces CI by about 37 g/MJ, which is more than enough to offset the baseline CI of 22.4 g/MJ. SAF made with cellulosic ethanol in today's electricity, hydrogen, and ammonia markets would be carbon negative according to our analysis. Substituting green hydrogen and ammonia would further offset emissions such that the net CI would be −21 g/MJ.

- The CCU cases (Cases 2.3.0–2.3.3) help generate 47% more fuel compared to Cases 2.1.x and 2.2.x with the same amount of corn stover by maximizing carbon utilization. However, from the CI reduction point of view, the base corn stover CCU case (Case 2.3.0) shows only 10% CI reductions compared to the petroleum counterpart due to its significant energy inputs for CCU. Like Case 1.3.x, the CCU cases can reduce emissions by adopting renewable energy inputs but cannot eliminate emissions during fuel production, unlike CCS cases. Renewable energy inputs help reduce the CI to become as low as 11.2 $gCO_2$/MJ (Case 2.3.3), which shows the potential of having near net-zero-carbon fuels.

*Key Learnings – TEA*

- The baseline cost of cellulosic ethanol to SAF is $4.55/GGE. This is substantially higher than the $3.24/GGE of corn starch ethanol to SAF, but it represents a very large reduction in CI.

- The increase of about $0.19/GGE for the substitution of green hydrogen represents a carbon abatement cost of approximately $280/tonne $CO_2$, and the increase of about $0.05/GGE for the substitution of green ammonia represents an approximate $260/tonne cost of abatement. These interventions cut across all variants in Cases 2.1–2.3.

- Carbon capture and sequestration, including the $10/tonne disposal cost, costs approximately $36/tonne, as evidenced by the results of Cases 2.2.1–2.2.3

- The strategy of recycling $CO_2$ into fuels (Cases 2.3.x) raises the baseline MFSP of stover-based SAF from $4.55 to $5.24 because the lower feedstock costs (resulting from an approximate doubling of the carbon efficiency of the process) are offset by the costs of electricity and hydrogen required for $CO_2$ conversion and upgrading.

# 3.3 Case 3 – Biomass Gasification and Fischer–Tropsch Synthesis

## 3.3.1 Process Design

The conceptual process design for the conversion of biomass to fuels via gasification and Fischer–Tropsch synthesis is shown in Figure 11. The biomass feedstock used in this assessment was assumed to be 50% clean pine and 50% forest residues, with a moisture content of 30 wt % at the plant gate. The feedstock cost was $63.23/dry ton per Idaho National Laboratory's *Woody Feedstocks 2020 State of Technology Report* [29]. The plant scale was set at 2,205 dry tons feedstock/day. Biomass is dried to a moisture content of 10 wt % and fed to an indirect gasifier, where biomass deconstructs to tars, chars, and raw syngas ($CO_2$, CO, and $H_2$). Char is combusted to provide heat for the gasifier. Some syngas is diverted to be used as a process fuel along with other unconverted light gases, which generates heat and electricity for the plant. Enough syngas is diverted such that a negligible amount of electricity is imported or exported in the base case design. The remainder of the raw syngas is sent to the tar reformer to convert hydrocarbons to additional CO and $H_2$. Steam is also utilized in the tar reformer to set the exiting syngas $H_2$:CO molar ratio equal to 2.15 via the water-gas shift reaction. Water is removed from the syngas stream in a quench step, and acid gases (primarily $CO_2$) are removed via an amine scrubbing step. The clean syngas stream is then converted to fuels via Fischer–Tropsch synthesis and separated into gasoline-, jet-, and diesel-range products via distillation. Light end products from Fischer–Tropsch synthesis are recycled and either combusted for process fuel or converted back to syngas in the tar reformer. A more detailed description of the process design is provided elsewhere [30-34].

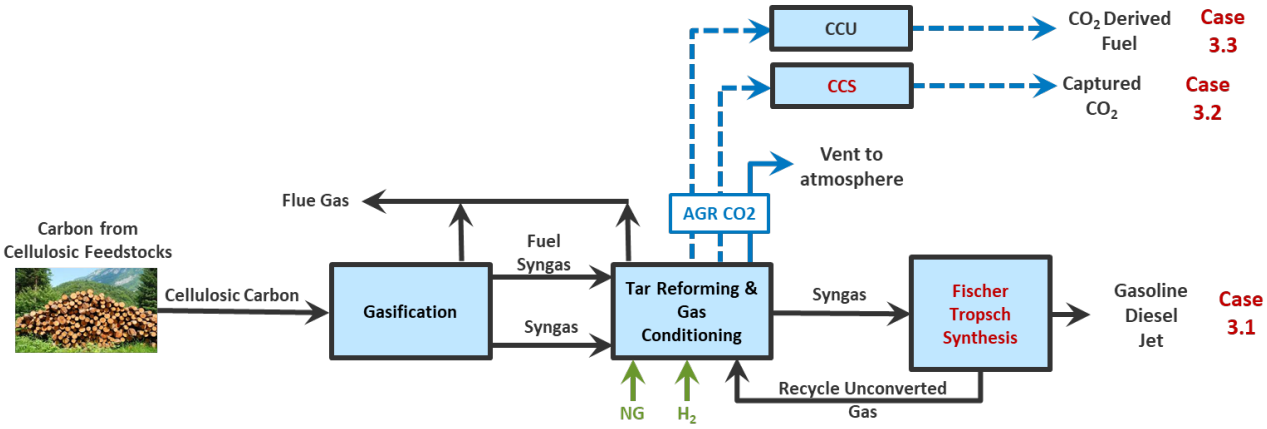


Figure 11. Block flow diagram for biomass to fuels via Fischer–Tropsch synthesis

The Fischer–Tropsch area was based off previous work by Zhang et al. [35]. The modeled reactor represented a cobalt-based slurry column operated at 230°C (446°F) and 26 bar (379 psia). Fresh syngas feed entered the reactor area at an $H_2$:CO molar ratio of 2.15, and the single-pass conversion of CO in the Fischer–Tropsch reactor was 85%. The product distribution was based on the Anderson-Schulz-Flory distribution, which predicts the carbon number

concentration based on a selected chain growth probability value (α). The relationship of molar concentration of hydrocarbons at a given carbon number ($x_n$) to the chain growth probability is given in Equation 2. As α increases, there is greater selectivity toward hydrocarbons with greater carbon number; thus, an α value that optimizes fuel-range hydrocarbons (C5–C22) is necessary. In this assessment, α = 0.84 was selected based on previous work [35].

$$\ln(x_n) = n * \ln(\alpha) + \ln\left((1-\alpha)/\alpha\right) \quad (2)$$

Where $n$ = carbon number.

Hydrocarbon products with fewer than five carbons (C1–C4) do not follow Anderson-Schulz-Flory distribution predictions and have therefore been adjusted based on previous work [35, 36]. Additionally, the olefin-to-paraffin ratio for each carbon number was determined experimentally by Todic et al. [37] and applied in this work.

The above conditions were used as the baseline assumptions for each of the Case 3 scenarios. Several scenarios (sub-cases) were introduced to understand the life cycle and economic opportunities and trade-offs for different renewable interventions and process designs. An overview of the sub-cases is given in Table 11.

Table 11. Summary of Case 3 scenarios and key interventions

| Case Number | AGR $CO_2$ | Flue Gas $CO_2$ | Electricity | Fuel | Hydrogen |
|---|---|---|---|---|---|
| Case 3.1.0 | Vented | Vented | N/A | Syngas + Offgases | N/A |
| Case 3.1.1.1 | Vented | Vented | N/A | Offgases + NG | N/A |
| Case 3.1.1.2 | Vented | Vented | N/A | Offgases + RNG | N/A |
| Case 3.1.2.1 | Vented | Vented | N/A | Syngas + Offgases | Fossil $H_2$ |
| Case 3.1.2.1b | Vented | Vented | N/A | Syngas + Offgases | Renewable $H_2$ |
| Case 3.1.2.2 | Vented | Vented | N/A | Syngas + Offgases | Fossil $H_2$ |
| Case 3.1.2.2b | Vented | Vented | N/A | Syngas + Offgases | Renewable $H_2$ |
| Case 3.1.2.3 | Vented | Vented | N/A | Syngas + Offgases | Fossil $H_2$ |
| Case 3.1.2.3b | Vented | Vented | N/A | Syngas + Offgases | Renewable $H_2$ |
| Case 3.1.2.4 | Vented | Vented | N/A | Syngas + Offgases | Fossil $H_2$ |
| Case 3.1.2.4b | Vented | Vented | N/A | Syngas + Offgases | Renewable $H_2$ |
| Case 3.2.0 | CCS | Vented | US mix | Syngas + Offgases | N/A |
| Case 3.2.1 | CCS | Vented | RE | Syngas + Offgases | N/A |
| Case 3.3.0 | CCU | Vented | US mix | Syngas + Offgases | Fossil $H_2$ |
| Case 3.3.1 | CCU | Vented | RE | Syngas + Offgases | Fossil $H_2$ |
| Case 3.3.2 | CCU | Vented | RE | Syngas + Offgases | Renewable $H_2$ |

Case 3.1.0 is the base-case scenario where the process design is as described above and no renewable interventions are introduced. Cases 3.1.1.1 and 3.1.1.2 import fossil natural gas and RNG, respectively, for process fuel rather than diverting syngas for process heating and power generation.

Cases 3.1.2.1 through 3.1.2.4 import $H_2$ to the tar reformer in increasing quantities (250, 1,000, 2,000, and 3,000 lbmol/h) to introduce the reverse water-gas shift reaction and reduce the amount of CO lost to $CO_2$. The sub-cases labeled with a "b" are the scenarios using renewable $H_2$.

CCS or CCU were considered in addition to the processes to help mitigate carbon loss to the atmosphere. Carbon is primarily lost to the atmosphere from two sources in this process design: as $CO_2$ from the AGR step and as $CO_2$ in the flue gas. The high-purity acid-gas removal $CO_2$ represents the low-cost option for CCS/CCU compared to the flue gas, which would require additional cleanup steps. Thus, this assessment only considered AGR $CO_2$ for the CCS (Case 3.2) and CCU cases (Case 3.3).

The CCS case (Case 3.2) compresses the AGR $CO_2$ from 2.2 bar (32 psia) to 152.7 bar (2,215 psia) and incorporates the additional capital and operating expenses required to compress, dehydrate, and sequester captured $CO_2$. Case 3.2.0 represents the CCS case in which grid electricity is used for sequestration, and Case 3.2.1 is the renewable electricity case.

The final scenarios are CCU scenarios (Case 3.3). In these cases, the captured $CO_2$ is routed through an electrolysis unit and electrochemically converted to CO. CO is purified from the $CO_2$-CO mixture out of the electrolyzer via pressure-swing adsorption and mixed with imported $H_2$ to create additional syngas with a molar ratio of 2.15 ($H_2$:CO). The additional syngas generated in the CCU process is mixed with the existing syngas stream to increase the Fischer–Tropsch fuel yield. Cases 3.3.0 to 3.3.2 investigate the impact of replacing grid electricity and gray $H_2$ with renewable sources.

### 3.3.2 LCA Results and Discussions

*LCA Cases and Inventories*

Case 3 represents pathways generating FT fuels from biomass gasification with and without CCS and CCU. Figure 12 shows the life cycle system boundary of Case 3, which includes feedstock production and transportation, FT fuel production, FT fuel transportation and distribution, and FT fuel combustion. Case 3.1.0 is the base case that uses biomass as a process fuel for FT fuel production. The biomass feedstock in this study consists of 50% clean pine and 50% forest residues (by mass). In Case 3.1.1, imported NG is used to support the process demand for FT fuel production instead of using biomass as a process fuel. In Case 3.1.2, additional $H_2$ is considered for tar reforming, which helps increase the FT fuel yield. In addition, Case 3.2 applies CCS to capture and sequester $CO_2$ from biomass gasification underground, whereas Case 3.3 applies CCU to convert the $CO_2$ from the biomass gasification process into additional FT fuels. During the FT fuel production process, wax is produced as a coproduct along with FT fuels, which is considered to displace residual oil based on the energy content.

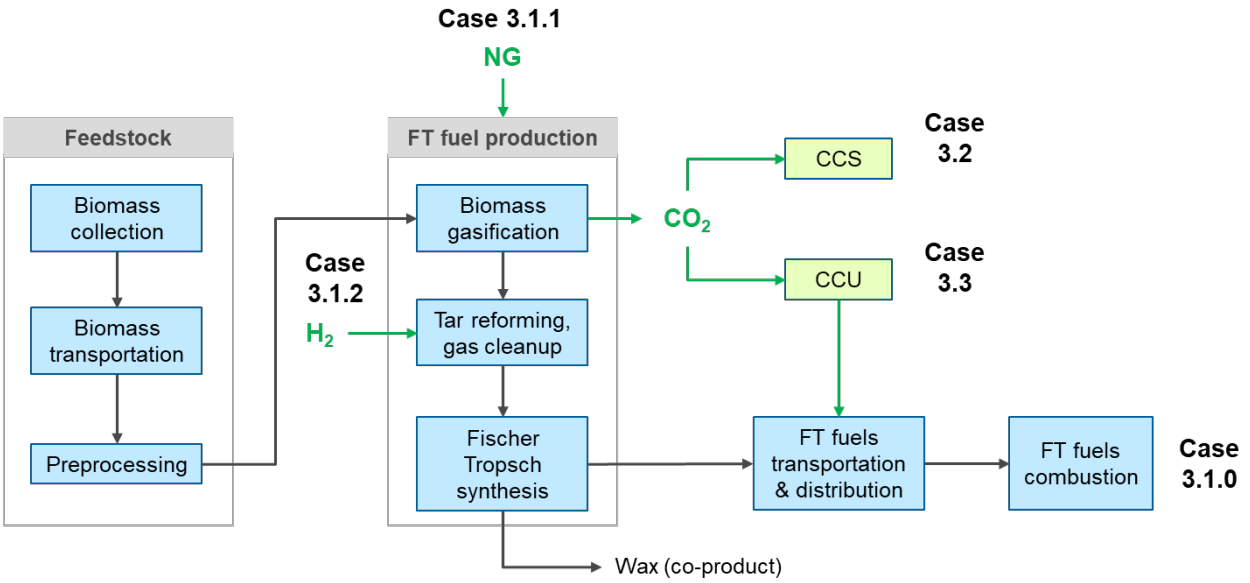


Figure 12. The schematic flow diagram of the life cycle pathways of Case 3, which includes biomass (50% clean pine and 50% forest residues by mass) feedstock production and transportation, FT fuel production, FT fuel transportation and distribution, and FT fuel combustion. Case 3.1.1 uses imported NG as a heat source instead of biomass. Case 3.1.2 uses additional $H_2$ for tar reforming to increase FT fuel yield. Cases 3.2 and 3.3 apply CCS and CCU, respectively, for high-purity $CO_2$ captured from biomass gasification.

Table 12 shows the life cycle inventory of Case 3. As Case 3.1.0 uses biomass as a feedstock and process fuel, there are no extra energy inputs other than catalyst/chemical inputs. This case needs 117 g (dry) biomass to generate 1 MJ of FT fuels. Along with FT fuels, 0.12 MJ of wax is produced, which gives 12.3 $gCO_2e/MJ_{wax}$ of displacement credits by assuming wax displaces residual oil. Case 3.1.1 imports NG to supply heat instead of burning biomass for heat, which reduces biomass inputs to 99 g (dry) by importing 0.30 MJ NG per megajoule of FT fuel. Cases 3.1.2.1–3.1.2.4 consider supporting different amounts of $H_2$ for tar reforming, ranging from 0.04–0.34 MJ per megajoule of FT fuel. The biomass inputs per megajoule of FT fuel production decrease by importing $H_2$ due to higher fuel yield. The catalyst/chemical inputs and coproduced wax are reduced with respect to the reduction of biomass inputs. Case 3.2 applies CCS for the biogenic $CO_2$ emissions from the biomass gasification process that are otherwise emitted. It has the same biomass inputs as in Case 3.1.0, while 0.02 MJ of electricity and 0.01 g of chemicals (tri-ethylene glycol) are used to capture and sequestrate 48.5 g of $CO_2$ per megajoule of FT fuel. In Case 3.3 (CCU), only 72 g (dry) of biomass is needed to produce 1 MJ FT fuel because the captured $CO_2$ is converted to FT fuels using additional $H_2$ and electricity inputs. Eight cases in Table 12 have sub-cases according to the type of energy source, as shown in Table 11.

Table 12. Life cycle inventory of Case 3: biomass gasification to FT fuel

| per MJ of FT fuel | Unit | Case 3.1.0 | Case 3.1.1 | Case 3.1.2.1 | Case 3.1.2.2 | Case 3.1.2.3 | Case 3.1.2.4 | Case 3.2 | Case 3.3 |
|---|---|---|---|---|---|---|---|---|---|
| Biomass (dry) | g | 117 | 99 | 114 | 105 | 94 | 86 | 117 | 72 |
| Natural gas | MJ | - | 0.30 | - | - | - | - | - | - |
| $H_2$ | MJ | - | - | 0.04 | 0.14 | 0.25 | 0.34 | - | 0.36 |
| Electricity | MJ | - | - | - | - | - | - | 0.02 | 0.43 |
| Catalysts/chemicals | g | 0.49 | 0.43 | 0.48 | 0.44 | 0.40 | 0.37 | 0.50 | 0.31 |
| Sequestrated $CO_2$ | g | - | - | - | - | - | - | 48.5 | - |
| Coproduced wax | MJ | 0.120 | 0.120 | 0.120 | 0.119 | 0.119 | 0.119 | 0.120 | 0.119 |

*LCA Results*

Figure 13 shows life cycle GHG emission results of biomass gasification to FT fuel pathways. Black dots represent the net GHG emissions of each case using grid electricity and $H_2$ from fossil NG SMR. Red dots represent the net GHG emissions of each case when using renewable electricity and $H_2$ from fossil NG SMR. Lastly, purple dots indicate the net GHG emissions of each case when using both renewable electricity and renewable $H_2$.

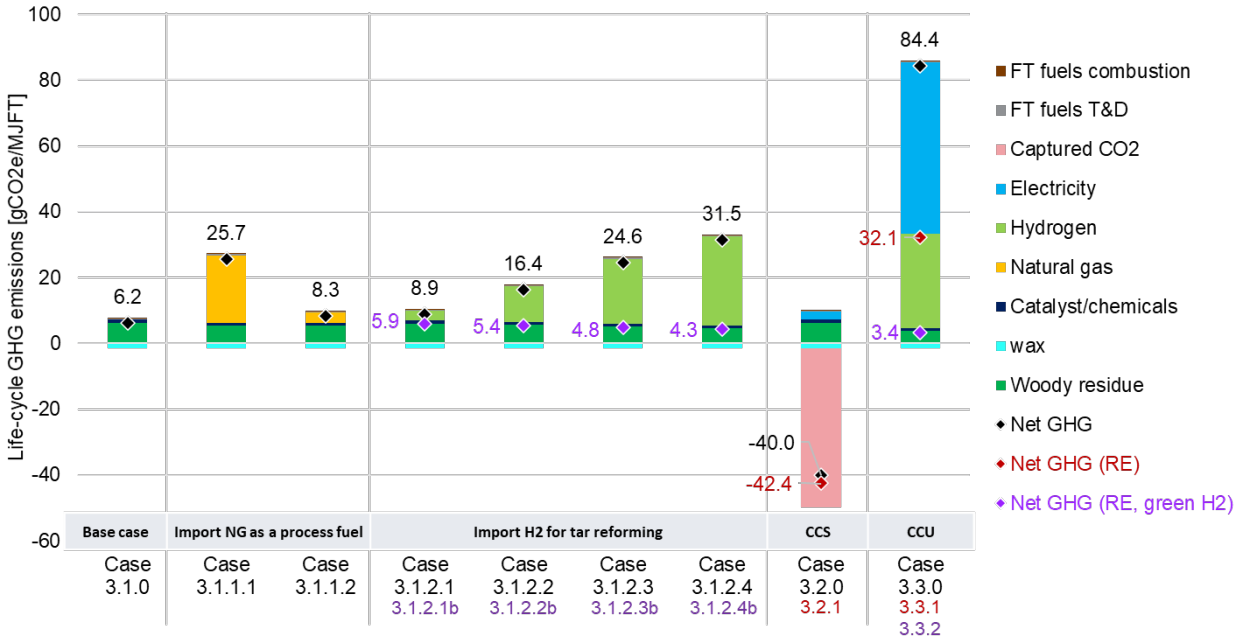


Figure 13. Life cycle GHG emissions ($gCO_2e/MJ$) of FT fuel production pathways via biomass gasification and FT synthesis. The net GHG emissions are indicated in black dots for each case using conventional energy sources, red dots for each case using renewable electricity, and purple dots for each case using renewable electricity and green $H_2$.

The CI of the base case (Case 3.1.0) FT fuel is 6.2 $gCO_2e/MJ$, which is 93% lower than petroleum jet fuel (84.5 $gCO_2e/MJ$). This is because the feedstock and all the process fuels are

from biomass, without any external fossil energy sources. Collecting, transporting, and preprocessing of woody residue (green) have GHG emissions of 6.3 $gCO_2e/MJ$. The rest (catalyst/chemical inputs, FT fuel distribution, and FT fuel combustion) generates 1.4 $gCO_2e/MJ$ of GHG emissions, while coproduced wax (cyan) gives −1.5 $gCO_2e/MJ$ of emissions credits.

Compared to the base case, GHG emissions of feedstock production are slightly reduced to 5.3 $gCO_2e/MJ$ in Cases 3.1.1.1–3.1.1.2 due to higher fuel yield, resulting in lower biomass requirements. However, the use of fossil NG generates 20.6 $gCO_2e/MJ$ in Case 3.1.1.1. Even using landfill gas-derived RNG generates an additional 3.2 $gCO_2e/MJ$ of GHG emissions, which increases overall CI compared to the base case (Case 3.1.0). The CIs of Cases 3.1.1.1 and 3.1.1.2 become 25.7 and 8.3 $gCO_2e/MJ$, respectively.

Cases 3.1.2.1–3.1.2.4 import $H_2$ for tar reforming. The additional $H_2$ inputs lead to requiring less biomass feedstock, catalyst, and chemical inputs per megajoule of fuel production. However, these bring additional GHG emissions for fossil NG SMR $H_2$ production, which are estimated to range from 3–27 $gCO_2e/MJ$ (yellow green), leading to higher life cycle GHG emissions compared to the base case. Meanwhile, Cases 3.1.2.1b–3.1.2.4b use renewable $H_2$ with zero CI, so those cases do not add GHG emissions (yellow green) while generating more FT fuel. The net GHG emissions with renewable $H_2$ (purple dots) reduces 1.5–5.1 $gCO_2e/MJ$ from Case 3.1.0.

Cases 3.2.0 and 3.2.1 capture and sequestrate 48.5 $gCO_2e/MJ$ of the $CO_2$ from the AGR process with an additional 0.02 MJ of electricity inputs for CCS. The impact of grid electricity is 2.4 $gCO_2e/MJ$ in Case 3.2.0, which could be removed by using renewable electricity in Case 3.2.1. The net GHG emissions become −40 $gCO_2e/MJ$ in Case 3.2.0 (black dot) and −42.4 $gCO_2e/MJ$ in Case 3.2.1 (purple dot).

Unlike CCS, CCU needs much more energy resources to convert $CO_2$ into FT fuels—0.43 MJ of electricity and 0.36 MJ of $H_2$. In Case 3.3.0, the CI of FT fuels is 84.4 $gCO_2e/MJ$, including 52.3 $gCO_2e/MJ$ from grid electricity and 28.8 $gCO_2e/MJ$ from NG SMR $H_2$. The CI can be decreased to 32.1 $gCO_2e/MJ$ (red dot) by replacing grid electricity to renewable electricity in Case 3.3.1 and further decreased to 3.4 $gCO_2e/MJ$ (purple dot) by using renewable electricity and renewable $H_2$ in Case 3.3.2.

Figure 14 shows the CIs, biomass inputs, and renewable energy consumptions of best cases in Case 3. The CI of FT fuel from the base case (Case 3.1.0) is 6.2 $gCO_2e/MJ$, with the significant GHG reductions from the use of biomass as a feedstock and a process fuel. External RNG input as a process fuel (Case 3.1.1.2) reduces 15% of biomass inputs but increases the net CI of FT fuel due to the RNG production and combustion. Importing $H_2$ for tar reforming (Case 3.1.2.4b) consumes 0.34 MJ of renewable hydrogen to reduce the CI by 1.9 $gCO_2e/MJ$ and also saves 26% of biomass compared to the base case.

Compared to the base case, implementing CCS reduces the CI by 48.5 $gCO_2e/MJ$ with using only 0.02 MJ of electricity. CCU consumes significant additional energy, 0.36 MJ of

renewable $H_2$ and 0.43 MJ of renewable electricity, to reduce the CI to 3.4 $gCO_2e/MJ$, which seems to be inefficient compared to the CCS case. Instead, CCU can save 39% of biomass feedstock to produce 1 MJ of FT fuel. In other words, there is an additional 0.64 MJ of FT fuel through CCU with the same amount of biomass input, which can bring additional economic and environmental advantages by displacing petroleum jet.

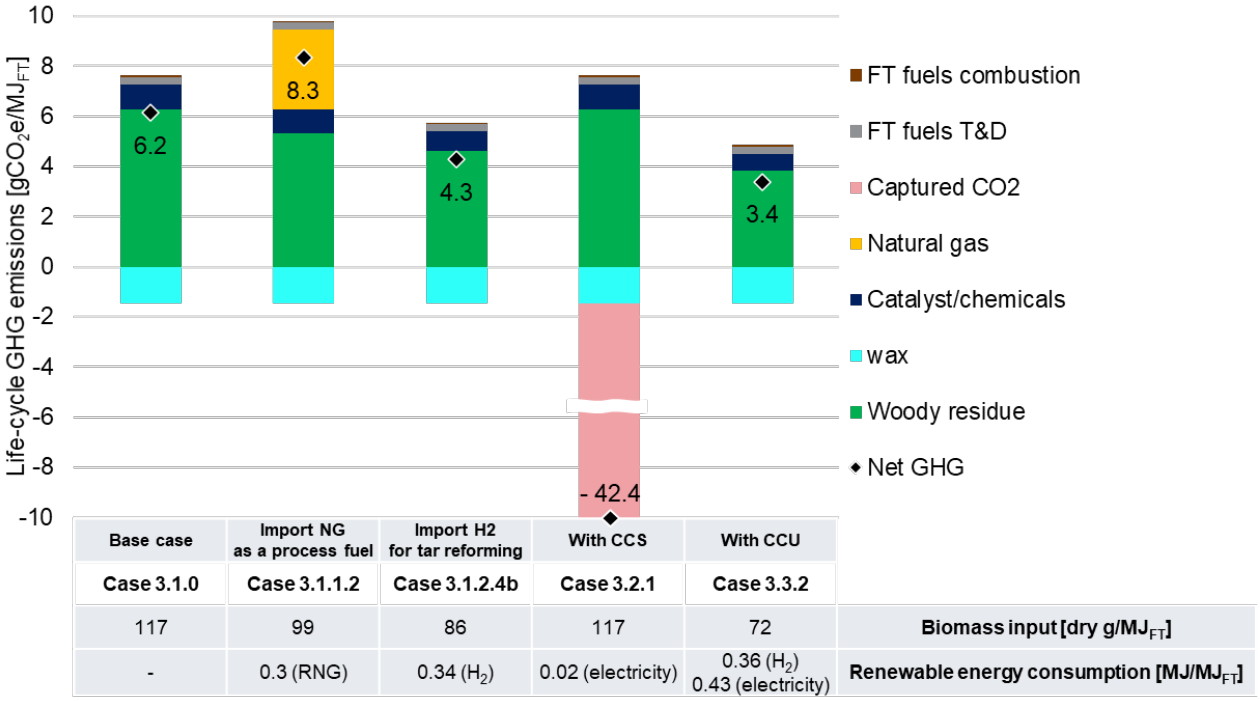


| Base case | Import NG as a process fuel | Import H2 for tar reforming | With CCS | With CCU | |
|---|---|---|---|---|---|
| Case 3.1.0 | Case 3.1.1.2 | Case 3.1.2.4b | Case 3.2.1 | Case 3.3.2 | |
| 117 | 99 | 86 | 117 | 72 | Biomass input [dry g/$MJ_{FT}$] |
| - | 0.3 (RNG) | 0.34 ($H_2$) | 0.02 (electricity) | 0.36 ($H_2$)<br>0.43 (electricity) | Renewable energy consumption [$MJ/MJ_{FT}$] |

Figure 14. Life cycle GHG emissions ($gCO_2e/MJ$) of selected scenarios, biomass inputs (dry g/MJ), and renewable energy consumption (MJ/MJ) of FT fuel production pathways via biomass gasification and FT synthesis

### 3.3.3 TEA Results and Discussions on Key Metrics (Cost, Carbon Efficiency, and Energy Efficiency)

*MFSP*

The TEA results for Case 3 include MFSP, carbon efficiency, energy efficiency, and TRL assessment for each of the sub-cases. The TEA results also include sensitivity assessments around the costs of electricity, hydrogen, and natural gas, where applicable. The MFSP for each scenario was derived using the methods and financial assumptions described earlier in this report. A summary of the MFSP results and cost contribution breakdown is given in Figure 15.

The base case scenario (Case 3.1.0) for the conversion of biomass to SAF resulted in a minimum fuel selling price of $2.58/GGE with a total fuel yield of 45.8 million GGE per year. A coproduct credit of $0.41/GGE was obtained through the sale of the wax coproduct. Of the total MFSP, about $1.34/GGE was attributed to capital costs and $1.00/GGE was attributed to feedstock costs. The TCI of the base case was nearly $473 million, with Fischer–Tropsch synthesis costs contributing 44%.

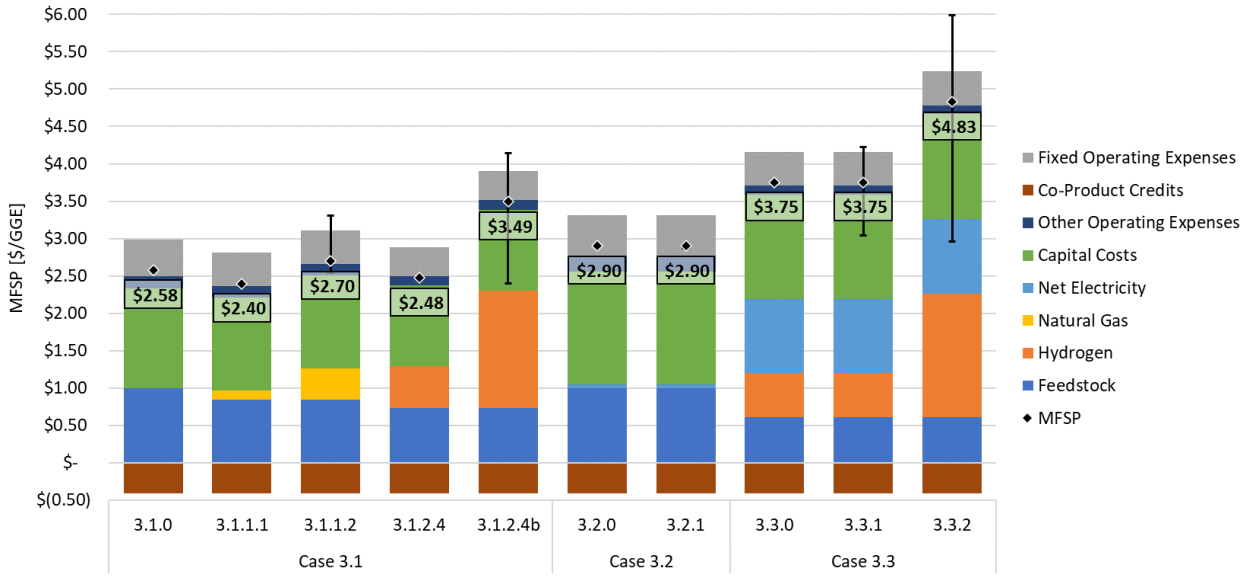


Figure 15. MFSP cost contribution breakdown of Case 3 scenarios

Cases 3.1.1.1 and 3.1.1.2 used imported natural gas to supplement heat and power generation instead of biomass-derived syngas. In the scenario where gray natural gas is used, the MFSP decreases by $0.18/GGE from the base case due to increased fuel yield (54.1 million GGE per year) and lower relative cost of natural gas compared to biomass. The renewable scenario (Case 3.1.1.2) resulted in the same fuel yield, but the MFSP increases by $0.12/GGE due to the higher baseline cost of RNG compared to gray natural gas ($12.00/MMBtu versus $3.39/MMBtu). Figure 15 displays error bars on the MFSP for Case 3.1.1.2 indicating the effect of high-cost ($29.44/MMBtu) and low-cost ($7.48/MMBtu) RNG. Low-cost RNG can achieve cost parity with the base case at $2.54/GGE.

Cases 3.1.2.1 through 3.1.2.4 varied the quantity of imported $H_2$. Figure 16 shows the results for these cases for carbon efficiency, energy efficiency, and MFSP. Note that the assessment shown in Figure 16 shows the results for the baseline green $H_2$ cost scenario ($4.50/kg $H_2$). Increasing imported $H_2$ increases carbon efficiency to a final value of 44% in the 3,000-lbmol $H_2$/h scenario (Case 3.1.2.4b). However, the MFSP also increases with increasing $H_2$ import to a final value of $3.49/GGE, a 35% increase from the base case (Case 3.1.0). The energy efficiency of the process showed minimal change with varying amounts of green $H_2$ import. Despite the increase in MFSP, Case 3.1.2.4b was selected as the base case for the $H_2$ import scenario and was used for comparison against other sub-cases. This scenario resulted in a fuel yield of 62.2 million GGE per year. Figure 15 shows the relative contribution of $H_2$ costs in the gray (Case 3.1.2.4) and green (Case 3.1.2.4b) $H_2$ scenarios. Scenarios where low-cost $H_2$ is available, including the gray $H_2$ scenario and the future low-cost green $H_2$ scenario, achieve MFSPs below the base case at $2.48/GGE and $2.45/GGE, respectively.

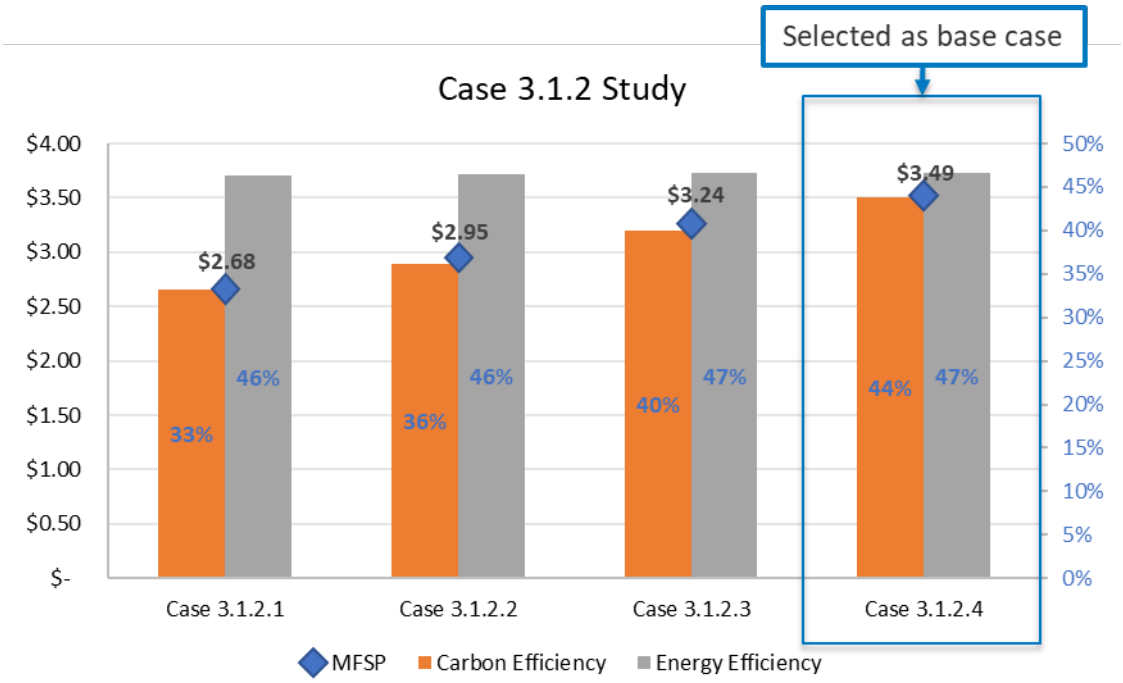


Figure 16. Case 3.1.2 case study investigating the effect of $H_2$ import quantities. Cases 3.1.2.1 through 3.1.2.4 imported 250, 1,000, 2,000, and 3,000 lbmol/h $H_2$, respectively.

Case 3.2 assessed the cost of implementing CCS technology to sequester carbon lost to the atmosphere from the acid gas removal step. The CCS scenario did not impact the overall fuel yield relative to the base case. The additional costs primarily stem from compression and dehydration capital expenses, compression power requirements, and the cost of final $CO_2$ storage, which was treated as an operating expense. Since the baseline cost for renewable electricity is assumed to be equal to current grid costs, CCS expenses increased the MFSP to $2.90/GGE in both the gray electricity and renewable electricity scenarios. The range of renewable energy costs in Case 3.2.1 resulted in a potential MFSP range of $2.87–$2.92/GGE.

The final scenario (Case 3.3) reincorporated AGR $CO_2$ into the final fuel product through electrosynthesis of $CO_2$ to CO. Reincorporating carbon lost to the atmosphere via electrolysis and syngas formation increased the fuel yield significantly, from 45.8 million GGE per year (Case 3.1.0) to 75.0 million GGE per year. However, the addition of the electrolyzer incurred significant capital expenses, nearly doubling the TCI from $473 million in the base case to $803 million. $H_2$ and electricity costs also contributed significantly to the MFSP in Case 3.3, as shown in Figure 15.

Case 3.3.0 used the cost of grid electricity and gray $H_2$ as a baseline, resulting in an MFSP of $3.75/GGE. Case 3.3.1 introduced renewable electricity ranging in price from $0.02–$0.10/kW and resulted in an MFSP range of $3.04–$4.22/GGE. Case 3.3.2 used both renewable electricity and green $H_2$ costs, increasing the MFSP to $4.83/GGE. In a future scenario where low-cost renewable electricity and green $H_2$ are available, an MFSP of $2.96/GGE is possible. In

the near term, however, renewable energy availability could raise the price of both electricity and green $H_2$, resulting in an upper bound of $5.99/GGE.

*Carbon Efficiency*

Carbon efficiency is a metric that describes the material efficiency of feedstock conversion to product. An overview of the carbon efficiency breakdown of each Case 3 sub-case is given in Figure 17. The figure shows the distribution of carbon flow to fuels, coproducts, and waste streams; the total carbon efficiency to fuels is highlighted by a yellow border.

For the base case scenario (Case 3.1.0), total carbon efficiency to fuels is 32.2%; 12.9% of the feedstock carbon ended up in the gasoline cut, 13.3% to the jet cut, and 6.1% to the diesel cut. A relatively smaller percentage of 3.9% represented the wax coproduct. The remaining 63.8% was lost to the atmosphere through AGR $CO_2$ or flue gas $CO_2$.

Case 3.1.1.1 increased efficiency of biomass-derived syngas to fuels by using natural gas as a process fuel and increased carbon efficiency to fuels to 34.9%. The remaining cases targeted the 22.4% of feedstock carbon lost via AGR $CO_2$ due to its high purity. Through the addition of $H_2$ and the reverse water-gas shift reaction, Case 3.1.2.4 achieved a total carbon efficiency of 43.8% and reduced AGR carbon losses to 10.8%.

Case 3.2.0 completely mitigated AGR $CO_2$ emissions through CCS; however, this strategy does not increase the carbon efficiency to fuels. The CCU scenario (Case 3.3.0) achieved the greatest carbon efficiency boost, reaching 52.9% total efficiency to fuels. This scenario eliminates carbon lost in the acid-gas removal step, though some of that carbon is still lost to waxes and lighter hydrocarbons, so the total 22.4% of recovered carbon is not reflected in the fuel yield.

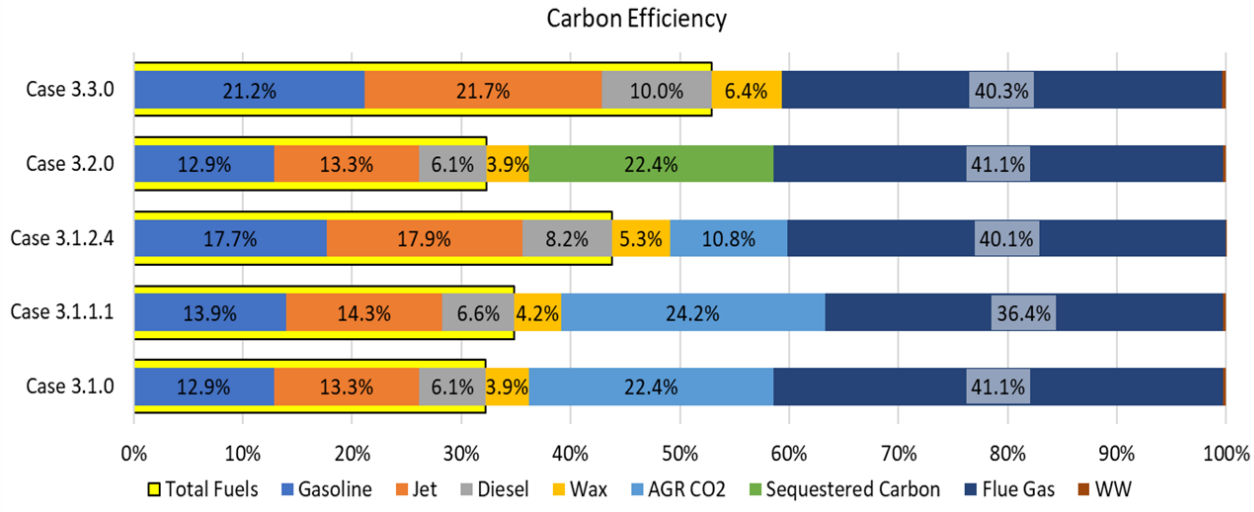


Figure 17. Carbon efficiency breakdown of Case 3 scenarios. Yellow border represents total carbon efficiency to fuels.

*Energy Efficiency*

Case 3.1.0 relied entirely on energy in the biomass feedstock for fuel production and heat and power generation. Therefore, the energy efficiency of the process is defined as the ratio of the lower heating value of the total fuels divided by the lower heating value of the biomass feedstock. Figure 18 shows the results for energy efficiency of each sub-case. The base case resulted in an energy efficiency of 46.2%.

Case 3.1.1.1 slightly increased the energy efficiency of the process by utilizing natural gas as a process fuel, which led to greater fuel production from biomass. Natural gas consumption contributed about 14% of the total energy consumption of the process. Imported $H_2$ in Case 3.1.2.4 made up 26% of the total energy consumption, with the remainder being allocated to biomass feedstock. This also only slightly improved energy efficiency to 46.6%.

The CCS scenario (Case 3.2.0) decreased overall energy efficiency by 0.4% due to the additional power requirement of the compression and dehydration equipment, without a corresponding increase in fuel yield.

Despite the largest increase in fuel yield, Case 3.3.0 resulted in the largest decrease in energy efficiency (down to 42.8%) due to the significant power requirement of the electrolyzer and the amount of $H_2$ needed for syngas formation. In total, electricity accounted for 18% of the total energy consumption, $H_2$ accounted for 25%, and feedstock made up the remaining 57% in the CCU case.

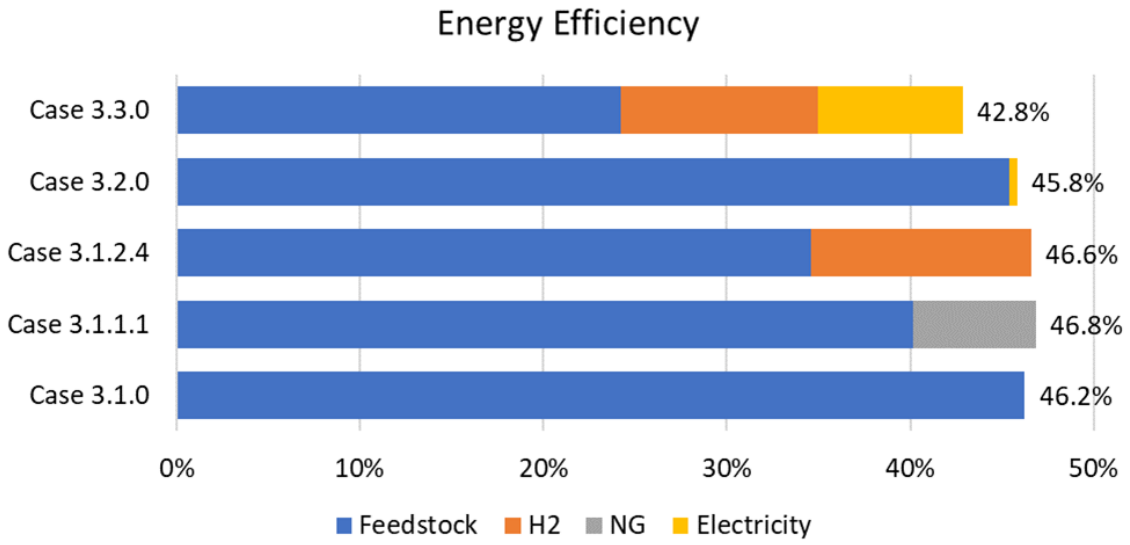


Figure 18. Energy efficiency breakdown for Case 3 scenarios

## 3.3.4 Key Learnings

*Key Learnings – LCA*

- LCA results present the low CIs of the FT fuel pathways produced from biomass gasification and FT synthesis. The CI of FT fuel from the base case (Case 3.1.0) is 6.2 $gCO_2e/MJ$, which is 93% lower than the CI of petroleum jet fuel, mainly by using biomass as a process fuel to meet heat and electricity demand. External RNG input as a process fuel (Case 3.1.1.2) reduces the biomass inputs but increases the net CI of FT fuel to 8.3 $gCO_2e/MJ$. The CI of Case 3.1.2.4b that imports an additional 0.34 MJ of renewable $H_2$ can be reduced to 4.3 $gCO_2e/MJ$ (reduction of 1.9 $gCO_2e/MJ$) while generating 0.64 MJ of additional FT fuel compared to the base case (Case 3.1.0).

- $CO_2$ from the acid gas removal process is captured and sequestrated (Case 3.2) or utilized (Case 3.3). With the additional 0.02 MJ of electricity inputs, CCS technology reduces the CI of FT fuel to −42.4 $gCO_2e/MJ$. On the other hand, CCU technology needs significant amounts of renewable $H_2$ (0.36 MJ) and electricity (0.43 MJ) to reduce the CI to 3.4 $gCO_2e/MJ$ while saving 39% of biomass input.

*Key Learnings – TEA*

- Gasification and Fischer–Tropsch synthesis technologies present a near-term viable pathway for biomass-derived fuel production. This pathway benefits from a high TRL (about 8) and a low baseline MFSP, as shown in Case 3.1.0. The baseline case also does not require external energy inputs other than the biomass feedstock, and therefore reduces the process dependency on renewable resource (i.e., renewable electricity, RNG, green $H_2$) availability and cost.

- Despite the low MFSP in Case 3.1.0, the baseline scenario results in poor carbon efficiency to fuels (32.2%), with a significant fraction of biomass carbon lost to the atmosphere as $CO_2$. Utilizing RNG for process heating and power, as in Case 3.1.1.2, is a low-cost, low-complexity method to slightly improve carbon efficiency. Importing green $H_2$ is also a near-term option for boosting carbon efficiency; however, current costs for renewable $H_2$ are high and could lead to a cost increase of about $1/GGE.

- CCS is another near-term carbon mitigation strategy with a high TRL that could readily be implemented and remove a large fraction of $CO_2$ emissions, with a low cost burden. Since renewable electricity can be purchased at or near grid prices, a fully renewable CCS system is achievable. However, CCS does not increase either carbon or energy efficiency, which could detract from the pathway's ability to meet future volumetric fuel targets.

- With a readily available and pure stream of $CO_2$ from the AGR process, CCU technologies present a strategy for reincorporating $CO_2$ to fuels. Implementing a CCU system results in the largest increase in carbon efficiency, up to 52.9%. However, this jump in efficiency is also associated with a decrease in energy efficiency and a large cost burden, especially in the renewable scenario, which would be necessary to approach a

net-zero-carbon fuel. Further R&D is required to move the TRL of CCU, which is currently about 3. Additionally, since this process is highly dependent on the availability of low-cost renewable electricity and green $H_2$, more time for optimization of these technologies will enhance the feasibility of this pathway. Thus, CCU should be viewed as a long-term strategy for carbon mitigation and utilization in the pathway of biomass to fuels via FT.

# 3.4 Case 4 – Wet Waste HTL

## 3.4.1 Process Design

Case 4 is based on HTL of wet waste feedstock and subsequent catalytic upgrading of the produced biocrude into hydrocarbon fuel blendstocks in the gasoline, diesel, and jet range. The process block flow diagram of this conversion pathway is shown in Figure 19. The United States generated approximately 77 million dry tons of wet waste in 2016, including wastewater residuals, manure, food waste, and fats, oils, and grease [20]. Approximately 65% of the wet waste availability in the United States is not utilized for any beneficial purpose, such as for fertilizer, biodiesel, or compost [20]. Since wet wastes are abundant, they can be a significant contributor to the nation's renewable energy goals and provide an economically and environmentally sustainable alternative for current waste disposal practices. HTL is a process that applies high-temperature and high-pressure water in the condensed phase to convert wet biomass feedstock to multiphase products consisting of an organic phase, an aqueous phase, solids, and gases. The HTL process is well suited for processing wet waste feedstocks since it eliminates drying that is typically required for other biomass conversion technologies. The organic product, also known as "biocrude," is analogous to petroleum crude in that it contains a mixture of hydrocarbons in the gasoline/jet/diesel range. However, it contains higher oxygen and nitrogen than petroleum, so a catalytic upgrading process such as hydroprocessing is required to improve compatibility with petroleum fuels.

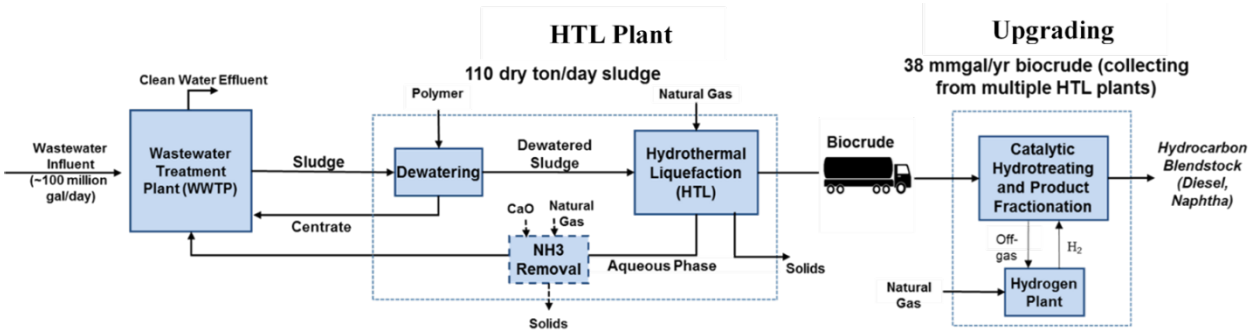


Figure 19. Sludge HTL and biocrude upgrading block flow

The process model for the conceptual conversion plant is based on a report prepared by Pacific Northwest National Laboratory [38] and represents a future target case with improved process performance parameters and economics relative to the state of the art. There are two separated main conversion processes to produce hydrocarbon fuel from wet waste feedstocks: (1) HTL of wet waste feedstock to produce biocrude and (2) hydroprocessing of HTL biocrude or biocrude upgrading to produce hydrocarbon fuel blendstocks. In addition to the HTL step and the upgrading step, on-site hydrogen plant, steam generation, steam turbine for power generation, and wastewater treatment are also included in the process design and simulation. Additional work is necessary to determine the optimal method for removing ammonia from the HTL aqueous phase. Given that there are wastewater treatment plants that could accept untreated

aqueous phase from the HTL plant, the pathway state-of-technology assessments conducted since the original design case was published include configurations both with and without the aqueous-phase ammonia removal step [38, 39] As indicated by the dotted line around the "$NH_3$ Removal" block in Figure 19, both configurations are considered in this study as well. The primary process steps shown in Figure 19 are summarized in the following paragraphs, while details can be found in the Bioenergy Technologies Office's HTL design case report [38].

*HTL of Wet Waste Feedstock*

The size of wastewater treatment plants is highly variable. A base case scale of the HTL step assumed 110 dry tons/day sludge (including ash) from a wastewater facility, which is the approximate minimum size that is economically feasible (due to economies of scale). Base on the assumption of the HTL plant owned and operated by the wastewater treatment plant, the sludge is available at no cost. An avoided sludge disposal cost (or renewable fuel credits) is not considered for conservative assumptions. A data set of the sludge production and existing municipal wastewater treatment plant scale in the United States can also be found in the report by Seiple, Coleman, and Skaggs [40]. In order to minimize both capital and operating costs of the HTL process, sludge feedstock is dewatered to 25% solid content before processing in the HTL reactor. After the dewatering step, slurry feed is pumped to 3,000 psia and preheated by the hot HTL reactor effluent to 550°F (288°C) before it is fed to the HTL flow reactor. Trim heat is generated from burning a mixture of natural gas and HTL offgas to operate HTL under 656°F (347°C). The HTL process converts the feedstock to an organic biocrude phase, an aqueous phase, solids, and gases. The reactor effluent is passed through a hot filter to remove the solids, and the remaining biocrude-aqueous-gas mixture is sent to a three-phase separator at 140°F (60°C) and 30 psia. The biocrude product is transported to a centralized upgrading facility, where biocrude is assumed to be collected from 10 multiple HTL plants in the area. The aqueous phase containing remaining soluble organics, ammonia, and metal salts is treated and sent back to the HTL reactor.

*Treatment of HTL Aqueous Phase*

The HTL aqueous-phase treatment process includes pH adjusting, ammonia stripping, and a thermal oxidation unit (THROX). Lime (CaO) is used to raise the pH to 11 to shift the $NH_3/NH_4^+$ equilibrium to the gas phase. After lime pretreatment, dissolved ammonia gas in the aqueous phase is removed by an air-stripping packed column, which also removes volatile oxygenates. The mixture of air, ammonia, and volatile compounds is then sent to THROX, where ammonia and organics are catalytically combusted to nitrogen ($N_2$), $CO_2$, and water.

*HTL Biocrude Upgrading*

Catalytic hydroprocessing is designed to upgrade the HTL biocrude to hydrocarbon fuel blendstocks by converting oxygen, nitrogen, and sulfur compounds to water, carbon dioxide, ammonia, and sulfur dioxide. The upgrading plant is assumed to process biocrude from 10 HTL plants within a 100-mile radius, and it is a scale of approximately 2,700 barrels of biocrude per

stream day. The biocrude is desalted to remove inorganic compounds prior to sending it to the hydrotreater. The hydrotreating process is under hydrogen pressure at 1,500 psia and 700°F (347°C). Hydrogen for the upgrading steps is produced by process offgases and natural gas via an on-site steam reforming process. Hydrocarbon products from the hydrotreater are a mixture of lights, paraffins, olefins, naphthenes, and aromatics that can be fractioned to gasoline, jet, and diesel blendstocks. A heavy oil-range material is also produced. The heavy cut is subsequently sent to a single-step hydrocracking process, producing additional fuel products. Wastewater from the upgrading process contains a high concentration of ammonia, which is required to be treated before sending to a wastewater treatment plant.

*On-Site Hydrogen Production and Electricity Generation*

On-site hydrogen production is designed as a natural gas-based hydrogen plant with a conventional multi-tube fired reactor and a commercial catalyst. The steam reforming reactor produces hydrogen from process offgases from the hydroprocessing steps (hydrotreating and hydrocracking). Additional purchased natural gas is required to fulfill the hydrogen requirement. Saturated and superheated steam is also generated by recuperating heat from steam reforming products. The generated steam is used in the reforming process and the hydrocarbon fractionation step. Available superheated steam is sent to generate power from the steam turbine.

Previous life cycle analysis suggests that electricity, natural gas, and lime usage are key process parameters giving the significant impact on life cycle greenhouse gas emissions. Electricity is used for hydrogen compression in the upgrading plant and for pumping in both HTL and upgrading plants. Natural gas is primarily used as the steam reformer feed to produce hydrogen required by the hydroprocessing. Natural gas is used for generating heat in both HTL and biocrude upgrading plants. Furthermore, natural gas is fed to THROX to oxidize and remove the ammonia from the HTL aqueous phase. Lime is used to raise the pH in the HTL aqueous-phase treatment process as well.

In order to reduce the process carbon emissions, fossil-derived resources were replaced by renewable resources—namely RNG, renewable electricity, and renewable hydrogen. Currently, additional work is still necessary to determine the optimal method for the HTL aqueous-phase treatment. The process flowsheet with ammonia removal is considered as the base case (Case 4.1.0) in this analysis to present the impacts of ammonia removal on process carbon intensity and process economics. The scenarios studied for Case 4 are summarized in Table 13.

From the process scenarios listed in Table 13, Cases 4.1.X are based on the process flowsheet without any additional step to remove ammonia from the HTL aqueous phase, while Cases 4.2.X are based on the process flowsheet with ammonia stripping and THROX to treat the aqueous phase before water is recycled back to the front-end process (Figure 19). Note that x refers to scenarios defined in Table 13. Cases 4.1.0 and 4.2.0 are the base case studies in which fossil-based resources and energy are adopted. Sensitivity cases for each process flowsheet were evaluated by incrementally introducing renewable electricity, RNG, and renewable hydrogen

into the conversion area, which excludes the feedstock supply and logistics. In Cases 4.1.1 and 4.2.1, U.S. grid electricity is replaced by renewable electricity and fossil natural gas is used. In Cases 4.1.2 and 4.2.2, fossil natural gas is replaced by landfill-based RNG when electricity is assumed to be non-renewable. Both electricity and natural gas are renewable in the analysis of Cases 4.1.3 and 4.2.3. In addition, renewable hydrogen is applied in Cases 4.1.4 and 4.2.4 to evaluate the impacts from reducing the natural gas consumption and steam reformer scale by using renewable hydrogen, such as hydrogen from electrolysis processes.

Table 13. Scenario analysis for Case 4. Renewable resources are incrementally introduced into wet waste HTL and biocrude upgrading process flowsheets.

| Case Number | HTL Aqueous-Phase Treatment | Electricity | Heat Sources and Steam Reforming Feed | NG Source | Hydrogen Sources | Notes |
|---|---|---|---|---|---|---|
| 4.1.0 | With $NH_3$ removal | Grid | Process offgases + NG | Fossil (NG) | On-site steam reforming | Base Case |
| 4.1.1 | With $NH_3$ removal | Renewable | Process offgases + NG | Fossil (NG) | On-site steam reforming | Base Case + RE |
| 4.1.2 | With $NH_3$ removal | Grid | Process offgases + RNG | Landfill (RNG) | On-site steam reforming | Base Case + RNG |
| 4.1.3 | With $NH_3$ removal | Renewable | Process offgases + RNG | Landfill (RNG) | On-site steam reforming | Base Case + RE & RNG |
| 4.1.4 | With $NH_3$ removal | Renewable | Process offgases + RNG | Landfill (RNG) | On-site steam reforming + renewable $H_2$ | Base Case + RE + RNG + Renewable $H_2$ |
| 4.2.0 | Without $NH_3$ removal | Grid | Process offgases + NG | Fossil (NG) | On-site steam reforming | Base Case |
| 4.2.1 | Without $NH_3$ removal | Renewable | Process offgases + NG | Fossil (NG) | On-site steam reforming | Base Case + RE |
| 4.2.2 | Without $NH_3$ removal | Grid | Process offgases + RNG | Landfill (RNG) | On-site steam reforming | Base Case + RNG |
| 4.2.3 | Without $NH_3$ removal | Renewable | Process offgases + RNG | Landfill (RNG) | On-site steam reforming | Base Case + RE & RNG |
| 4.2.4 | Without $NH_3$ removal | Renewable | Process offgases + RNG | Landfill (RNG) | On-site steam reforming + renewable $H_2$ | Base Case + RE + RNG + Renewable $H_2$ |

### 3.4.2 LCA Results and Discussions

*LCA Cases and Inventories*

Figure 20 shows the supply chain of Case 4 pathways that produce renewable diesel (RD) from the wastewater sludge (wet waste). Because sludge is a waste stream of wastewater facilities, sludge does not take upstream emissions burdens. Sludge is converted to biocrude through HTL and assumed to be transported 100 miles by truck to the biocrude upgrading plant. The biocrude is converted to RD through catalytic hydrotreating. RD is transported and distributed 30 miles by truck to the end-use site. We assumed that $CO_2$ emissions from RD combustion are carbon neutral. The HTL process also produces an aqueous phase containing a complex mixture of water-soluble organic and inorganic compounds. It might be necessary to remove ammonia from the HTL aqueous stream before sending the aqueous phase back to the wastewater treatment facility (Case 4.1). This analysis work also considers the advanced technology that does not require any step to remove ammonia from the HTL aqueous phase (Case 4.2).

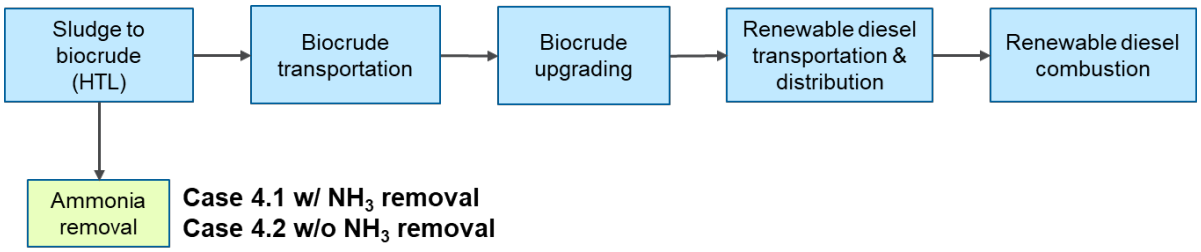


Figure 20. The schematic flow diagram of the supply chain of Case 4, which includes sludge to biocrude (HTL), biocrude upgrading, renewable diesel transportation and distribution, and renewable diesel combustion. Ammonia is removed from the aqueous stream from the HTL plant in Case 4.1.

Table 14 shows the energy and material inputs to produce 1 MJ of RD in Case 4. The life cycle inventory data are divided into two groups—sludge to biocrude and biocrude upgrading. In Case 4.1.0, the baseline case, 69.5 g (dry) of sludge is converted to 29.5 g of biocrude. The sludge-to-biocrude process consumes 0.049 MJ of electricity, 0.20 MJ of NG, and 7.7 g of catalysts/chemicals. Note that those inputs include 0.002 MJ of electricity, 0.07 MJ of NG, and 7.5 g of quicklime (CaO; CI of 1.3 $gCO_2e$ per gram of CaO) for the ammonia removal process. Therefore, Case 4.2.0 needs less energy and material inputs for the sludge-to-biocrude process. Cases 4.1.0–4.1.3 and Cases 4.2.0–4.2.3 only change the renewable energy sources with the same amount of energy inputs.

During the biocrude upgrading process, both process offgas and imported NG are used for on-site SMR to produce hydrogen. On the other hand, in Cases 4.1.4 and 4.2.4, only process offgas is used for the SMR $H_2$, while 0.07 MJ of renewable $H_2$ is imported from off-site (50 miles). The intermediate power generated during the NG SMR process is also reduced, so there is an additional 0.03 MJ of electricity input in Cases 4.1.4 and 4.2.4.

Table 14. Life cycle inventory of Case 4: wet waste sludge HTL to renewable diesel

| | | Unit | Cases 4.1.0–4.1.3 | Case 4.1.4 | Cases 4.2.0–4.2.3 | Case 4.2.4 |
|---|---|---|---|---|---|---|
| **Sludge to biocrude** | Sludge (dry) | g | 69.5 | 69.5 | 69.5 | 69.5 |
| | Electricity | MJ | 0.049 | 0.049 | 0.047 | 0.047 |
| | Natural gas | MJ | 0.20 | 0.20 | 0.13 | 0.13 |
| | Catalysts/chemicals | g | 7.7 | 7.7 | 0.18 | 0.18 |
| **Biocrude upgrading** | Biocrude | g | 29.5 | 29.5 | 29.5 | 29.5 |
| | Electricity | MJ | 0.010 | 0.013 | 0.010 | 0.013 |
| | Natural gas for SMR | MJ | 0.10 | - | 0.10 | - |
| | $H_2$ | MJ | - | 0.07 | - | 0.07 |
| | Catalysts/chemicals | g | 0.002 | 0.002 | 0.002 | 0.002 |

For RD production, it is likely that sludge is diverted from the conventional management practices because sludge is not intentionally generated (waste stream) and regulated to be treated regardless of the use of sludge. Since the conventional sludge management practices generate 249

g of GHG emissions per kilogram of dry sludge [3], we considered that using sludge feedstock brings avoided GHG emissions credits of −17.3 $gCO_2e/MJ$ RD.

*LCA Results*

Figure 21 shows life cycle GHG emissions of sludge-to-RD pathways, which are divided into two groups: Cases 4.1.0–4.1.4 with ammonia removal and Cases 4.2.0–4.2.4 without ammonia removal. The yellow bars in all the sub-cases represent −17.3 $gCO_2e/MJ$ of the avoided emissions from conventional management practices for the use of 69.5 g of sludge per megajoule of RD production.

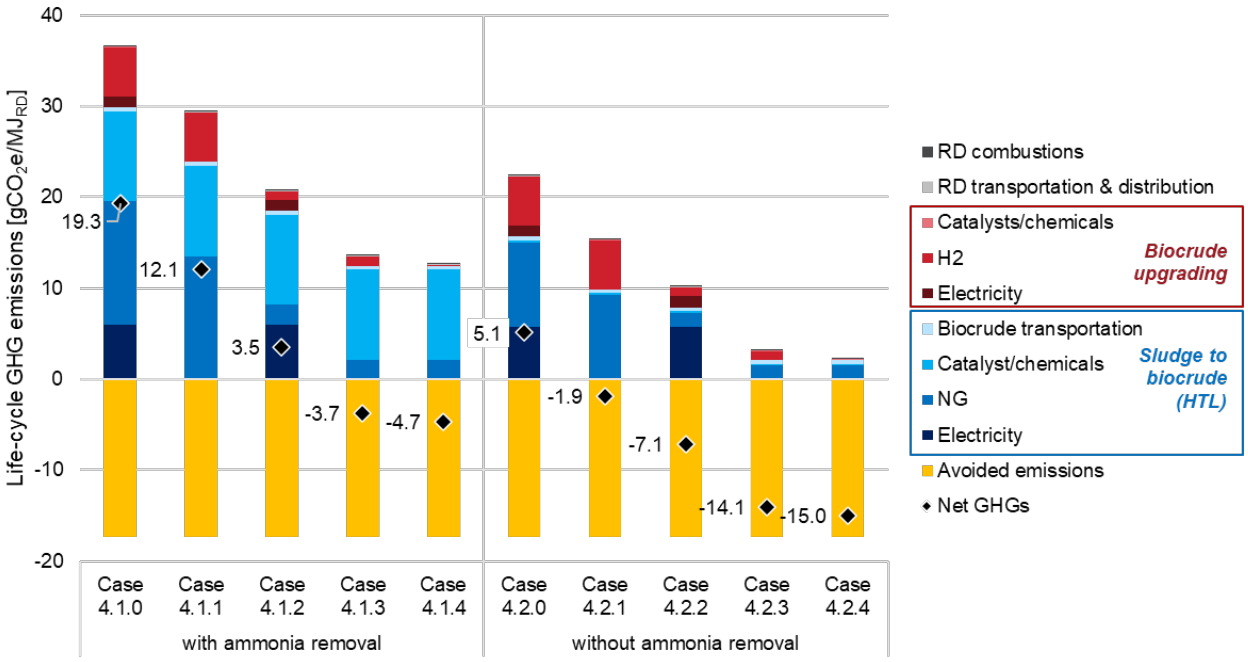


Figure 21. Life cycle GHG emissions ($gCO_2e/MJ$) of wet waste sludge to RD production via HTL

Case 4.1.0 uses the process fuels from a conventional energy system. The GHG emissions during the HTL (sludge-to-biocrude) process are 29.9 $gCO_2e/MJ$, with 45% from fossil NG, 33% from catalyst/chemical inputs, and 20% from grid electricity, including the impact of quicklime (CaO; CI of 1.3 $gCO_2e/g$ CaO) for ammonia removal process, leading to 9.7 $gCO_2e/MJ$ of GHG emissions. $H_2$ and electricity inputs for the biocrude upgrading process bring 5.4 and 1.2 $gCO_2e/MJ$, respectively. The CI of Case 4.1.0 is 19.3 $gCO_2e/MJ$ with significant avoided emissions credits (−17.3 $gCO_2e/MJ$), which is 79% lower than the CI of conventional diesel (90.5 $gCO_2e/MJ$). For Cases 4.1.1–4.1.3, grid electricity and fossil NG are replaced by renewable electricity and landfill-based RNG, which reduce the CIs by 7.2 and 15.7 $gCO_2e/MJ$, respectively. For Case 4.1.3, with renewable electricity and RNG, the CI becomes −3.7 $gCO_2e/MJ$. It is noted that landfill-based RNG is used for the heat source and also for on-site $H_2$ SMR. In Case 4.1.4, using renewable $H_2$ instead of landfill gas SMR $H_2$ gives 1 $gCO_2e/MJ$ of CI reduction compared to Case 4.1.3.

Compared to Case 4.1.0 with ammonia removal, the net GHG emissions of Case 4.2.0 are decreased by 14.2 $gCO_2e/MJ$ from deducted inputs of CaO (9.7 $gCO_2e/MJ$), fossil NG (4.3 $gCO_2e/MJ$), and grid electricity (0.2 $gCO_2e/MJ$) for the ammonia removal process. The CIs of Case 4.2 range from −15.0 to 5.1 $gCO_2e/MJ$, which are 94%–117% lower than the CI of conventional diesel.

### 3.4.3 TEA Results and Discussions on Key Metrics (Carbon Efficiency, Energy Efficiency, and Cost)

The TEA results are summarized in Figure 22 for the HTL biocrude production section and Figure 23 for the HTL biocrude upgrading section. The results are shown in terms of minimum biocrude selling price (in dollars per gallon gasoline equivalent), which is the biocrude intermediate selling price that makes the net present value of the process equal to zero under the $n^{th}$ plant assumptions. Uncertainty in the future cost of renewable resources—namely NG, electricity, and $H_2$ (as listed in Table 13)—is considered and shown as error bars in Figures 22 and 23. The biocrude selling prices for the two base case scenarios (using fossil-based resources throughout the process flowsheets) are $2.11/GGE and $1.79/GGE for Cases 4.1.0 and 4.2.0, respectively. Case 4.1.0 has a higher cost than Case 4.2.0 due to the extra capital cost ($0.15/GGE) and operating cost ($0.13/GGE for lime and natural gas) required for ammonia removal from the aqueous phase. Moreover, the ammonia removal step also increases labor and electricity costs, resulting in an MFSP increase by $0.04/GGE.

Process economics are evaluated from an additional four process scenarios as described in Table 13 considering incremental incorporation of renewable resources into the process flowsheet. The baseline cost of renewable electricity is assumed to be equal to the average grid electricity cost ($0.068/kWh in Table 3). Therefore, applying the renewable electricity in Cases 4.1.1 and 4.2.1 does not have any impact on the overall process economics. A range of renewable electricity costs ($0.02–$0.10/kWh vs. $0.068/kWh baseline) is also considered in this analysis. Using the lowest renewable electricity cost and highest electricity costs resulted in the error bars of Cases 4.1.1 and 4.2.1. These error bars are insignificant because electricity cost and electricity consumption are not major cost contributors (light blue bars in Figure 22) in the HTL biocrude production process. On the other hand, natural gas cost contributes more significantly (yellow bars in Figure 22) in the HTL biocrude production. While the baseline cost of renewable natural gas is assumed at $12/MMBtu (vs. $3.39/MMBtu fossil NG), using renewable natural gas in Cases 4.1.2 and 4.2.2 could potentially increase production costs by $0.24/GGE and $0.17/GGE for the process with and without the ammonia removal step, respectively. Renewable natural gas price could be up to nine times higher than fossil natural gas ($3.39/MMBtu NG vs. $7.48–$29.44/MMBtu RNG), which would add at least $0.50/GGE to the price of the HTL biocrude, as shown by the error bars presented in Cases 4.1.2, 4.1.3, and 4.1.4.

Cases 4.1.3 and 4.2.3 consider the use of both renewable electricity and renewable natural gas. The HTL biocrude costs are the same between Cases 4.1.2 and 4.1.3, and also the same

between Cases 4.2.2 and 4.2.3. This is because renewable and grid electricity have the same baseline costs at $0.068/kWh. In addition, green hydrogen such as electrolysis-based hydrogen is brought in the analysis of Cases 4.1.4 and 4.2.4. It is found that green hydrogen doesn't impact the TEA results for the biocrude production since hydrogen is not required for this conversion step.

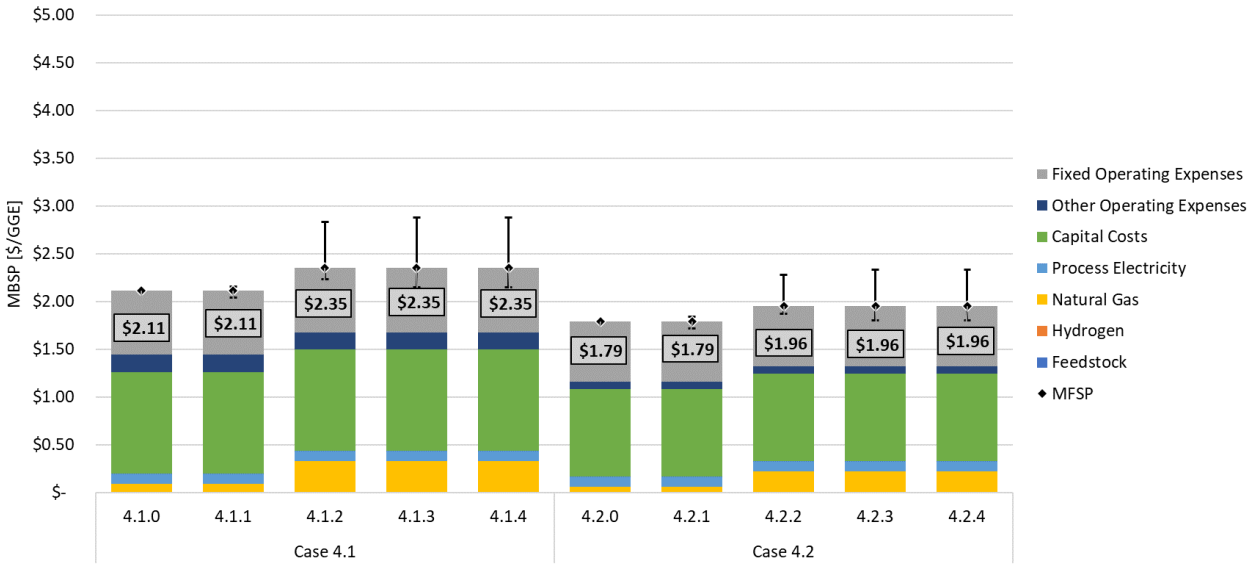


Figure 22. TEA results of HTL biocrude production from wet waste feedstock via the HTL process

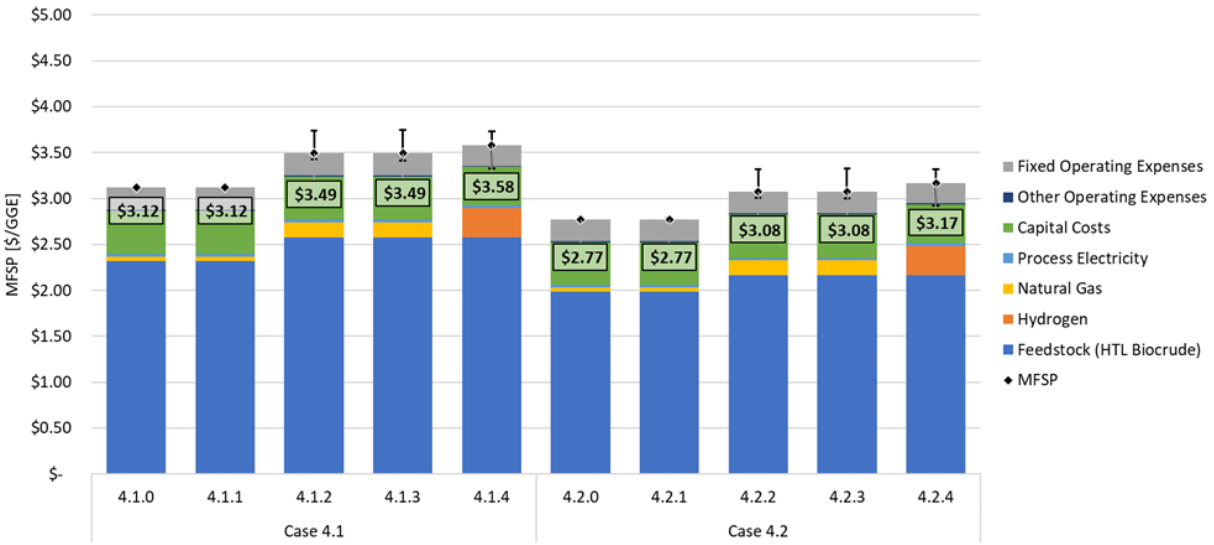


Figure 23. TEA results of hydrocarbon fuel blendstock production via hydroprocessing of HTL biocrude (HTL biocrude upgrading)

Figure 23 presents the minimum fuel selling prices of hydrocarbon fuel blendstocks from the wet waste HTL pathway. This analysis assumes that 10 HTL plants will supply 2,700 barrels per stream day of biocrude to a centralized biocrude upgrading plant. For each process scenario

analysis, a transportation cost of $0.09/GGE biocrude (assumption for a 100-mile shipping radius) is added to the HTL biocrude selling prices presented in Figure 22. TEA results in Figure 23 show that HTL biocrude cost (dark blue bars) is the biggest cost contribution among other operating and capital costs. The feedstock cost ranges from 68% (Case 4.2.4) to 75% (Cases 4.1.0 and 4.1.1) of the MFSP. Capital-related cost is the second-biggest cost contribution to MFSP. Labor or fixed operating expense is the third-biggest cost contribution to MFSP for the process without green hydrogen. Green hydrogen cost is approximately $0.10/GGE more expensive than the labor cost in Cases 4.1.4 and 4.2.4. Similar to the TEA results of HTL biocrude production, the more expensive cost of renewable natural gas gives significant impacts on the overall process economics. Replacing fossil natural gas by renewable natural gas would add at least $0.12/GGE to MFSP (Case 4.1.1 vs. Case 4.1.2 and Case 4.2.1 vs. Case 4.2.2).

Carbon efficiency and thermal efficiency were evaluated for the conversion steps only (wet waste HTL to biocrude and biocrude upgrading to hydrocarbon fuel). Carbon efficiency is defined as the ratio of carbon content of the product to carbon from feed plus NG, as expressed in Equation 3. The thermal efficiency (lower heating value basis) calculation is shown in Equation 4. It is the ratio of the heating value of hydrocarbon fuel product to the heating value of feed, NG, electricity, and hydrogen (renewable $H_2$ for Cases 4.1.4 and 4.2.4). Both carbon and thermal efficiencies are summarized in Table 15.

$$C_{eff} = \frac{C_{product}}{C_{feed}+C_{NG}} \quad (3)$$

$$Ther_{eff} = \frac{LHV_{product}}{LHV_{feed}+LHV_{NG}+LHV_{H2}+Electricity} \quad (4)$$

Table 15. Carbon efficiency and thermal efficiency for conversion processes

| Case Study | Wet Waste HTL | | Case Study | Biocrude Upgrading | | Note |
|---|---|---|---|---|---|---|
| | Carbon Efficiency | Thermal Efficiency | | Carbon Efficiency | Thermal Efficiency | |
| 4.1.0 to 4.1.4 | 65.5% | 68.8% | 4.1.0 to 4.1.3 | 83.2% | 85.9% | With $NH_3$ removal process |
| | | | 4.1.4 | 88.9% | 88.0% | With $NH_3$ removal process + green $H_2$ |
| 4.2.0 to 4.2.4 | 67.5% | 72.0% | 4.2.0 to 4.2.3 | 83.2% | 85.9% | Without $NH_3$ removal process |
| | | | 4.2.4 | 88.9% | 88.0% | Without $NH_3$ removal process + green $H_2$ |

*Carbon Efficiency*

The results in Table 15 were generated under the assumption of comparable carbon content and energy content between NG and RNG. Carbon input is carbon content of sludge and natural gas for the HTL process, and it is carbon content of biocrude and natural gas for the upgrading process. Carbon output is carbon content of HTL biocrude for the HTL process, and it is carbon content of hydrocarbon fuel for the upgrading process. Since carbon efficiency depends on the carbon input and the carbon output, the carbon efficiency is kept constant for each process flowsheet design (with vs. without ammonia removal step), even though the renewable resource

is incrementally applied. For the HTL process, the carbon efficiency of the process flowsheet without ammonia removal (Cases 4.2.X) is better than that of the process flowsheet with ammonia removal (Cases 4.1.X) due to natural gas used in the THROX reactor. Note that x refers to scenarios defined in Table 13. For the upgrading process, carbon efficiency is improved when green hydrogen is applied (Cases 4.1.4 and 4.2.4) due to less natural gas required to produce less amount of hydrogen via the steam reforming process.

*Thermal Efficiency*

For a conversion process (HTL process or upgrading process), process thermal efficiency is a ratio of energy content of the product to total energy content of the feed. Correspondingly, for the thermal efficiency comparison, both natural gas and electricity consumption in the ammonia removal step reduce the process thermal efficiency of the HTL process. Thermal efficiency of the process flowsheet with ammonia removal (Case 4.1.X) is reported at 69%, while it is up to 72% for the flowsheet without ammonia removal (Case 4.2.X). In addition, for the upgrading process, the thermal efficiency is improved in Cases 4.1.4 and 4.2.4. This is because green hydrogen is used and the process requires less natural gas for the steam reforming process.

### 3.4.4 Key Learnings

*Key Learnings – LCA*

- Using wastewater sludge as a feedstock of RD brings two advantages from an LCA perspective. First, like other biofuels, the biogenic carbon in sludge is carbon neutral when released into atmosphere as $CO_2$ emissions. In addition, using sludge leads to avoiding GHG emissions from conventional sludge management practices. As a result, the CI of the base case (Case 4.1.0) is 19.3 $gCO_2e/MJ$, which is 79% lower than conventional diesel. With the intervention of all renewable energy sources in Case 4.1.4, the CI of renewable diesel is reduced to −3.8 $gCO_2e/MJ$. It shows the potential of reaching net-zero fuels with the help of avoided emissions.

- Using quicklime (CaO) for the ammonia removal generates 9.7 $gCO_2e/MJ$ in Case 4.1. However, considering that the future technology may not need the ammonia removal process (Case 4.2), the CIs of RD go down to 5.1 $gCO_2e/MJ$ in Case 4.2.0, and further decrease to −14.1 $gCO_2e/MJ$ using renewable energy sources in Case 4.2.4.

- When comparing to the algae HTL case analyzed in a previous study [2], the wet waste HTL pathway has a lower CI, mainly due to avoiding emissions related to algae growth (e.g., $CO_2$ capture and transportation and energy inputs for algae growth) and additional GHG emissions credits from the conventional sludge management practices. It presents the benefit of using waste feedstocks compared to typical biomass feedstocks.

*Key Learnings – TEA*

- Biocrude minimum selling prices for two base case scenarios (using fossil-based resources throughout the process flowsheets) are $2.11/GGE and $1.79/GGE for the process flowsheet with and without aqueous phase treatment.

- Minimum fuel selling prices for two base case scenarios (using fossil-based resources throughout the process flowsheets) are $3.12/GGE and $2.77/GGE for the process flowsheet with and without aqueous phase treatment.

- For the range of electricity cost studied, process economics are not significantly impacted. This is because electricity cost and electricity consumption are not major cost contributors for the HTL process.

- Natural gas cost is one of the largest operating costs in the wet waste HTL and biocrude upgrading pathway. Using renewable natural gas could increase the biocrude production cost by $0.20–$0.50 per GGE biocrude (for the cases including HTL aqueous-phase ammonia removal). Moreover, the most expensive cost of RNG (at $29.44/MMBtu) could increase the final product fuel cost by at least $0.10/GGE.

- Renewable hydrogen could increase the MFSP by $0.10/GGE.

# 3.5 Case 5 – DAC $CO_2$ to SAF

## 3.5.1 Process Design

This assessment provides a conceptual process design for $CO_2$ to SAF via DAC and Fischer–Tropsch synthesis. The process model from $CO_2$ to SAF was built in Aspen Plus and excluded the DAC system. The DAC performance metrics used in this analysis, including cost and energy consumption, were reported in a review by Fasihi et al. [41]. This analysis selected a low-temperature solid sorbent DAC system as the basis due to their favorability for both cost and energy use relative to high-temperature aqueous solution DAC systems [42]. The energy requirement, capital costs, assumed scale, and other key parameters for the selected DAC system are shown in Table 16.

Table 16. Key parameters of the DAC system (adopted from Fasihi et al. [41], converted key metrics to U.S. ton and U.S. dollar basis)

| Metric | Value | Unit |
|---|---|---|
| Technology type | Low-temperature solid sorbent | |
| Baseline capacity | 3,968 | ton $CO_2$/year |
| Capital scaling exponent | 0.89 | Assumed |
| Capital expenses | 1,216 | \$/ton $CO_2$ annually |
| Electricity demand | 630 | kWh/ton |
| Thermal demand | 1,890 | kWh/ton |

The baseline plant scale for Case 5 was selected to reflect a similar scale as that of Case 3 to create an even comparison between the Fischer–Tropsch synthesis and highlight the impact of exchanging the upstream technologies. The base case scenario for Case 3 (Case 3.1.0) yields about 46 million GGE of fuel per year. To achieve a similar scale, Case 5 scenarios require about 620,000 tons $CO_2$ per year. The high-purity $CO_2$ from the DAC system is fed to a $CO_2$ electrolyzer with a single-pass conversion of $CO_2$ of 43%. CO is separated from the $CO_2$-CO mixture via pressure swing adsorption, and unconverted $CO_2$ is recycled to the electrolyzer. CO is compressed to 28.5 bar (415 psia) and mixed with imported $H_2$ to an $H_2$:CO ratio of 2.15. The syngas is then directed to the Fischer–Tropsch synthesis area. FT synthesis is operated under the same conditions as those described in Case 3. Products are separated into gasoline-, diesel-, and jet-range hydrocarbons via distillation. Light hydrocarbons are combusted as a process fuel to generate heat and electricity in a combined heat and power unit, and flue gases are vented to the atmosphere in the base case. FT synthesis also produces a wax product, which is sold as a coproduct. A simplified process flow diagram for the $CO_2$-to-SAF pathway is depicted in Figure 24.

A summary of the $CO_2$-to-SAF cases is given in Table 17. The base case scenario (Case 5.1) for the $CO_2$-to-SAF pathway requires imported electricity and natural gas for the DAC process, electricity for electrochemical conversion of $CO_2$ to CO, and $H_2$ for syngas formation. The sub-cases labeled 5.1.0 through 5.1.3 assess the impact of successively implementing renewable electricity, RNG, and renewable $H_2$ on the TEA and LCA results.

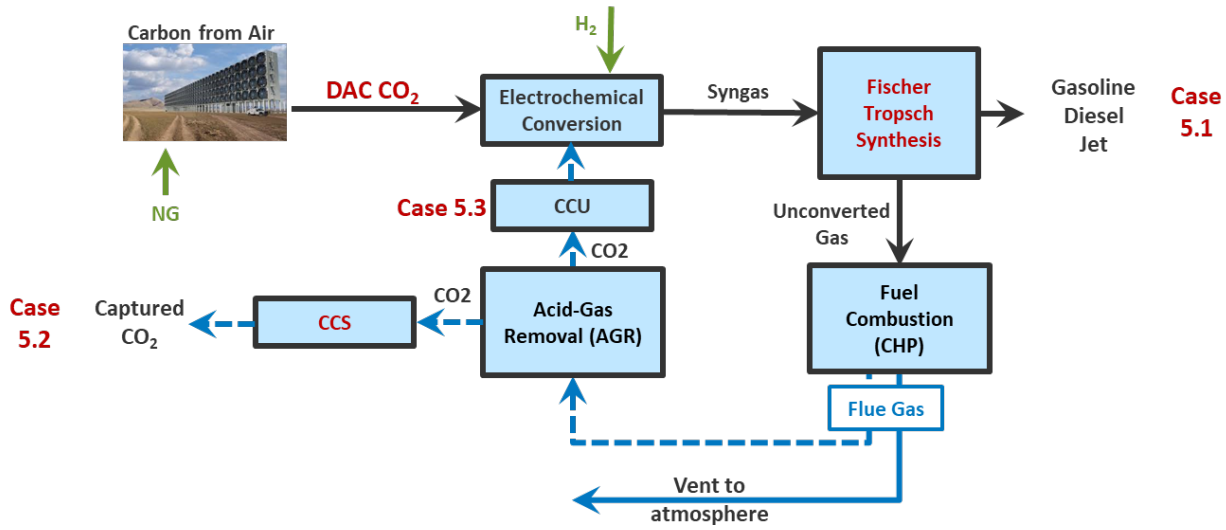


Figure 24. Block flow diagram for Case 5, $CO_2$ to fuels via DAC, electrochemical conversion, and Fischer–Tropsch synthesis

Additionally, Case 5 also implements CCS (Case 5.2) and CCU (Case 5.3) scenarios. In this process design, the primary source of carbon loss is through flue gas $CO_2$. Therefore, an amine scrubbing system is installed in both the CCS and CCU cases to capture and purify the flue gas $CO_2$. The amine scrubber is assumed to capture 96% of the flue gas carbon. The CCS scenario, Case 5.2, compresses the captured $CO_2$ to 152.7 bar (2,215 psia) with interstage dehydration, as described in previous cases. Case 5.3 (CCU) recycles the captured $CO_2$ to the electrolysis unit to maximize carbon utilization for fuel production. Like Case 5.1, these scenarios also consider the sequential addition of renewable interventions to understand their effect on both cost and environmental impacts.

Table 17. Summary of Case 5 scenarios and key interventions

| Case Number | AGR $CO_2$ | Flue Gas $CO_2$ | Electricity | Fuel | Hydrogen |
|---|---|---|---|---|---|
| Case 5.1.0 | N/A | Vented | U.S. mix | Offgases + NG | Fossil $H_2$ |
| Case 5.1.1 | N/A | Vented | RE | Offgases + NG | Fossil $H_2$ |
| Case 5.1.2 | N/A | Vented | RE | Offgases + RNG | Fossil $H_2$ |
| Case 5.1.3 | N/A | Vented | RE | Offgases + RNG | Renewable $H_2$ |
| Case 5.2.0 | N/A | CCS | U.S. mix | Offgases + NG | Fossil $H_2$ |
| Case 5.2.1 | N/A | CCS | RE | Offgases + NG | Fossil $H_2$ |
| Case 5.2.2 | N/A | CCS | RE | Offgases + RNG | Fossil $H_2$ |
| Case 5.2.3 | N/A | CCS | RE | Offgases + RNG | Renewable $H_2$ |
| Case 5.3.0 | N/A | CCU | U.S. mix | Offgases + NG | Fossil $H_2$ |
| Case 5.3.1 | N/A | CCU | RE | Offgases + NG | Fossil $H_2$ |
| Case 5.3.2 | N/A | CCU | RE | Offgases + RNG | Fossil $H_2$ |
| Case 5.3.3 | N/A | CCU | RE | Offgases + RNG | Renewable $H_2$ |

### 3.5.2 LCA Results and Discussions

*LCA Cases and Inventories*

Figure 25 shows the schematic diagram of Case 5, FT fuel production using DAC $CO_2$ captured from the air. Captured $CO_2$ is then converted to CO through electrochemical conversion ($CO_2$ electrolysis) and mixed with $H_2$. FT synthesis is a chemical reaction process producing FT fuels using imported $H_2$ and CO from $CO_2$ electrolysis. The FT synthesis process has a 75% carbon conversion efficiency. The remaining 25% of carbon is combusted and vented to the atmosphere in Case 5.1, while the flue gas is captured again for CCS in Case 5.2 or for CCU in Case 5.3. The process also coproduced wax, similar to Case 3.

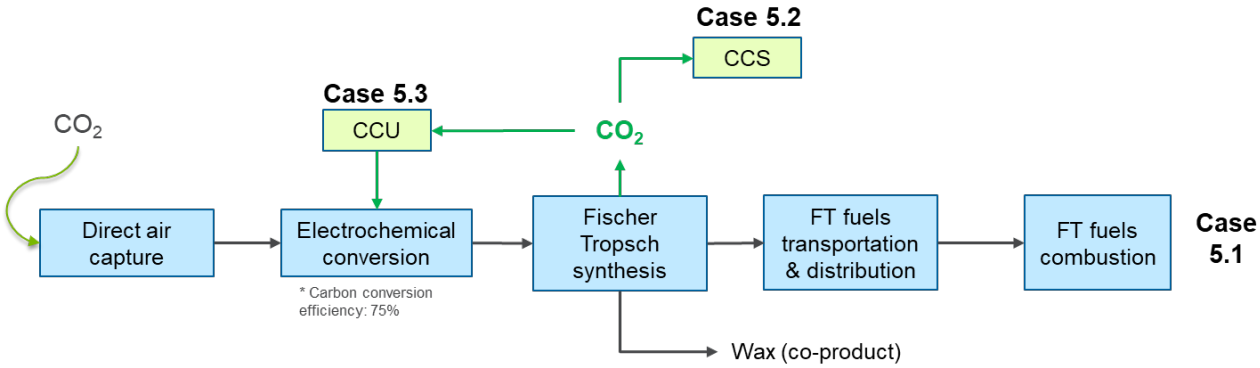


Figure 25. The schematic flow diagram of the life cycle pathways of Case 5, which include direct air capture, electrochemical conversion, FT synthesis, FT fuel transportation and distribution, and FT fuel combustion. Case 5.2 applies additional CCS and Case 5.3 applies additional CCU.

Table 18 presents the energy and material inputs and outputs of Case 5. In Cases 5.1 and 5.2, the input DAC $CO_2$ feedstock is 105 g to produce 1 MJ of FT fuels. Case 5.2 captures and sequesters 25 g of $CO_2$ with an additional 0.01 MJ of electricity and 0.01 g of chemical inputs. To produce 1 MJ of FT fuel, Case 5.3 also needs 105 g of $CO_2$ from 80 g of DAC $CO_2$ and 25 g of additional $CO_2$ captured from the electrochemical conversion process.

Table 18. Life cycle inventory of Case 5: DAC $CO_2$ to FT fuel

| per MJ of FT fuels | Unit | Case 5.1 | Case 5.2 | Case 5.3 |
|---|---|---|---|---|
| DAC $CO_2$ feedstock | g | 105 | 105 | 80 |
| Natural gas for DAC | MJ | 0.8 | 0.8 | 0.6 |
| Electricity for DAC | MJ | 0.3 | 0.3 | 0.2 |
| Electricity for electrochemical conversion | MJ | 1.4 | 1.4 | 1.4 |
| Electricity for CCS | MJ | N/A | 0.01 | N/A |
| $H_2$ for FT synthesis | MJ | 1.2 | 1.2 | 1.2 |
| Catalysts/chemicals | g | 0.06 | 0.07 | 0.06 |
| Sequestrated $CO_2$ | g | N/A | 25 | N/A |
| Coproduced electricity | MJ | 0.13 | 0.13 | 0.13 |
| Coproduced wax | MJ | 0.12 | 0.12 | 0.12 |

For Cases 5.1–5.3, NG and electricity are used to capture 105 g or 80 g of $CO_2$ in the air. Electricity input for the electrochemical conversion process is 1.4 MJ to produce 1 MJ of FT fuels from 105 g of $CO_2$ in all cases. Coproduced electricity is assumed to be used internally for electrochemical conversion. Wax is assumed to displace residual oil, providing displacement GHG emissions credits.

*LCA Results*

LCA results of Case 5 are presented in terms of the life cycle GHG emissions in Figure 26. The group of blue, green, and orange bars represent GHG emissions during DAC, fuel conversion/CCU, and CCS process, respectively. For all the cases, $CO_2$ emissions are considered carbon neutral because carbon is from the atmosphere, while $CH_4$ and $N_2O$ emissions lead to small amounts of combustion GHG emissions (0.1 $gCO_2e/MJ$).

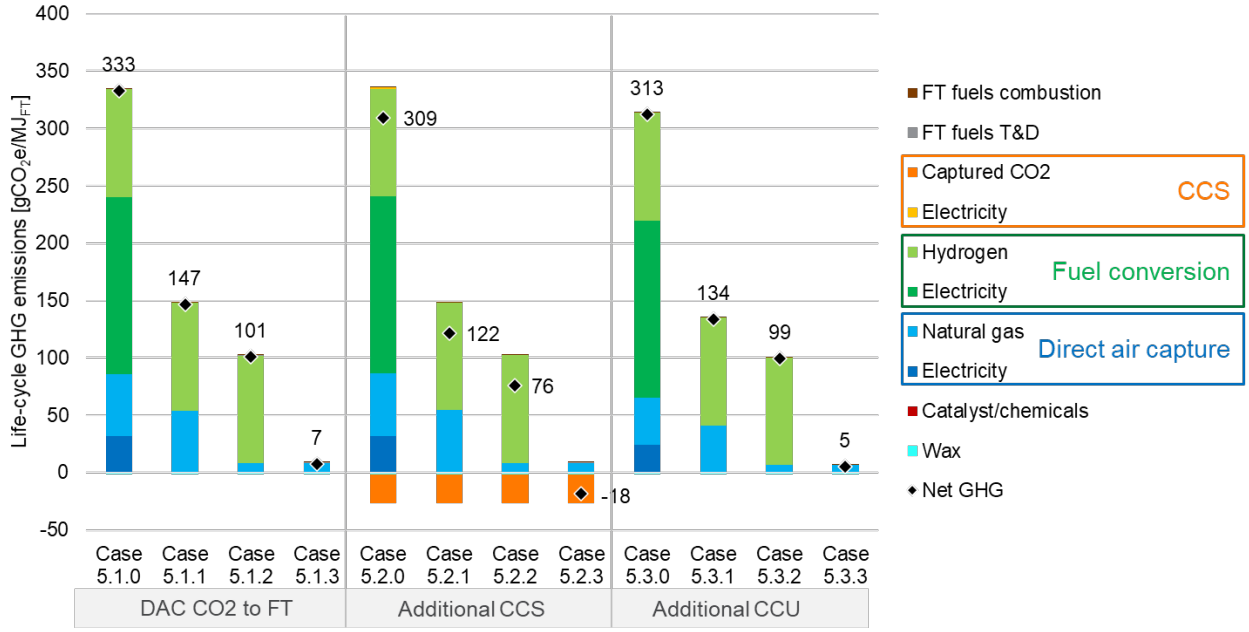


Figure 26. Life cycle GHG emissions ($gCO_2e/MJ$) of DAC $CO_2$ to FT fuel production via electrochemical conversion and FT synthesis

In Case 5.1.0, life cycle GHG emissions are estimated at 333 $gCO_2e/MJ$, which is 3.9 times higher than the CI of conventional jet fuel (84.5 $gCO_2e/MJ$). GHG emissions from the fuel conversion process are 154 $gCO_2e/MJ$ by using grid electricity and 94 $gCO_2e/MJ$ by using NG SMR $H_2$. In addition, the DAC process generates the GHG emissions by using fossil NG (54 $gCO_2e/MJ$) and grid electricity (32 $gCO_2e/MJ$). Wax, catalyst/chemicals, FT fuels transportation and distribution, and combustion are minor contributors with −1.5, 0.2, 0.3, and 0.05 $gCO_2e/MJ$, respectively. In Cases 5.1.1–5.1.3, renewable energy sources are incrementally applied to reduce the CIs. Using renewable electricity, landfill gas-derived RNG, and renewable $H_2$ reduce 186, 46, and 94 $gCO_2e/MJ$ of GHG emissions, respectively. In Case 5.1.3, DAC $CO_2$ FT with all renewable

energy inputs, the CI becomes 7 $gCO_2e/MJ$, which reduces the CI 92% compared to the petroleum jet fuel.

In Cases 5.2.0–5.2.3, additional CCS brings −25.5 $gCO_2e/MJ$ of emissions. Grid electricity for CCS adds 1.3 $gCO_2e/MJ$, which makes the CI of Case 5.2.0 309 $gCO_2e/MJ$. By using the renewable electricity, NG, and $H_2$, the CIs are reduced to 121, 76, and −18 $gCO_2e/MJ$, respectively in Cases 5.2.1–5.2.3.

Cases 5.3.0–5.3.3 implement CCU to produce additional FT fuel using the captured $CO_2$ from flue gas along with 80 g of DAC $CO_2$. Thus, GHG emissions from the DAC process decrease 24% compared to Case 5.1. However, the fuel conversion is the same as in the base cases; 105 g of $CO_2$ is converted to 1 MJ of FT fuel. GHG emissions from the fuel conversion process become 154 $gCO_2e/MJ$ when using conventional energy sources, which means CCU alone may not provide CI reduction benefits compared to Case 5.1 while generating more fuels. Similarly, by employing renewable energy inputs, the CI of DAC with additional CCU can reach 5 $gCO_2e/MJ$ in Case 5.3.3.

### 3.5.3 TEA Results and Discussions on Key Metrics (Carbon Efficiency, Energy Efficiency, and Cost)

*MFSP*

Figure 27 summarizes the results for Case 5. The results show the relative cost contributions of different capital and operating expenses for each of the sub-cases. Each sub-case result also highlights the cost uncertainty for renewable resources by including error bars for the minimum and maximum cost scenarios.

The MFSP of the base case scenario (Case 5.1.0) was $10.95/GGE, with a total fuel yield of 43.8 million GGE per year. The two largest cost drivers were $CO_2$ feedstock costs, which contributed $3.81/GGE, and process electricity, which contributed $2.92/GGE. It is important to note that the $CO_2$ feedstock costs include the associated capital and operating expenses required by the DAC system. The operating expenses for DAC $CO_2$ include both natural gas and electricity; cost variations for the green scenarios of these resources will be reflected within the feedstock cost.

The base case scenario with all green interventions (i.e., renewable electricity, RNG, and green $H_2$) is shown by Case 5.1.3 and resulted in an MFSP of $15.26/GGE. A significant portion of the increase is due to the high baseline cost of green $H_2$, which contributes a total of $5.40/GGE versus only $1.93/GGE in Case 5.1.0. The overall MFSP range for Case 5.1.3 spans from $8.52/GGE in the low-cost scenario to $20.80/GGE in the high-cost scenario.

Implementing CCS to sequester flue gas $CO_2$ raised the MFSP by $0.19/GGE in each scenario (Cases 5.2.0–5.2.3). The resulting MFSP for the all-renewable intervention case (Case 5.2.3) ranges from $8.70–$21.01/GGE. Cases 5.3.0–5.3.3 assessed utilizing flue gas capture to

recover and recycle lost carbon. Relative to the base case, additional capital and operating expenses were incurred from the amine scrubber system; however, the MFSP decreased by about $1.01/GGE in each sub-case. This interesting result is primarily due to the cost of flue gas carbon capture being significantly less than that of direct air capture. Thus, by recovering "high-cost" lost carbon (DAC carbon), the process feedstock is supplemented by a "low-cost" $CO_2$ source. The total fuel yield increased to 57.9 million GGE per year in Case 5.3 at the same total DAC feedstock flow rate (620,000 tons $CO_2$ per year).

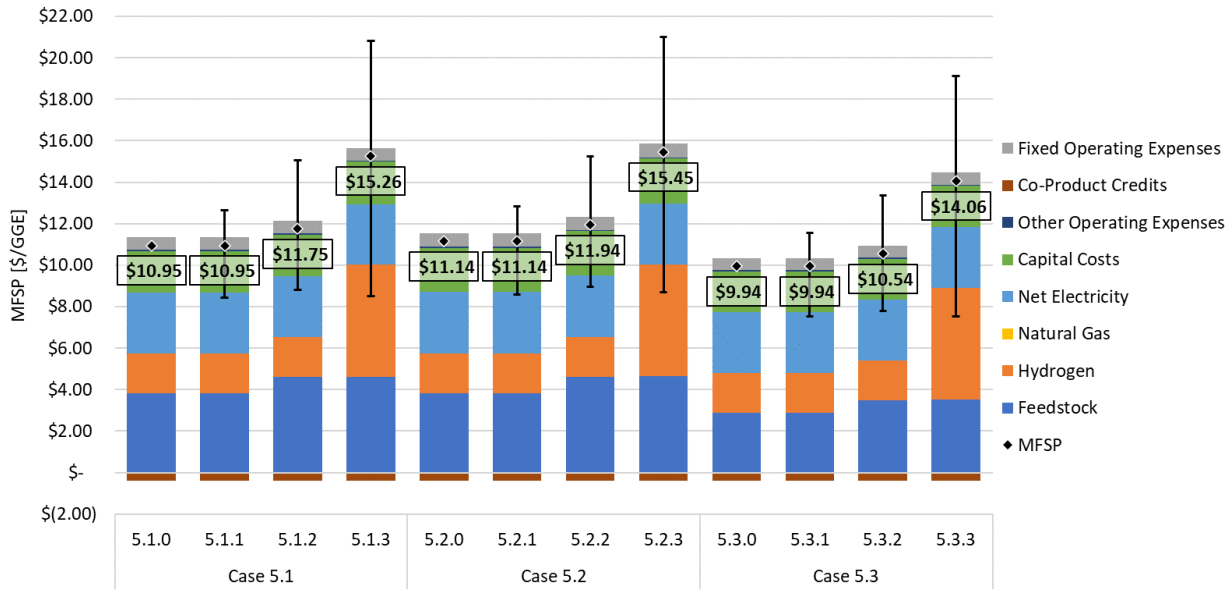


Figure 27. MFSP cost contribution breakdown of Case 5 scenarios ($/GGE)

*Carbon Efficiency*

The carbon efficiency of Case 5 was calculated downstream from the DAC system, and thus the denominator for efficiency was $CO_2$ fed to the electrolyzer. This ignores the carbon efficiency of the DAC system itself. Under these assumptions, Case 5.1.0 resulted in a total carbon efficiency to fuels of 66.8%, as shown in Figure 28. Another 8% of the total fed carbon was attributed to the wax coproduct, and the remaining carbon was vented to the atmosphere in the combined heat and power flue gas.

Cases 5.2 and 5.3 implemented two strategies to minimize the carbon vented to the atmosphere: CCS and CCU. Case 5.2.0 did not improve total carbon efficiency to fuels; however, 96% of the carbon vented to the atmosphere in Case 5.1.0 was captured and sequestered. Case 5.3.0 recycled the captured carbon to the electrolyzer to generate CO and ultimately more syngas for fuel production. This case resulted in the greatest carbon efficiency at 88.2%, with only 1.2% of the carbon being vented to the atmosphere.

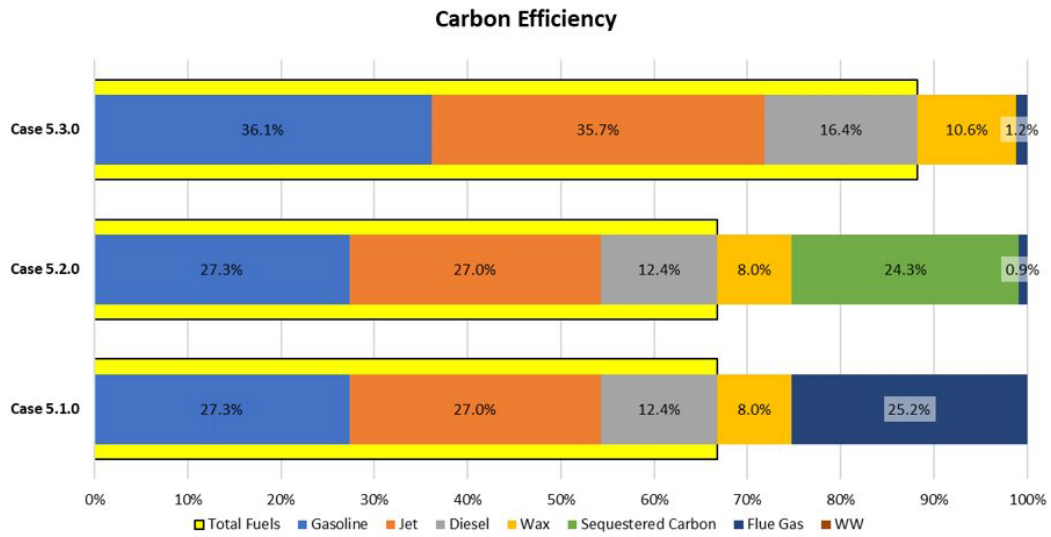


Figure 28. Carbon efficiency breakdown of Case 5 scenarios. Yellow border represents total carbon efficiency to fuels.

*Energy Efficiency*

The energy efficiency was calculated as the ratio of the lower heating value of fuels produced, divided by the lower heating value of the energy inputs. $CO_2$ does not have any inherent heating value, and as such did not contribute to the energy consumption, as illustrated in Figure 29.

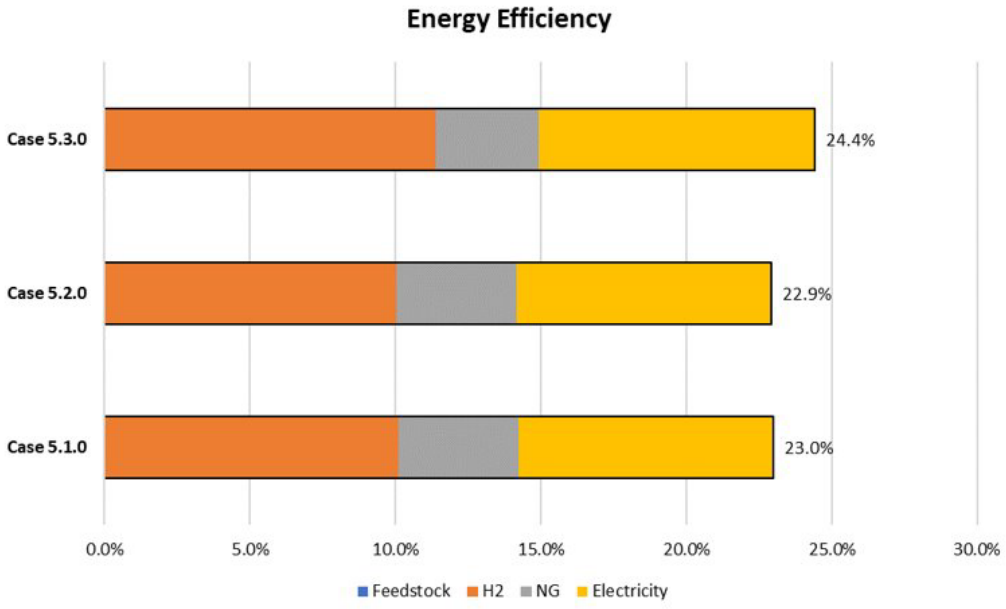


Figure 29. Energy efficiency breakdown for Case 5 scenarios

As shown in Figure 29, each Case 5 sub-case resulted in an energy efficiency between 22.9%–24.4%. Hydrogen and electricity were the largest contributors to the energy consumption. Case 5.2.0 resulted in the lowest energy efficiency at 22.9% due to the additional electricity consumption from compression without a corresponding increase in fuel yield. Case 5.3.0 was the most energy efficient of the three cases at 24.4%. The boost in efficiency resulted from an increased fuel yield due to less energy-intensive $CO_2$ separation from flue gas versus ambient air.

### 3.5.4 Key Learnings

*Key Learnings – LCA*

- DAC $CO_2$ to FT fuel is an energy-intensive technology that requires 1.2 MJ of $H_2$, 0.4 MJ of NG, and 0.5 MJ of electricity per MJ fuel. Thus, without using renewable energy, the DAC $CO_2$ FT process does not provide CI reduction benefits. Using conventional energy sources makes the CI of FT fuel 3.9 times higher (333 $gCO_2e$/MJ) compared to conventional jet fuel (84.5 $gCO_2e$/MJ) in Case 5.1.0. CCS or CCU may not help reduce the CIs if the same conventional energy sources are used. Case 5.2.0 (CCS) and Case 5.3.0 (CCU) show similar CIs—309 and 313 $gCO_2e$/MJ, respectively—compared to the base Case 5.1.0.

- Because DAC $CO_2$ to FT highly relies on electricity, natural gas, and $H_2$, shifting to renewable energy sources significantly reduces the CIs of the products. For example, the CI becomes 7 $gCO_2e$/MJ using the renewable energy sources in Case 5.1.3.

- Further, unconverted carbon in DAC $CO_2$ can be captured again for CCS (Case 5.2) or CCU (Case 5.3). Energy use of the amine capturing system for capturing $CO_2$ from the flue gas is lower than the low-temperature solid sorbent DAC system due to the higher $CO_2$ concentration of the fuel gas stream compared to the atmosphere. With the additional 0.02 MJ of electricity for CCS, the CI of FT fuel is decreased by 25.5 $gCO_2e$/MJ. For the CCU case, $CO_2$ captured from the flue gas replaces 24% of DAC $CO_2$ feedstock. As a result, implementation of CCU can reduce 0.2 MJ of NG and 0.02 MJ of electricity per megajoule of FT fuel compared to the base case. Once renewable energy sources are used, the CIs of CCS (Case 5.2.3) and CCU (Case 5.3.3) become −18 and 5 $gCO_2e$/MJ, respectively.

*Key Learnings – TEA*

- Both DAC and $CO_2$-to-CO electrolysis are nascent technologies, at TRLs of 2–3, which require significant R&D efforts to be implemented at commercial scale. However, coupling these technologies with the established Fischer–Tropsch technology shows potential for the development of a novel pathway with high carbon efficiency in the baseline design (66.8% in Case 5.1.0) and benefits from the unique decarbonization

potential of DAC. However, low TRL and reliance on renewable resources, namely green $H_2$ and renewable electricity, lead to very high fuel cost in the near term.

- Additional carbon mitigation strategies such as CCS and CCU reduce the amount of $CO_2$ released to the atmosphere in this process. CCS technologies are relatively higher TRL, and sequestration has key environmental benefits, but this strategy does not recover the costs of expensive DAC $CO_2$ and does not improve carbon or energy efficiency to fuels. The CCU strategy requires only the addition of an amine flue-gas scrubbing system and can utilize the existing $CO_2$-to-CO framework to improve both carbon and energy efficiency to fuels. As such, more economic value (i.e., reduced fuel costs with improved efficiency) is added by recycling carbon in this process design versus sequestration.

- Each scenario for DAC shows high energy intensity values, indicating inefficient use of high-value renewable resources. Future developments for DAC can improve energy efficiency through reduction of $CO_2$ desorption energy and higher $CO_2$ capture efficiencies. Similarly, future improvements in $CO_2$ electrolysis to reduce the electricity requirements would help to improve the overall energy efficiency of the $CO_2$-to-fuels pathway.

- Due to low TRL and high near-term costs, the DAC $CO_2$-to-SAF pathway should be considered a long-term option for SAF and other fuel production. Improvements to resource costs and technological developments on the DAC and electrolysis technologies can potentially reduce cost and improve energy efficiency enough to make commercialization of this high-carbon-efficiency pathway viable in the long term.

# 4. Discussion

## 4.1 LCA

To achieve GHG emissions reduction goals, we need low- or zero-carbon fuels in many energy and transportation sectors such as aviation, marine, and rail where liquid fuels are needed. The NZTT has analyzed multiple fuel production pathways to examine the potential of producing low- or zero-carbon fuels, which has been continued from our earlier analysis [2]. This study includes five fuel production pathways using biomass and waste feedstocks such as corn, corn stover, woody biomass/forest residues, wastewater sludge, and $CO_2$ from the atmosphere. The conversion processes we analyzed are fermentation, gasification-FT, HTL, and electrochemical-FT, which generate multiple fuel products such as gasoline, diesel, and jet fuels. We also examined CCS and CCU, along with renewable energy options (electricity, $H_2$, and natural gas), which are essential to have net-zero-carbon fuels.

Table 19 presents the life cycle GHG emissions (CIs) of all the cases evaluated in this study. Since renewable and/or CCU/CCS options require significant electricity and $H_2$ inputs while reducing the CIs of the fuels, we parameterized total electricity and $H_2$ inputs to generate a megajoule of fuel. In addition, NG and feedstock inputs are presented to help compare trade-offs among the cases.

First, the results show that the use of renewable energy inputs (electricity, $H_2$, and NG) helps reduce the CIs of the benchmark fuel production pathways. For example, when all these renewable options are applied, CIs are reduced from 78 (Case 1.1.0) to 28 $gCO_2e/MJ$ (Case 1.1.4) for SAF production from corn ethanol; 22 (Case 2.1.0) to 13 $gCO_2e/MJ$ (Case 2.1.3) for SAF production from corn stover ethanol; 19 (Case 4.1.0) to −4 $gCO_2e/MJ$ (Case 4.1.4) for RD production from wet waste HTL; and 333 (Case 5.1.0) to 7 $gCO_2e/MJ$ (Case 5.1.3) for SAF production from DAC. Since the benchmark of Case 3 (Case 3.1.0) utilizes biomass (renewable) to meet the heat and power demand, which already generates quite a low CI of 6 $gCO_2e/MJ$, using renewable energy inputs does not help reduce CI further in this case.

All CCS options added to the benchmark configuration that capture and sequester process $CO_2$ emissions provide significant emissions reductions. Depending on available $CO_2$ emissions that can be captured per megajoule of fuel production, additional CI reduction is estimated at 24–41 $gCO_2e/MJ$. With CCS, it is possible to achieve net negative CI values. Note that CCS leads to a slight increase in electricity consumption for $CO_2$ capture and compression.

On the other hand, when captured $CO_2$ is rather utilized, significant additional energy inputs (electricity and $H_2$) are needed to convert $CO_2$ into valuable products such as SAF. Thus, it is essential to couple with renewable energy inputs to lower the CIs. If conventional energy inputs are used (grid electricity, fossil NG SMR, and fossil NG), CCU cases present CIs even higher than the petroleum fuels. CCU coupled with renewable energy can reduce the CIs while

providing additional fuel outputs from the same amount of feedstocks. However, carbon in fuels would be eventually emitted into the atmosphere, which makes CCU-derived fuels carbon neutral. Although CCU cases do not make carbon-negative fuels, they generate additional products with low CI values.

Both Case 1 and Case 2 generate ethanol through fermentation, which is then converted into SAF. The major difference between the two cases is their feedstocks (corn and corn stover), which leads to the major difference in the LCA results. The benchmark case of Case 1 has a CI of 78 $gCO_2e/MJ$, which is higher than the CI of corn ethanol (53 $gCO_2e/MJ$) [2] due to the additional processes converting ethanol to SAF. With renewable energy inputs, this can be reduced to 28 $gCO_2e/MJ$. In this case, the feasibility of supporting renewable energy sources is the critical part to achieve this. When CCS is considered for high-purity $CO_2$ generated from corn ethanol production (fermentation process) coupled with renewable energy inputs, CI can be reduced to −10 $gCO_2e/MJ$ with additional electricity inputs for $CO_2$ capture and compression. In this case, the infrastructure for $CO_2$ capture/storage would be the key factor. When it comes to CCU, this option significantly reduces the corn feedstock inputs per megajoule of fuel production, from 119 to 81 g/MJ (32% reduction), with the cost of additional electricity and $H_2$ inputs. If we can support renewable electricity and $H_2$ to utilize $CO_2$, the system can generate 47% more fuels from the same amount of corn feedstock with a CI of 21 $gCO_2e/MJ$.

The benchmark of Case 2, corn stover ethanol to jet, has a CI of 22 $gCO_2e/MJ$, which is much smaller than that of Case 1 using corn ethanol. This is mainly because of the difference in feedstocks (corn vs. corn stover). Unlike corn, corn stover is a byproduct of corn farming, so it does not take upstream burdens (energy and chemical uses) associated with corn production. In addition, a portion of corn stover is used to support heat and electricity requirements for ethanol production. Thus, this pathway involves much fewer carbon emissions compared to corn ethanol production, where fossil energy inputs are used. Thus, shifting energy inputs to renewables does not provide significant emissions reduction benefits. When all renewable options are considered, the CI becomes 13 $gCO_2e/MJ$. Due to the low benchmark CI, adding CCS brings the CI down to −19 $gCO_2e/MJ$ with conventional energy inputs, which can be further reduced to −23 $gCO_2e/MJ$ coupled with renewable energy inputs. CCU, on the other hand, may increase the CI when conventional energy inputs are used because of additional electricity and $H_2$ requirements in order to convert $CO_2$ into fuels. If renewable energy inputs are used, the CI can be as low as 11 $gCO_2e/MJ$. Due to additional fuel production from CCU, feedstock inputs would decrease from 150 to 102 g/MJ (32%), while requiring additional electricity and $H_2$ inputs.

We have also evaluated two FT fuel production pathways using woody biomass and $CO_2$ feedstocks for Cases 3 and 5, respectively. The benchmark of Case 3 presents the lowest CI (6 $gCO_2e/MJ$) among all benchmark cases. It is mainly because the fuel conversion processes rely on biomass inputs to meet heat and electricity demand. On the other hand, the benchmark of Case 5 has the highest CI of 333 $gCO_2e/MJ$ among all the benchmark cases, mainly because of significant electricity and $H_2$ inputs to convert DAC $CO_2$ into CO. Thus, even when using the same downstream conversion processes (syngas to FT fuels), the types of feedstocks play an

important role in determining the CI values of the final products. For Case 3, we have evaluated multiple options importing NG or $H_2$. However, these do increase the CI unless the imported $H_2$ is renewable. This means that maximizing the use of internal products is a way to reduce the CIs, especially when the internal products are from biomass. Applying CCU/CCS options leads to similar impacts on the CIs compared to other pathways.

Case 4 uses wastewater sludge to generate RD via HTL. Compared to other cases, the sludge HTL case has quite low feedstock input (69.5 g/MJ) to produce a megajoule of fuel, which means the conversion process has a relatively higher conversion efficiency compared to other cases. Case 4 is the only case that reached negative CIs without CCS with the help of avoided emissions. We have accounted for avoided emissions from conventional sludge management practices. If sludge is not used for RD production, it is likely it is managed in a conventional facility where $CH_4$ emissions are generated, which is why we have emissions credits (negative emissions) associated with the business-as-usual cases. Coupled with renewable energy inputs, Case 4 can reach −3.7 $gCO_2e$/MJ. Note that the value includes the impact of the ammonia removal process, which is expected to be removed in the future. Then, the CI can be further reduced to −14.1 $gCO_2e$/MJ. Compared to the algae-HTL pathway evaluated in the previous report [2], using wastewater sludge provides lower CI values due to the avoided emissions.

As the LCA results show, there are ways to reduce the CIs of various fuel production pathways (combinations of feedstocks, conversion technologies, and final products). However, we also found that there might be trade-offs. In addition, while CCU would increase the production of fuels, it would add up burdens to support additional “renewable” energy requirements. While CCS provides CI reduction with the cost of small marginal electricity inputs, there might be infrastructure constraints (pipeline and/or underground storage) in order for this technology to be applied. Most of all, all these emissions reduction options should be considered along with the TEA results (MFSP) to make the options practically feasible.

Note that the infrastructure impact was not considered in the LCA results. Although this impact, compared to operational impacts, is typically considered small in LCA, further analysis is warranted to capture the contribution from infrastructure such as renewable electricity and $H_2$ production and/or storage.

NZTT will further investigate the CIs of more pathways under the guidance of the Driving Research and Innovation for Vehicle efficiency and Energy sustainability (U.S. DRIVE) partnership and the U.S. Department of Energy to identify how to achieve net-zero-carbon fuels production in the near future. We will also examine both the technical challenges of these fuel production pathways and the opportunities. We believe the LCA results of various conditions documented in this report will help decisions on net-zero-carbon fuel production technologies.

Table 19. CIs of selected cases in this study, along with the electricity, $H_2$, NG, and feedstock inputs for the conversion processes

| Case | | Description | Intervention of Renewable Resources | Feedstock | Product | CI [$gCO_2e/MJ$] | Electricity Inputs [MJ/MJ] | $H_2$ Inputs [MJ/MJ] | NG Inputs [MJ/MJ] | Feedstock Inputs [g/MJ] [a] |
|---|---|---|---|---|---|---|---|---|---|---|
| Case 1 Corn to Ethanol to SAF | Case 1.1.0 | Benchmark | - | Corn | SAF | 78 | 0.09 | 0.06 | 0.49 | 119 |
| | Case 1.1.1 | | RE | Corn | SAF | 67 | 0.09 | 0.06 | 0.49 | 119 |
| | Case 1.1.2 | | RE and RNG | Corn | SAF | 39 | 0.09 | 0.06 | 0.49 | 119 |
| | Case 1.1.3 | | RE, RNG, and renewable $H_2$ | Corn | SAF | 34 | 0.09 | 0.06 | 0.49 | 119 |
| | Case 1.1.4 | | RE, RNG, renewable $H_2$, and GA | Corn | SAF | 28 | 0.09 | 0.06 | 0.49 | 119 |
| | Case 1.2.0 | With additional CCS | - | Corn | SAF w/ CCS | 40 | 0.10 | 0.06 | 0.49 | 119 |
| | Case 1.2.1 | | RE | Corn | SAF w/ CCS | 28 | 0.10 | 0.06 | 0.49 | 119 |
| | Case 1.2.2 | | RE and RNG | Corn | SAF w/ CCS | 1 | 0.10 | 0.06 | 0.49 | 119 |
| | Case 1.2.3 | | RE, RNG, and renewable $H_2$ | Corn | SAF w/ CCS | −4 | 0.10 | 0.06 | 0.49 | 119 |
| | Case 1.2.4 | | RE, RNG, renewable $H_2$, and GA | Corn | SAF w/ CCS | −10 | 0.10 | 0.06 | 0.49 | 119 |
| | Case 1.3.0 | With additional CCU | - | Corn + $CO_2$ | SAF | 120 | 0.27 | 0.41 | 0.49 | 81 |
| | Case 1.3.1 | | RE | Corn + $CO_2$ | SAF | 86 | 0.27 | 0.41 | 0.49 | 81 |
| | Case 1.3.2 | | RE and RNG | Corn + $CO_2$ | SAF | 58 | 0.27 | 0.41 | 0.49 | 81 |
| | Case 1.3.3 | | RE, RNG, and renewable $H_2$ | Corn + $CO_2$ | SAF | 25 | 0.27 | 0.41 | 0.49 | 81 |
| | Case 1.3.4 | | RE, RNG, renewable $H_2$, and GA | Corn + $CO_2$ | SAF | 21 | 0.27 | 0.41 | 0.49 | 81 |
| Case 2 Corn Stover to Ethanol to SAF | Case 2.1.0 | Benchmark | - | Corn stover | SAF | 22 | −0.03 | 0.06 | N/A | 150 |
| | Case 2.1.1 | | RE | Corn stover | SAF | 22 | −0.03 | 0.06 | N/A | 150 |
| | Case 2.1.2 | | RE and renewable $H_2$ | Corn stover | SAF | 17 | −0.03 | 0.06 | N/A | 150 |
| | Case 2.1.3 | | RE, renewable $H_2$, and GA | Corn stover | SAF | 13 | −0.03 | 0.06 | N/A | 150 |
| | Case 2.2.0 | With additional CCS | - | Corn stover | SAF w/ CCS | −19 | −0.01 | 0.06 | N/A | 150 |
| | Case 2.2.1 | | RE | Corn stover | SAF w/ CCS | −19 | −0.01 | 0.06 | N/A | 150 |
| | Case 2.2.2 | | RE and renewable $H_2$ | Corn stover | SAF w/ CCS | −24 | −0.01 | 0.06 | N/A | 150 |
| | Case 2.2.3 | | RE, renewable $H_2$, and GA | Corn stover | SAF w/ CCS | −27 | −0.01 | 0.06 | N/A | 150 |
| | Case 2.3.0 | With additional CCU | - | Corn stover + $CO_2$ | SAF | 76 | 0.20 | 0.41 | N/A | 102 |
| | Case 2.3.1 | | RE | Corn stover + $CO_2$ | SAF | 46 | 0.20 | 0.41 | N/A | 102 |
| | Case 2.3.2 | | RE and renewable $H_2$ | Corn stover + $CO_2$ | SAF | 14 | 0.20 | 0.41 | N/A | 102 |
| | Case 2.3.3 | | RE, renewable $H_2$, and GA | Corn stover + $CO_2$ | SAF | 11 | 0.20 | 0.41 | N/A | 102 |
| Case 3 Biomass Gasification to FT Fuel | Case 3.1.0 | Benchmark, no external energy inputs | - | woody biomass | SAF | 6 | N/A | N/A | N/A | 117 |
| | Case 3.1.1.1 | Import NG for process fuel | Fossil NG | woody biomass | SAF | 26 | N/A | N/A | 0.30 | 99 |
| | Case 3.1.1.2 | | RNG | woody biomass | SAF | 8 | N/A | N/A | 0.30 | 99 |
| | Case 3.1.2.1 | Import gray $H_2$ for tar reforming (250, 1,000, 2,000, 3,000 lbmol/h) | NG SMR $H_2$ | woody biomass | SAF | 9 | N/A | 0.04 | N/A | 114 |
| | Case 3.1.2.2 | | NG SMR $H_2$ | woody biomass | SAF | 16 | N/A | 0.14 | N/A | 105 |
| | Case 3.1.2.3 | | NG SMR $H_2$ | woody biomass | SAF | 25 | N/A | 0.25 | N/A | 94 |
| | Case 3.1.2.4 | | NG SMR $H_2$ | woody biomass | SAF | 31 | N/A | 0.34 | N/A | 86 |
| | Case 3.1.2.1b | Import renewable $H_2$ for tar reforming (250, 1,000, 2,000, 3,000 lbmol/h) | Renewable $H_2$ | woody biomass | SAF | 6 | N/A | 0.04 | N/A | 114 |
| | Case 3.1.2.2b | | Renewable $H_2$ | woody biomass | SAF | 5 | N/A | 0.14 | N/A | 105 |
| | Case 3.1.2.3b | | Renewable $H_2$ | woody biomass | SAF | 5 | N/A | 0.25 | N/A | 94 |
| | Case 3.1.2.4b | | Renewable $H_2$ | woody biomass | SAF | 4 | N/A | 0.34 | N/A | 86 |
| | Case 3.2.0 | With additional CCS | - | woody biomass | SAF w/ CCS | −40 | 0.02 | N/A | N/A | 117 |
| | Case 3.2.1 | | RE | woody biomass | SAF w/ CCS | −42 | 0.02 | N/A | N/A | 117 |
| | Case 3.3.0 | With additional CCU | - | woody biomass + $CO_2$ | SAF | 84 | 0.43 | N/A | N/A | 72 |
| | Case 3.3.1 | | RE | woody biomass + $CO_2$ | SAF | 32 | 0.43 | 0.36 | N/A | 72 |
| | Case 3.3.2 | | RE and renewable $H_2$ | woody biomass + $CO_2$ | SAF | 3 | 0.43 | 0.36 | N/A | 72 |
| Case 4 Wet Waste HTL to RD | Case 4.1.0 | With ammonia removal | - | Wastewater sludge | RD | 19 | 0.059 | N/A | 0.29 | 69.5 |
| | Case 4.1.1 | | RE | Wastewater sludge | RD | 12 | 0.059 | N/A | 0.29 | 69.5 |
| | Case 4.1.2 | | RNG | Wastewater sludge | RD | 3 | 0.059 | N/A | 0.29 | 69.5 |
| | Case 4.1.3 | | RE and RNG | Wastewater sludge | RD | −4 | 0.059 | N/A | 0.29 | 69.5 |
| | Case 4.1.4 | | RE, RNG, and renewable $H_2$ | Wastewater sludge | RD | −4 | 0.062 | 0.071 | 0.20 | 69.5 |
| | Case 4.2.0 | Without ammonia removal | - | Wastewater sludge | RD | 5 | 0.057 | N/A | 0.23 | 69.5 |
| | Case 4.2.1 | | RE | Wastewater sludge | RD | −2 | 0.057 | N/A | 0.23 | 69.5 |
| | Case 4.2.2 | | RNG | Wastewater sludge | RD | −7 | 0.057 | N/A | 0.23 | 69.5 |
| | Case 4.2.3 | | RE and RNG | Wastewater sludge | RD | −14 | 0.057 | N/A | 0.23 | 69.5 |
| | Case 4.2.4 | | RE, RNG, and renewable $H_2$ | Wastewater sludge | RD | −14 | 0.060 | 0.071 | 0.13 | 69.5 |
| Case 5 DAC $CO_2$ to SAF | Case 5.1.0 | Benchmark | - | DAC $CO_2$ | SAF | 333 | 0.3 | 1.2 | 0.8 | 105 |
| | Case 5.1.1 | | RE | DAC $CO_2$ | SAF | 147 | 0.3 | 1.2 | 0.8 | 105 |
| | Case 5.1.2 | | RE and RNG | DAC $CO_2$ | SAF | 101 | 0.3 | 1.2 | 0.8 | 105 |
| | Case 5.1.3 | | RE, RNG, and GA | DAC $CO_2$ | SAF | 7 | 0.3 | 1.2 | 0.8 | 105 |
| | Case 5.2.0 | With additional CCS | - | DAC $CO_2$ | SAF w/ CCS | 309 | 0.3 | 1.2 | 0.8 | 105 |
| | Case 5.2.1 | | RE | DAC $CO_2$ | SAF w/ CCS | 122 | 0.3 | 1.2 | 0.8 | 105 |
| | Case 5.2.2 | | RE and RNG | DAC $CO_2$ | SAF w/ CCS | 76 | 0.3 | 1.2 | 0.8 | 105 |
| | Case 5.2.3 | | RE, RNG, and GA | DAC $CO_2$ | SAF w/ CCS | −18 | 0.3 | 1.2 | 0.8 | 105 |
| | Case 5.3.0 | With additional CCU | - | DAC $CO_2$ + flue gas $CO_2$ | SAF | 313 | 0.3 | 1.2 | 0.6 | 79 |
| | Case 5.3.1 | | RE | DAC $CO_2$ + flue gas $CO_2$ | SAF | 134 | 0.3 | 1.2 | 0.6 | 79 |
| | Case 5.3.2 | | RE and RNG | DAC $CO_2$ + flue gas $CO_2$ | SAF | 99 | 0.3 | 1.2 | 0.6 | 79 |
| | Case 5.3.3 | | RE, RNG, and GA | DAC $CO_2$ + flue gas $CO_2$ | SAF | 5 | 0.3 | 1.2 | 0.6 | 79 |

[a] Captured $CO_2$ is not included in the feedstock inputs for Cases 1.3.x, 2.3.x, 3.3.x, and 5.3.x

# 4.2 TEA

Even though many assumptions used for the TEA were kept consistent throughout this study, comparing TEA results across the five different cases can be difficult. This is because each pathway is analyzed based on different assumptions of process scale, product type and functional unit, and different TRLs. Production costs (and resultant MFSPs) comprise capital cost-related components (capital depreciation, income tax, and return on investment) and operating costs (materials, utilities, and labor). The production costs of all the case studies and scenarios analyzed are summarized in Table 20.

RNG and renewable $H_2$ are assumed to have a higher price than fossil NG and fossil $H_2$. Higher prices of these renewable resources (compared to fossil base) increase MFSPs. Additional carbon mitigation strategies such as CCS and CCU reduce the amount of $CO_2$ released to the atmosphere in this process. CCS technologies are relatively higher TRL, and sequestration has key environmental benefits, but this strategy does increase costs. The CCU strategy requires only the addition of an amine flue-gas scrubbing system and can utilize the existing $CO_2$-to-CO framework to improve both carbon and energy efficiency to fuels. As such, more economic value (i.e., reduced fuel costs with improved efficiency) is added by recycling carbon in this process design versus sequestration. However, this jump in efficiency is also associated with a decrease in energy efficiency and a large cost burden, especially in the renewable scenario, which would be necessary to approach a net-zero-carbon fuel. Further R&D is required to move the TRL of CCU, which is currently at a TRL of about 3. Additionally, since this process is highly dependent on the availability of low-cost renewable electricity and green $H_2$, more time for optimization of these technologies will enhance the feasibility of this pathway. Thus, CCU should be viewed as a long-term strategy for carbon mitigation and utilization in the biomass-to-fuels via FT pathway.

Table 20. Summary of TEA results; positive cost impacts and negative cost impacts from the sensitivity study are presented in green and red, respectively.

| Case | Scenarios | Feedstock Rate (U.S. tons/yr) | Product Rate (million GGE/yr) | MFSP ($/GGE) | Reasons for Cost Changes from Benchmark |
|---|---|---|---|---|---|
| Case 1.1.0 | Corn ethanol to SAF benchmark | 342,500 | 25.1 | 3.24 | Benchmark |
| Case 1.1.1 | Benchmark with RE | | | 3.24 | |
| Case 1.1.2 | Benchmark with RE and RNG | | | 3.70 | Higher operating cost for RNG |
| Case 1.1.3 | Benchmark with RE, RNG, and renewable $H_2$ | | | 3.88 | Higher operating cost for RNG and renewable $H_2$ |
| Case 1.1.4 | Benchmark with RE, RNG, renewable $H_2$, and GA | | | 4.34 | Higher operating cost for RNG, renewable $H_2$, and GA |
| Case 1.2.0 | Benchmark with additional CCS | | | 3.43 | Higher capital and operating costs for CCS |
| Case 1.2.1 | Benchmark with additional CCS with RE | | | 3.43 | |
| Case 1.2.2 | Benchmark with additional CCS with RE and RNG | | | 3.90 | Higher operating cost for RNG |
| Case 1.2.3 | Benchmark with additional CCS with RE, RNG, and renewable $H_2$ | | | 4.08 | Higher operating cost for RNG and renewable $H_2$ |
| Case 1.2.4 | Benchmark with additional CCS with RE, RNG, renewable $H_2$, and GA | | | 4.54 | Higher operating cost for RNG, renewable $H_2$, and GA |
| Case 1.3.0 | Benchmark with additional CCU | | 37.0 | 4.53 | Higher capital and operating costs for CCU even with higher fuel production |
| Case 1.3.1 | Benchmark with additional CCU with RE | | | 4.53 | |
| Case 1.3.2 | Benchmark with additional CCU with RE and RNG | | | 5.00 | Higher operating cost for RNG |
| Case 1.3.3 | Benchmark with additional CCU with RE, RNG, and renewable $H_2$ | | | 5.18 | Higher operating cost for RNG and renewable $H_2$ |
| Case 1.3.4 | Benchmark with additional CCU with RE, RNG, renewable $H_2$, and GA | | | 5.49 | Higher operating cost for RNG, renewable $H_2$, and GA |
| Case 2.1.0 | Corn stover ethanol to SAF benchmark | 724,200 | 35.8 | 4.55 | |
| Case 2.1.1 | Benchmark with RE | | | 4.55 | |
| Case 2.1.2 | Benchmark with RE and RNG | | | 4.74 | Higher operating cost for RNG |
| Case 2.1.3 | Benchmark with RE, RNG, and renewable $H_2$ | | | 4.80 | Higher operating cost for RNG and renewable $H_2$ |
| Case 2.2.0 | Benchmark with additional CCS | | | 4.72 | Higher capital and operating costs for CCS |
| Case 2.2.1 | Benchmark with additional CCS with RE | | | 4.72 | |
| Case 2.2.2 | Benchmark with additional CCS with RE and RNG | | | 4.92 | Higher operating cost for RNG |
| Case 2.2.3 | Benchmark with additional CCS with RE, RNG, and renewable $H_2$ | | | 4.96 | Higher operating cost for RNG and renewable $H_2$ |
| Case 2.3.0 | Benchmark with additional CCU | | 52.7 | 5.26 | Higher capital and operating costs for CCU even with higher fuel production |
| Case 2.3.1 | Benchmark with additional CCU with RE | | | 5.26 | |
| Case 2.3.2 | Benchmark with additional CCU with RE and RNG | | | 5.45 | Higher operating cost for RNG |
| Case 2.3.3 | Benchmark with additional CCU with RE, RNG, and renewable $H_2$ | | | 5.50 | Higher operating cost for RNG and renewable $H_2$ |
| Case 3.1.0 | Biomass gasification to FT fuel benchmark | 724,200 | 45.8 | 2.58 | |
| Case 3.1.1.1 | Benchmark with importing NG | | 54.1 | 2.40 | |
| Case 3.1.1.2 | Benchmark with importing RNG | | | 2.70 | Higher operating cost for RNG |
| Case 3.1.2.1 | Benchmark with import gray $H_2$ for tar reforming 250 lbmol/h | | 47.2 | 2.57 | Higher operating cost for $H_2$ |
| Case 3.1.2.1b | Benchmark with import green $H_2$ for tar reforming 250 lbmol/h | | | 2.68 | Higher operating cost for renewable $H_2$ |
| Case 3.1.2.2 | Benchmark with import gray $H_2$ for tar reforming 1,000 lbmol/h | | 51.3 | 2.53 | Higher operating cost for $H_2$ |
| Case 3.1.2.2b | Benchmark with import green $H_2$ for tar reforming 1,000 lbmol/h | | | 2.95 | Higher operating cost for renewable $H_2$ |

| | | | | | |
|---|---|---|---|---|---|
| Case 3.1.2.3 | Benchmark with import gray $H_2$ for tar reforming 2,000 lbmol/h | | 56.8 | 2.50 | Higher operating cost for $H_2$ |
| Case 3.1.2.3b | Benchmark with import green $H_2$ for tar reforming 2,000 lbmol/h | | | 3.24 | Higher operating cost for renewable $H_2$ |
| Case 3.1.2.4 | Benchmark with import gray $H_2$ for tar reforming 3,000 lbmol/h | | 62.2 | 2.48 | Higher operating cost for $H_2$ |
| Case 3.1.2.4b | Benchmark with import green $H_2$ for tar reforming 3,000 lbmol/h | | | 3.49 | Higher operating cost for renewable $H_2$ |
| Case 3.2.0 | Benchmark with additional CCS | | 45.8 | 2.90 | Higher capital and operating costs for CCS |
| Case 3.2.1 | Benchmark with additional CCS with RE | | | 2.90 | |
| Case 3.3.0 | Benchmark with additional CCU | | 75.0 | 3.75 | Higher capital and operating costs for CCU even with higher fuel production |
| Case 3.3.1 | Benchmark with additional CCU with RE | | | 3.75 | |
| Case 3.3.2 | Benchmark with additional CCU with RE and renewable $H_2$ | | | 4.83 | Higher operating cost for renewable $H_2$ |
| Case 4.1.0 | Wet waste HTL to fuel with $NH_3$ removal from aqueous phase (benchmark w/ $NH_3$ removal) | 363,000 (dry sludge) | 36.8 | 3.12 | Benchmark (flowsheet with $NH_3$ removal) |
| Case 4.1.1 | Benchmark w/ $NH_3$ removal, RE | | | 3.12 | Insignificantly different due to comparable prices between renewable and non-renewable electricity costs |
| Case 4.1.2 | Benchmark w/ $NH_3$ removal, RNG | | | 3.49 | Higher operating cost for RNG |
| Case 4.1.3 | Benchmark w/ $NH_3$ removal, RE and RNG | | | 3.49 | Higher operating cost for RNG |
| Case 4.1.4 | Benchmark w/ $NH_3$ removal, RE, RNG, and renewable $H_2$ | | | 3.58 | Higher operating cost for RNG and renewable $H_2$ |
| Case 4.2.0 | Wet waste HTL to fuel without $NH_3$ removal from aqueous phase (benchmark w/o $NH_3$ removal) | | | 2.77 | Benchmark (flowsheet without $NH_3$ removal) |
| Case 4.2.1 | Benchmark w/o $NH_3$ removal, RE | | | 2.77 | Insignificantly different due to comparable prices between renewable and non-renewable electricity costs |
| Case 4.2.2 | Benchmark w/o $NH_3$ removal, RNG | | | 3.08 | Higher operating cost for RNG |
| Case 4.2.3 | Benchmark w/o $NH_3$ removal, RE and RNG | | | 3.08 | Higher operating cost for RNG |
| Case 4.2.4 | Benchmark w/o $NH_3$ removal, RE, RNG, and renewable $H_2$ | | | 3.17 | Higher operating cost for RNG and renewable $H_2$ |
| Case 5.1.0 | DAC $CO_2$ to SAF | 620,200 | 43.8 | 10.95 | |
| Case 5.1.1 | Benchmark with RE | | | 10.95 | |
| Case 5.1.2 | Benchmark with RE and RNG | | | 11.75 | Higher operating cost for RNG |
| Case 5.1.3 | Benchmark with RE, RNG, and renewable $H_2$ | | | 15.26 | Higher operating cost for RNG and renewable $H_2$ |
| Case 5.2.0 | Benchmark with CCS | | | 11.14 | |
| Case 5.2.1 | Benchmark with CCS with RE | | | 11.14 | |
| Case 5.2.2 | Benchmark with CCS with RE and RNG | | | 11.94 | Higher operating cost for RNG |
| Case 5.2.3 | Benchmark with CCS with RE, RNG, and renewable $H_2$ | | | 15.45 | Higher operating cost for RNG and renewable $H_2$ |
| Case 5.3.0 | Benchmark with CCU | | 57.9 | 9.94 | |
| Case 5.3.1 | Benchmark with CCU with RE | | | 9.94 | |
| Case 5.3.2 | Benchmark with CCU with RE and RNG | | | 10.54 | Higher operating cost for RNG |
| Case 5.3.3 | Benchmark with CCU with RE, RNG, and renewable $H_2$ | | | 14.06 | Higher operating cost for RNG and renewable $H_2$ |

# 5. Conclusion

This report summarizes analysis conducted to assess the environmental and economic feasibility of net-zero-carbon fuels for transportation applications. The analysis was performed collaboratively between four national laboratories: Argonne National Laboratory, Lawrence Livermore National Laboratory, the National Renewable Energy Laboratory, and Pacific Northwest National Laboratory; and our university partner at the University of California, Berkeley. These institutions brought independent perspectives on energy and carbon management to bear on the challenge of net-zero fuels and benefited greatly from insights provided by the U.S. Department of Energy and the industrial members of the Net-Zero Carbon Fuels Technical Team.

We assessed the following pathways: production of jet fuel from corn feedstock with conventional ethanol as an intermediate; production of jet fuel from corn stover with cellulosic ethanol production as an intermediate; production of synthetic fuels from wood and forestry waste using indirect gasification and FT conversion; production of fuel blendstock from wastewater-derived biosolids using hydrothermal liquefaction; and production of jet fuel from carbon dioxide captured directly from air via electrochemical conversion followed by FT synthesis.

We conclude that multiple pathways exist to produce commercial net-zero carbon fuels. Most pathways require both technical maturation of core conversion processes and one or more process inputs (e.g., feedstock, electricity, process heat) to be substantially decarbonized to deliver a net-zero product. We have shown this for multiple variations on each of five different core pathways using carefully harmonized life cycle assessment and techno-economic analysis.

The project team assessed the following variations on each of those pathways, combining lower-CI and higher-carbon-efficiency variations as appropriate: adoption of renewable electricity for use in a biorefinery or upgrading process, use of renewable natural gas instead of conventional natural gas, use of “green” hydrogen produced from renewable electricity instead of conventional hydrogen produced from steam methane reforming, use of “green” ammonia produced from green hydrogen instead of conventional ammonia, capture and sequestration of $CO_2$ in selected exhaust streams at biorefineries, and capture and conversion (to fuels) of $CO_2$ in selected exhaust streams.

For Case 1, we conclude that ethanol-to-jet processes, which are currently being demonstrated at sub-industrial scale (TRL 8), can be combined with fully commercial ethanol production to deliver SAF at $3.24/GGE and a CI 7% below conventional fuel. Sustainable process inputs such as renewable electricity and RNG can substantially reduce the CI of aviation fuel further. Adding commercially available carbon capture and sequestration further reduces the CI by more than 30 g/MJ, making net-zero (and potentially net-negative) jet fuel a near-term possibility. Adding CCU, currently a TRL 3 technology, is the only way to substantially improve the carbon efficiency of the process, but it is not projected to lower the overall costs or achieve

net-negative emissions. We project that the cost of a net-zero fuel would be approximately $3.90/GGE.

For Case 2, we conclude that the ethanol-to-jet process described in Case 1 could be combined with cellulosic ethanol to deliver a much lower-CI aviation fuel. Cellulosic ethanol has been demonstrated at commercial scale (TRL 8-9) but is not widely deployed. This pathway, without further intervention, can deliver jet fuel at 21.8 g/MJ and $4.55/GGE. Incorporating sustainable inputs such as RNG and green hydrogen can address approximately 25% of these remaining emissions, albeit at relatively high costs per unit $CO_2$. Incorporating CCS can make the pathway comfortably net negative at $4.72/GGE. Adding CCU can improve the carbon efficiency of the process and lower the carbon intensity from Cases 2.1 when electricity and hydrogen inputs are fully decarbonized.

For Case 3, we conclude that biomass gasification with Fischer–Tropsch fuel synthesis represents a promising pathway to low-CI transportation fuels, assuming that it can be scaled up from its current TRL status of about 8. If adopted at industrial scale, such fuels are modeled to have a cost of $2.58/GGE and a CI starting around 6 g/MJ. Variants on the baseline process, such as those that replace biomass-derived process heat, electricity, and hydrogen, may reduce process complexity at the expense of higher CI. CCS enables this pathway to become impressively carbon negative (approximately −40 g/MJ) but requires more costly solvent capture than Cases 1 and 2.

For Case 4, we conclude that hydrothermal liquefaction of biosolids from wastewater is also a promising pathway to low-CI transportation fuels. This is the only pathway that exhibited significant “avoided emissions” due to diversion of the feedstock away from traditional disposal pathways. The TRL of this pathway is currently about 7. If this pathway can be demonstrated as operable without the energy-intensive ammonia removal step, it would exhibit a CI of 22 g/MJ (5 g/MJ if considering avoided emissions) with conventional inputs and 2 g/MJ (−14 g/MJ with avoided emissions) with sustainable inputs. At full scale and maturity, delivering fuel from this pathway is projected to cost between $2.77 and $3.58/GGE.

For Case 5, we conclude it is possible to produce fuels produced from $CO_2$ captured from the air. However, with current technology, these fuels are projected to have much higher carbon intensity than conventional fuels. With a fully decarbonized energy system, including zero-carbon electricity and zero-carbon hydrogen, such fuels could achieve near-zero net emissions. They are, however, projected to cost between $10 and $15/GGE.

Leveraging insights learned from this analysis, the NZTT analysis team will continue to explore additional pathways (the combinations of feedstocks, conversion technologies, and products) to expand the coverage of net-zero-carbon fuel production pathways, as well as to perform expanded analysis on the cases reported here to include logistic, system-level, and technical considerations. The uniqueness and key contribution of this study is that both LCA constraints and TEA perspectives are investigated simultaneously, so consequently this

integrated study can quantify the impacts of a variety of economic and environmental metrics. Applying this simultaneous analysis approach to several highly varying technologies allows for the identification of overarching trends such as those highlighted in previous sections. This current analysis, together with future studies, can inform strategic decisions for development of future net-zero-carbon fuel production technologies.

# 6. References


[1] EPA. (2020). *Inventory of U.S. Greenhouse Gas Emissions and Sinks*. Available: https://www.epa.gov/ghgemissions/inventory-us-greenhouse-gas-emissions-and-sinks

[2] U.S. DRIVE, "Net-Zero Carbon Fuels Technical Team Analysis Summary Report 2020," 2021. Available: https://www.energy.gov/eere/vehicles/articles/us-drive-net-zero-carbon-fuels-technical-team-analysis-summary-report-2020

[3] M. Wang, A. Elgowainy, U. Lee, A. Bafana, P. Benavides, A. Burnham, *et al.*, "Greenhouse gases, regulated emissions, and energy use in technologies model®(2021 Excel)," *Comput. Software,* 2021.

[4] R. Pachauri and L. J. I. P. o. C. C. G. Mayer, Switzerland, "Intergovernmental Panel on Climate Change.(Eds.) Climate Change 2014: Synthesis Report," 2015.

[5] S. Jones, Y. Zhu, D. Anderson, R. Hallen, D. Elliott, A. Schmidt, *et al.*, "Process Design and Economics for the Conversion of Algal Biomass to Hydrocarbons: Whole Algae Hydrothermal Liquefaction and Upgrading.," Pacific Northwest National Laboratory, Richland, WA PNNL-23227, 2014. Available: http://www.pnnl.gov/main/publications/external/technical_reports/PNNL-23227.pdf

[6] S. D. Phillips, J. K. Tarud, M. J. Biddy, and A. Dutta, "Gasoline from Woody Biomass via Thermochemical Gasification, Methanol Synthesis, and Methanol-to-Gasoline Technologies: A Technoeconomic Analysis (vol 50, pg 11734, 2011)," *Industrial & Engineering Chemistry Research,* vol. 50, pp. 14226-14226, Dec 21 2011.

[7] R. Davis, J. Markham, C. Kinchin, N. Grundl, E. Tan, and D. Humbird, "Process design and economics for the production of algal biomass: algal biomass production in open pond systems and processing through dewatering for downstream conversion," National Renewable Energy Laboratory, Golden, CO NREL/TP-5100-64772, 2016. Available: http://www.nrel.gov/docs/fy16osti/64772.pdf

[8] A. Dutta, E. C. Tan, D. Ruddy, C. P. Nash, D. P. Dupuis, D. Hartley, *et al.*, "High-Octane Gasoline from Lignocellulosic Biomass via Syngas and Methanol/Dimethyl Ether Intermediates: 2018 State of Technology and Future Research," National Renewable Energy Lab.(NREL), Golden, CO (United States)2018.

[9] E. C. Tan, D. Ruddy, C. P. Nash, D. P. Dupuis, A. Dutta, D. Hartley, *et al.*, "High-Octane Gasoline from Lignocellulosic Biomass via Syngas and Methanol/Dimethyl Ether Intermediates: 2018 State of Technology and Future Research," National Renewable Energy Lab.(NREL), Golden, CO (United States)2018.

[10] R. Davis and L. Laurens, "Algal Biomass Production via Open Pond Algae Farm Cultivation: 2019 State of Technology and Future Research," National Renewable Energy Lab.(NREL), Golden, CO (United States)2020.

[11] ICF, "STUDY ON THE USE OF BIOFUELS (RENEWABLE NATURAL GAS) IN THE GREATER WASHINGTON, D.C. METROPOLITAN AREA " 2020.

[12] National Renewable Energy Laboratory. (2016). *H2A Production Model, Version 3*. Available: http://www.hydrogen.energy.gov/h2a_production.html

[13] D. Klein‐Marcuschamer, B. A. Simmons, and H. W. Blanch, "Techno‐economic analysis of a lignocellulosic ethanol biorefinery with ionic liquid pre‐treatment," *Biofuels, Bioproducts and Biorefining,* vol. 5, pp. 562-569, 2011.

[14] B. Heydorn, "SRI Consulting Chemical Economics Handbook," *SRI Consulting, Menlo Park, CA,* 1998.

[15] E. C. D. Tan, M. Talmadge, A. Dutta, J. Hensley, L. J. Snowden‐Swan, D. Humbird, *et al.*, "Conceptual process design and economics for the production of high‐octane gasoline blendstock via indirect liquefaction of biomass through methanol/dimethyl ether intermediates," *Biofuels, Bioproducts and Biorefining,* vol. 10, pp. 17-35, 2015.

[16] S. Greenberg, K. Canaday, A. Vance, R. McKaskle, and J. Koenig, "A detailed approach for cost analysis for early CCS projects: A case study from the Illinois Basin-Decatur Project," in *14th Greenhouse Gas Control Technologies Conference Melbourne*, 2018, pp. 21-26.

[17] T. Grant, "Quality Guidelines for Energy System Studies: Carbon Dioxide Transport and Storage Costs in NETL Studies," NETL2019.

[18] S. Ma, R. Luo, J. I. Gold, A. Z. Yu, B. Kim, and P. J. A. Kenis, "Carbon nanotube containing Ag catalyst layers for efficient and selective reduction of carbon dioxide," *Journal of Materials Chemistry A,* vol. 4, pp. 8573-8578, 2016.

[19] D. Peterson, J. Vickers, and D. DeSantis, "Hydrogen Production Cost from PEM Electrolyzers - 2019," Department of Energy2020.

[20] Bioenergy Technologies Office, "biofuels and bioproducts from wet and gaseous waste streams: Challenges and Opportunities," 2017. Available: https://energy.gov/sites/prod/files/2017/01/f34/biofuels_and_bioproducts_from_wet_and_gaseous_waste_streams_full_report_2.pdf

[21] RFA. (2020). *Annual Industry Outlook | Renewable Fuels Association*. Available: https://ethanolrfa.org/publications/outlook/

[22] SRI Consulting, "CEH Marketing Research Report: Ethylene," 2011.

[23] A. Dutta, M. Talmadge, J. Hensley, M. Worley, D. Dudgeon, D. Barton*, et al.*, "Process Design and Economics for Conversion of Lignocellulosic Biomass to Ethanol, Thermaochemical Pathway by Indirect Gasification and Mixed Alcohol Synthesis," National Renewable Energy Laboratory, Golden, CO NREL/TP-5100-51400, 2011.

[24] C. W. Lanier, "Process for the production of olefins," US Patent 3,663,647, 1972.

[25] H. W. Stache, Ed., *Anionic Surfactants: Organic Chemistry* (Surfactant Science Series. New York: Marcel Dekker, 1995, p.^pp. Pages.

[26] S. Herron, A. Zoelle, and W. M. Summers, "Cost of Capturing CO2 from Industrial Sources," NETL2014.

[27] I. F. P. News. (2020). *Costs of Corn and Soybean Production in 2020, ISU Report*. Available: https://farmpolicynews.illinois.edu/2020/01/costs-of-corn-and-soybean-production-in-2020-isu-report/

[28] Z. Qin, J. B. Dunn, H. Kwon, S. Mueller, and M. M. Wander, "Influence of spatially dependent, modeled soil carbon emission factors on life‐cycle greenhouse gas emissions of corn and cellulosic ethanol," *Gcb Bioenergy,* vol. 8, pp. 1136-1149, 2016.

[29] D. S. Hartley, D. N. Thompson, and H. Cai, "Woody Feedstocks 2020 State of Technology Report," Idaho National Laboratory, Idaho Falls, Idaho2021.

[30] R. M. Swanson, J. A. Satrio, R. C. Brown, A. Platon, and D. D. Hsu, "Techno-Economic Analysis of Biofuels Production Based on Gasification," National Renewable Energy Laboratory, National Renewable Energy Laboratory NREL/TP-6A20-46587, 2010.

[31] A. Dutta and S. D. Phillips, "Thermochemical ethanol via direct gasification and mixed alcohol synthesis of lignocellulosic biomass. Report No. TP-510-45913. ," National Renewable Energy Lab.(NREL), Golden, CO (United States)2009. Available: http://www.nrel.gov/docs/fy09osti/45913.pdf.

[32] A. Dutta, J. Hensley, R. Bain, K. Magrini, E. C. D. Tan, G. Apanel*, et al.*, "Technoeconomic Analysis for the Production of Mixed Alcohols via Indirect Gasification of Biomass Based on Demonstration Experiments," *Industrial & Engineering Chemistry Research,* vol. 53, pp. 12149-12159, 2014/07/30 2014.

[33] A. Dutta, M. Talmadge, J. Hensley, M. Worley, D. Dudgeon, D. Barton*, et al.*, "Techno-Economics for Conversion of Lignocellulosic Biomass to Ethanol by Indirect Gasification and Mixed Alcohol Synthesis," *Environmental Progress & Sustainable Energy,* vol. 31, pp. 182-190, Jul 2012.

[34] Eric C.D. Tan, Michael Talmadge, Abhijit Dutta, Jesse Hensley, Josh Schaidle, and M. Biddy, "Process Design and Economics for the Conversion of Lignocellulosic. Biomass to Hydrocarbons via. Indirect Liquefaction," 2015.

[35] Y. Zhang, A. H. Sahir, E. C. Tan, M. S. Talmadge, R. Davis, M. J. Biddy*, et al.*, "Economic and environmental potentials for natural gas to enhance biomass-to-liquid fuels technologies," *Green chemistry,* vol. 20, pp. 5358-5373, 2018.

[36] A. H. Sahir, Y. Zhang, E. C. Tan, L. J. B. Tao, Bioproducts, and Biorefining, "Understanding the role of Fischer‐Tropsch reaction kinetics in techno‐economic analysis for co‐conversion of natural gas and biomass to liquid transportation fuels," *Biofuels, Bioproducts and Biorefining,* vol. 13, pp. 1306-1320, 2019.

[37] B. Todic, L. Nowicki, N. Nikacevic, and D. B. Bukur, "Fischer–Tropsch synthesis product selectivity over an industrial iron-based catalyst: Effect of process conditions," *Catalysis Today,* vol. 261, pp. 28-39, 2016.

[38] L.J. Snowden-Swan, J. Zhu, M.D. Bearden, T.E. Seiple, S.B. Jones, A.J. Schmidt*, et al.*, "Conceptual Biorefinery Design and Research Targeted for 2022: Hydrothermal Liquefacation Processing of Wet Waste to Fuels," PNNL-27186, Pacific Northwest National Laboratory, Richland, WA.2022. Available: https://www.pnnl.gov/main/publications/external/technical_reports/PNNL-27186.pdf

[39] H. Cai, L. Ou, M. Wang, R. Davis, A. Dutta, K. Harris*, et al.*, "Supply Chain Sustainability Analysis of Renewable Hydrocarbon Fuels via Indirect Liquefaction, Ex Situ Catalytic Fast Pyrolysis, Hydrothermal Liquefaction, Combined Algal Processing, and Biochemical Conversion: Update of the 2020 State-of-Technology Cases," Argonne National Lab.(ANL), Argonne, IL (United States)2021.

[40] T. E. Seiple, A. M. Coleman, and R. L. Skaggs, "Municipal wastewater sludge as a sustainable bioresource in the United States," *J Environ Manage,* vol. 197, pp. 673-680, Jul 15 2017.

[41] M. Fasihi, O. Efimova, and C. Breyer, "Techno-economic assessment of CO2 direct air capture plants," *Journal of Cleaner Production,* vol. 224, pp. 957-980, 2019.

[42] N. McQueen, K. V. Gomes, C. McCormick, K. Blumanthal, M. Pisciotta, and J. Wilcox, "A review of direct air capture (DAC): scaling up commercial technologies and innovating for the future," *Progress in Energy,* 2021.